Observing speed for SPIRE feedhorn and filled array options

Prepared by: Matt Griffin **Version: 2**
Date: 24 January 2000

This is the final version of this document before the Array Selection meeting

Updates from the January 10 version:

1. The definition of the filter passbands in the observing speed worksheet has been changed slightly to make the treatment consistent with the SPIRE photmetric model (this makes the observing speed figures for the filled array case marginally better).

2. The observing speed calculations (now Appendix A) have been updated (changes are small).

3. A new section (6.3) on the sensitivity of the results to various assumed parameters is included.

4. Figures and appendices have been re-numbered.

5. Appendix B, an updated version of the SPIRE photometer sensitivity model, has been added. It is now consistent with the treatment and assumptions of this note.

6. Appendix E, a note by Bruce Swinyard on frame compression for the filled array options, has been added.

7. Some changes and additions to the main text have been made here and there based on comments received.

Significant changes to the text of Version 1 are typed in green.

1. Introduction

This note is a revised, and extended version of the note *Comparison of sensitivities of 0.5Fλ, 1.0Fλ and 2.0Fλ arrays for the BOL* by Matt Griffin, Jamie Bock, and Walter Gear, 15 Dec. 1997 (BOL/QMW/N/0026.10).

I consider the 0.5Fλ square pixel and 2.0Fλ feedhorn cases (1.0Fλ horns are no longer being considered for SPIRE). The relative mapping speeds of the filled array and feedhorn options are estimated for pointed and scanning observations. Mapping speeds are estimated both for observations of the sky intensity distribution and for measurements of point sources. The speed improvements achievable in principle (for the completely background-limited case) are calculated, and the important effect of finite detector NEP on mapping speed is also considered. Finally, some practical issues concerning the scan rate, 1/f noise and the detector speed of response are discussed.

Two other filled array options are now included (in Section 8):

(i) the case of a single filled array type for both 250 and 350 μm, optimised for 300 μm;

(ii) the case of 1.0Fλ filled array pixels, to examine the effects of using larger pixels for all wavelengths for the filled arrays (this is presumably as large or larger than one would want to make them).

The analysis is based mainly on the photometer, but similar considerations should apply to the FTS. Throughout, subscripts F and H are used to denote the filled array and feedhorn options, respectively.

The modelling of the SPIRE beam profiles and the simulation of SPIRE observations have demonstrated that the main difference in principle between the 0.5Fλ filled array and 2Fλ feedhorn options for SPIRE is in mapping speed. This is because there are only small differences in the beam profile on the sky for the two cases, and because there are no fundamental differences in the form of data and their treatment. The SPIRE photometer beam profiles computed by Martin Caldwell for the 0.5Fλ filled array and 2.0Fλ feedhorn options are shown in Fig. 1. The FWHM values for the filled array and feedhorn options are as follows:

λ (μm)	FWHM (arcseconds)	
	0.5Fλ filled pixel	**2.0Fλ feedhorn**
250	16.5	17.1
350	23.1	24.4
500	32.8	34.6

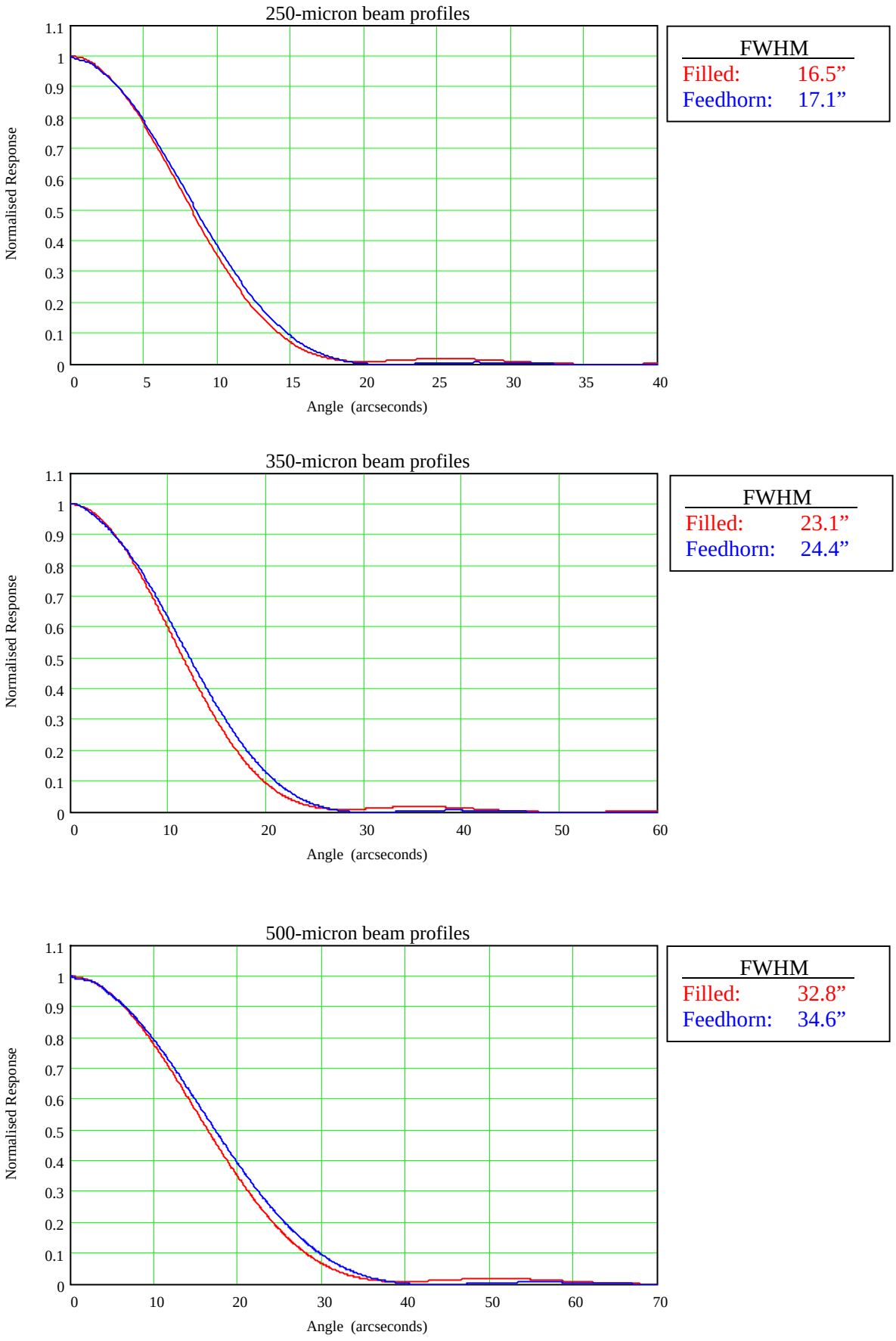

Fig. 1: SPIRE photometer beam profiles

2. Assumptions

In estimating the theoretical relative performance of the two options, we make the following assumptions.

1 The point spread function is purely diffraction limited. This will not be the case in SPIRE – the assumption is really that the effect of imperfect psf on sensitivity will be the same for both options.

2 Detector centre-centre spacing is $0.5F\lambda$ for the filled array case and $2.0F\lambda$ for the feedhorn case.

3 Feedhorns are single-moded (throughput = λ^2) .

4 The optical efficiency of the instrument and the absorption efficiency of the detectors are the same for both options.

5 There is no stray light or out-of-band radiation.

6 No excess noise or inefficiency are added by microphonics, multiplexing, pixel co-addition, on-board data processing, data compression, or anything else.

7 In all cases, overheads when chopping, jiggling or dithering are taken to be negligible.

8 The small differences (4 - 6%) in the beam widths between the filled and feedhorn options can be neglected.

9 The numbers of detectors, N_F and N_H, in the arrays are as follows:

	250 μm	**350 μm**	**500 μm**
N_F (0.5Fλ)	32 x 64 = 2048	24 x 48 = 1152	16 x 32 = 512
N_H (2.0Fλ)	9 x 17 = 153	7 x 13 = 91	5 x 9 = 45
$\beta = N_F/N_H$	13.4	12.7	11.4

10 When the signals from several pixels or map points are combined, simple co-addition is assumed: the total signal is the sum of the signals in all the pixels being combined and the noise is taken to increase as the square root of number of pixels.

3. Definitions

Parameter	Description	Units	Nominal value
D	Telescope aperture diameter	m	3.28
T_{tel}	Telescope temperature	K	80
ε_{tel}	Telescope emissivity		0.04
λ	Central wavelength	μm	250, 350, 500
$\Delta\lambda$	Filter bandwidth	μm	$\lambda/3$
F	Focal ratio of the final optics		5
η_{opt}	Telescope-to-detector transmission efficiency		0.30
η_d	Detector quantum efficiency		0.80
d_F	Square pixel centre-centre spacing		$0.5F\lambda$
g	Inactive gap between filled array pixels	μm	CEA: 70 GSFC: ?
d_F	Feedhorn centre-centre spacing		$2.0F\lambda$
P_s	Total source power collected by telescope from a point source	W	
P_{sig}	Source power incident on the on-axis pixel	W	
$A\Omega$	Throughput	m^2Sr	
η_{pix}	Fraction of the total power from a point source coupled to a detector centred on the source		
α	Fraction of single-moded feedhorn throughput which is truncated by the SPIRE cold stop		0.8
t	Integration time per pixel	s	
NEP_{ph}	Photon noise limited NEP referred to the background power absorbed by the detector	$W\ Hz^{-1/2}$	
NEP_{det}	Detector optical NEP at the signal frequency	$W\ Hz^{-1/2}$	3×10^{-17}
P_B	Telescope background power incident on a detector	W	
σ	S/N ratio for a given detector or map point		
$B_\nu(T)$	Planck function	$W\ m^{-2}\ Sr^{-1}\ Hz^{-1/2}$	
T_{sky}	Sky brightness temperature	K	
S_ν	Point source flux density	$W\ m^{-2}\ Hz^{-1/2}$	
β	Ratio of detector numbers for filled and feedhorn arrays (N_F/N_H)		
γ	Ratio of detector NEP to photon noise NEP		
θ	Angular offset for seven-point observation of a point source (feedhorn option)	arcseconds	6

4. Values of η_{pix} and $A\Omega$ for the various options

4.1 η_{pix} for 2.0Fλ feedhorns

For the feedhorn case, η_{pix_H} is usually given as ≈ 0.7 for 2.0Fλ horns (the effect of a small wall thickness is negligible). Martin Caldwell had computed the horn coupling efficiency for the SPIRE feedhorn option, deriving a figure of 0.74 for the 500-μm band with a 30-mm long horn. The efficiency should be slightly better for the shorter wavelengths as the horn length is greater in relation to the wavelength.

4.2 $A\Omega$ for the feedhorn

For single-moded feedhorns, the total throughput is $A\Omega_H = \lambda^2$. For the telescope background, there will actually be a reduction by some factor α due to the fact that some of the power radiated by the horn is terminated on the cold pupil stop which is designed to match the FIRST secondary mirror system stop. We assume that $\alpha = 0.8$.

4.3 η_{pix} for the filled array pixel

For an individual square pixel in a filled array, η_{pix_F} is determined by the fraction of the power in the PSF that is contained in the pixel, which may be calculated by integrating under the intercepted part of the PSF. This is plotted in Fig. 2 for a diffraction limited system (where the PSF is the Airy diffraction pattern). In practice η_{pix_F} will be less by an amount roughly equal to the Strehl ratio, but we ignore this effect here. For 0.5Fλ pixels with no gap, we have $\eta_{pix\_F} = 0.177$. For a 70-μm gap, we have η_{pix_F} = (0.143, 0.152, 0.160) at (250, 350, 500) μm.

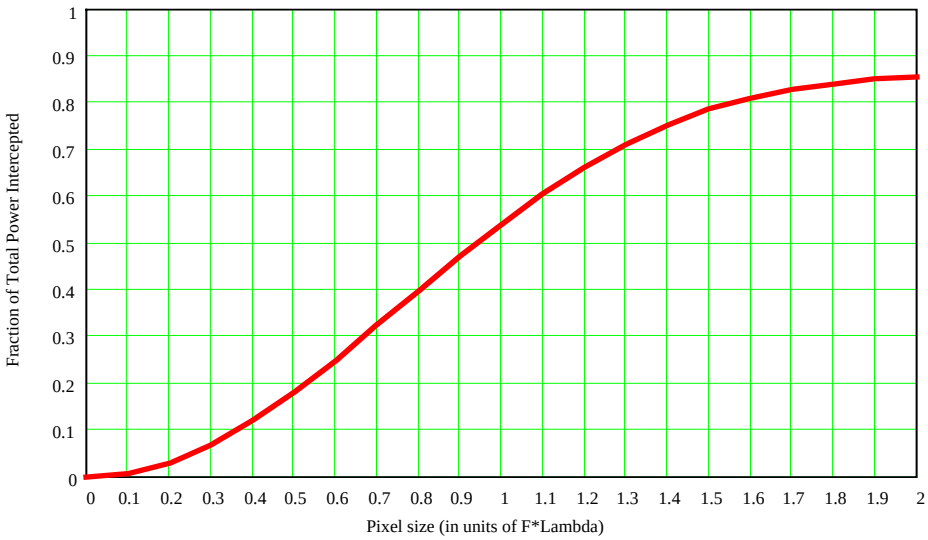

Fig. 2: Fraction of the power in the diffraction-limited psf intercepted by an on-axis square pixel

4.4 $A\Omega$ for the filled array pixel

Here we assume that the square pixel of side is illuminated by a top-hat beam of solid angle $\pi/(4F^2)$, so that the throughput is

$$A\Omega_F = [0.5F\lambda - g]^2 \left[\frac{\pi}{4F^2}\right] \qquad (1)$$

For zero gap, $A\Omega_F = \frac{\pi\lambda^2}{16} = 0.196\lambda^2$.

5. Signal-to-noise ratios and relative mapping speed

5.1 Measurement of sky intensity distribution

The telescope background power absorbed by each pixel is

$$P_B = A\Omega B_\nu(T_{tel})\Delta\nu\varepsilon_{tel}\eta_{opt}\eta_d \,. \qquad (2)$$

Neglecting the Bose-Einstein correction, which is negligible in this case, the photon noise limited NEP, referred to the power *absorbed* by the detector, is

$$NEP_{ph} = \left[2A\Omega B_\nu(T_{tel})\Delta\nu\varepsilon_{tel}\eta_{opt}\eta_d h\nu\right]^{0.5}. \qquad (3)$$

The overall NEP, referred to the power absorbed by the detector, is

$$NEP_{tot} = \left[NEP_{ph}{}^2 + NEP_{det}{}^2\right]^{0.5}. \qquad (4)$$

Let $NEP_{det} = \gamma NEP_{ph}$. Therefore,

$$NEP_{tot} = NEP_{ph}\left[1+\gamma^2\right]^{0.5}. \qquad (5)$$

The detective quantum efficiency of the whole system is defined as

$$DQE = \left[\frac{NEP_{ideal}}{NEP_{actual}}\right]^2 . \qquad (6)$$

where NEP_{ideal} is the photon noise NEP for a noiseless detector of unit quantum efficiency, and NEP_{actual} is the achieved NEP referred to the power incident on the detector.

In this case, $DQE = \eta_d/(1+\gamma^2)$. (7)

Let the sky brightness be given by $B_\nu(T_{sky})$. The signal power absorbed by a detector is

$$P_{sig} = A\Omega B_\nu(T_{sky})\Delta\nu\eta_{opt}\eta_d \,. \qquad (8)$$

After an integration time, t, the signal-to-noise ratio, σ, for the on-axis pixel is

$$\sigma = \frac{P_{sig}(2t)^{0.5}}{NEP_{tot}} . \qquad (9)$$

We then have, from (3), (5), and (8),

$$\sigma = \frac{B_\nu(T_{sky})\left(A\Omega\Delta\nu\eta_{opt}\eta_{bol}t\right)^{0.5}}{\left[B_\nu(T_{tel})\varepsilon_{tel}h\nu(1+\gamma^2)\right]^{0.5}} . \qquad (10)$$

For simplicity in comparing the two cases, we can lump together all of the quantities that are assumed to be independent of the detector type:

$$\sigma = K_1\left[\frac{A\Omega t}{1+\gamma^2}\right]^{0.5}, \qquad (11)$$

where K_1 is a constant. This is the result we would expect, with the signal-to-noise scaling as the square root of the number of photons collected during the integration time. For a given integration time per point,

$$\frac{\sigma_F}{\sigma_H} = \left[\frac{A\Omega_F}{A\Omega_H} \frac{(1+\gamma_H{}^2)}{(1+\gamma_F{}^2)} \right]^{0.5} . \qquad (12)$$

The relative mapping speed *per map point* for filled and feedhorn arrays is proportional to $\sigma_F/\sigma_H{}^2$:

$$\frac{\text{Speed}_F}{\text{Speed}_H} = \frac{A\Omega_F}{A\Omega_H} \frac{(1+\gamma_H{}^2)}{(1+\gamma_F{}^2)} \qquad \text{per individual point in the map.} \qquad (13)$$

The filled array has β times more pixels than the feedhorn array, so the relative mapping speed is given by

$$\frac{\text{Speed}_F}{\text{Speed}_H} = \beta \frac{A\Omega_F}{A\Omega_H} \frac{(1+\gamma_H{}^2)}{(1+\gamma_F{}^2)} \qquad \text{for the whole map.} \qquad (14)$$

5.2 Measurement of the signal from a point source on-axis

In this case the requirement is to measure the flux density of the point source, and the coupling efficiency of the individual pixel to the point spread function is important. The background power and photon noise limited NEP are as given above in equations (2) and (3). The signal power absorbed by the on-axis detector is

$$P_{sig} = S_\nu A_{tel} \Delta\nu \eta_{opt} \eta_{pix} \eta_d . \qquad (15)$$

Equation (10) is then modified as follows:

$$\sigma = \frac{S_\nu A_{tel} \Delta\nu \eta_{opt} \eta_{pix} \eta_d (2t)^{0.5}}{\left[2A\Omega B_\nu(T_{tel}) \Delta\nu \varepsilon_{tel} \eta_{opt} \eta_d h\nu (1+\gamma^2) \right]^{0.5}} . \qquad (16)$$

We can again combine together all of the quantities that are assumed to be independent of the pixel size:

$$\sigma = K_2 \frac{\eta_{pix} t^{0.5}}{\left[A\Omega(1+\gamma^2 \right]^{0.5}} , \qquad (17)$$

where K_2 is a constant.

Comparing the S/N achieved for a given integration time (with the on-axis detector alone) for the two cases, we have

$$\frac{\sigma_F}{\sigma_H} = \left[\frac{\eta_{pix\_F}}{\eta_{pix\_H}} \right] \left[\frac{A\Omega_H}{A\Omega_F} \frac{(1+\gamma_H{}^2)}{(1+\gamma_F{}^2)} \right]^{0.5} . \qquad (18)$$

For the feedhorn array, the nearest neighbour detectors are too far away to take in any appreciable source power, so the detection is for the on-axis pixel only. No jiggle pattern is needed, so the total integration time is used on-source. In the case of the filled array, however, the signals from

neighbouring pixels can be co-added to improve the S/N. We assume that the eight nearest neighbour pixels are co-added to the central one. The signal is therefore increased by a (slightly wavelength dependent) factor of approximately 4.3. The noise is increased by a factor of (total no. of pixels being co-added)$^{0.5}$ = $9^{0.5}$ = 3. The S/N is therefore enhanced by a factor of 4.3/3 = 1.43. We can actually do slightly better if the signals are weighted appropriately (see Appendix A), and achieve a S/N enhancement by a factor of 1.58.

$$\frac{\sigma_F}{\sigma_H} = 1.58 \left[\frac{\eta_{pix\_F}}{\eta_{pix\_H}}\right]\left[\frac{A\Omega_H}{A\Omega_F}\frac{(1+\gamma_H{}^2)}{(1+\gamma_F{}^2)}\right]^{0.5}. \qquad (19)$$

The relative observing speed for filled and feedhorn arrays is given by the square of this number:

$$\frac{\text{Speed}_F}{\text{Speed}_H} = 2.5 \left[\frac{\eta_{pix\_F}}{\eta_{pix\_H}}\right]^2\left[\frac{A\Omega_H}{A\Omega_F}\frac{(1+\gamma_H{}^2)}{(1+\gamma_F{}^2)}\right]. \qquad (20)$$

5.3 Seven-point observation of a point source with the feedhorn option

Should the pointing accuracy of FIRST be such that we cannot rely on blind pointing to capture the flux of a point source, then, for the feedhorn option, it will be necessary to carry out a small map around the source. The best approach is probably to perform a seven-point map in which the nominal position and six positions around it are visited by a detector. The spacing, θ, should be larger than the maximum expected pointing error. The signals from the seven map points can be co-added to derive the total flux density. Assuming that the beam profile is a Gaussian, we can derive the S/N as follows:

Let t be the total integration time available.
Let the S/N that would be achieved with perfect pointing for one on-axis pixel be equal to 1.
Let the central pixel be pointing directly at the source (an offset will produce gains in some positions and losses in others so the result will be much the same).

Compare the S/N achieved by co-adding the seven pixels with that achieved for the central pixel alone:

- The signal is (central pixel) + (6 pixels at spacing θ) so the total signal is increased by

$$1 + 6\exp\left[-\left[\frac{\theta}{(0.601)\text{FWHM}}\right]^2\right].$$

- The noise per pixel is increased by $7^{0.5}$ as the integration time is shared between the seven pixels
- The noise per pixel is increased by a further $7^{0.5}$ by the co-addition of the seven pixels
- So the S/N is reduced by $\frac{1}{7}\left[1 + 6\exp\left[-\left[\frac{\theta}{(0.601)\text{FWHM}}\right]^2\right]\right]$.

For SPIRE, a suitable value for θ would be 6". This is comfortably greater than the largest expected pointing error (~ 3 arcseconds). It corresponds to 1/3 of the 18" beam at 250 μm and 1/6 of the 35" beam at 500 μm. The factors by which the feedhorn option S/N is reduced through having to do a seven-point map are (0.77, 0.87, 0.94) at (250, 350, 500) μm.

5.4 Extraction of point sources from maps

For SPIRE, an important goal is to carry out such surveys of clean areas of sky and to extract point sources from the maps. The nominal observing mode is to scan the telescope continuously while taking data. The scan rate must be chosen such that the beam crossing time is long compared to the detector time constant to avoid loss of angular resolution in the scan direction. Chopping and/or dithering can also be carried out in making maps. In these modes, the individual detector signals must be telemetered to the ground: on-board differencing will add significantly to the confusion noise, increasing the confusion limit by a factor of ~ 1.6 (cf. Minutes of Detector Array Group meeting, Caltech, May 1999).

Scanning observations with the feedhorn arrays produce a fully sample image of the sky provided the scan direction is chosen to give the necessary overlap between the beams. For chopped observations with feedhorn arrays, a "jiggle-pattern" must be performed to get a fully sampled map.

Consider a fully-sampled map of a given area with a given total integration time and a fixed spacing between the samples. In practice the sampling grid may be more complex, but that will not have much effect on the result of this comparison. Regardless of the exact details (jiggling or scanning), in the filled array case we have β times more integration time per sample than for the feedhorn case. For simplicity, assume that the map contains a point source that happens to be centred on one of the map points. If the map is critically sampled ($0.5F\lambda/D$) then the filled array can generate it by spatial multiplexing while the feedhorn array does it by a combination of spatial and temporal multiplexing. If it is over-sampled (say, $0.25\lambda/D$) then both arrays use a combination of spatial and temporal multiplexing. In any case, what matters for the mapping speed is the final S/N per map point, which is considered below.

Two slightly different methods of estimation the mapping speed advantage for the filled array are presented below. The results they give are essentially the same.

Method 1: Assume that the beam profile on the sky is the same for both options.

This assumption has been shown by beam modelling of SPIRE to be essentially valid (the filled array beam profile is actually very slightly narrower than that for the feedhorn).

Let S_o be the signal in the central position.
Let ΔS be the noise level in each position.
Let $\sigma_o = S_o/\Delta S$ be the S/N for the central position.
Let n appropriate map points be co-added to enhance S/N on a point source.
The beam width on the sky is FWHM = $1.22\lambda/D$.

Signal in pixel i is

$$S_i = S_o \exp\left[-\left[\frac{\theta_i}{(0.601)\mathrm{FWHM}}\right]^2\right] \text{ where } \theta_i \text{ is the angular offset from the source.}$$

The FWHM is approximately the same for both $2.0F\lambda$ feedhorns and $0.5F\lambda$ pixels, so the S_i values scale in the same way for both options. The final signal level is

$$S_{tot} = \sum \mathrm{Sig}_i = K_3 S_o \qquad (K_3 \text{ is the same constant for both options}).$$

The final noise level is $\Delta S_{tot} = n^{0.5}\Delta S$.

The final S/N is thus $$\sigma_{\mathrm{Final}} = \frac{K_3 S_o}{n^{0.5}\Delta S} = \frac{K_3}{n^{0.5}}\sigma_o, \qquad (21)$$

which scales with the S/N on the centre position.

The S/N on the centre position is $\sigma_o = K_2 \frac{\eta_{pix} t^{0.5}}{(A\Omega)^{0.5}}$. (22)

The filled array has β times more detectors and so has β times longer integration time per point. Taking the ratio of the S/N values for the filled and feedhorn arrays we then have:

$$\frac{\sigma_F}{\sigma_H} = \left[\frac{\eta_{pix\_F}}{\eta_{pix\_H}}\right]\left[\frac{A\Omega_H}{A\Omega_F}\frac{(1+\gamma_H{}^2)}{(1+\gamma_F{}^2)}\right]^{0.5} \beta^{0.5}. \quad (23)$$

The mapping speed advantage for the filled array is the square of this number:

$$\frac{\text{Speed}_F}{\text{Speed}_H} = \beta\left[\frac{\eta_{pix\_F}}{\eta_{pix\_H}}\right]^2\left[\frac{A\Omega_H}{A\Omega_F}\frac{(1+\gamma_H{}^2)}{(1+\gamma_F{}^2)}\right]. \quad (24)$$

Method 2: Convolve the pixel with the diffraction pattern to estimate the signals for the filled array case

Consider a fully-sampled map of a given area with a given total integration time and a fixed spacing of 0.25λ/D. Other reasonable values of the angular step will produce similar results. Although the samples will not be on a square grid for the feedhorn option, this too will not make any significant difference to the conclusions.

Assume again that the map contains a point source that happens to be centred on one of the map points. The S/N ratio if we consider the on-axis point alone is given by eq. (23). This S/N can be enhanced by co-adding neighbouring map points as shown in Fig. 3 below:

2.0Fλ feedhorn case: The signals in the offset positions are determined by the Gaussian beam profile on the sky, and may be represented as follows:

Beam FWHM = 1.22λ/D; Grid step = 0.25λ/D

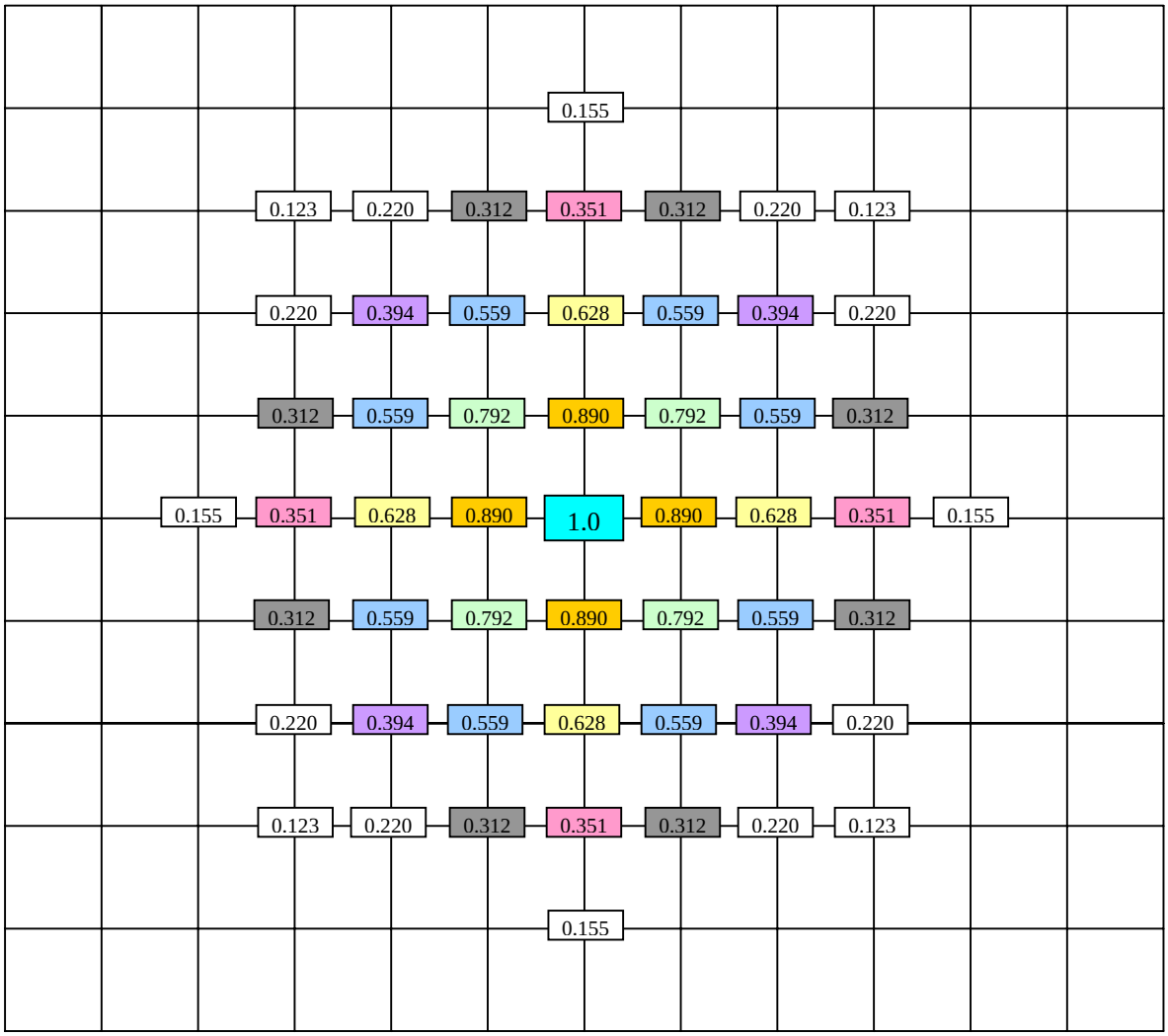

Fig. 3: Normalised signal vs. offset position for regular grid map with 2Fλ feedhorn detectors

Various different sets of pixels could be chosen for co-addition:

(a) Include the 45 points with signal > 0.2:
Tot. Sig. = 1.0 + 4(0.890) + 4(0.792) + 4(0.628) + 8(0.559) + 4(0.394) + 4(0.351) + 8(0.312) + 8(0.220)
Tot. Sig. = 21.95
Tot. Noise = $45^{0.5}$
S/N improvement over central point = **3.27**

(b) Include the 37 points with signal > 0.3:
Tot. Sig. = 1.0 + 4(0.890) + 4(0.792) + 4(0.628) + 8(0.559) + 4(0.394) + 4(0.351) + 8(0.312)
Tot. Sig. = 20.19
Tot. Noise = $37^{0.5}$
S/N improvement over central point = **3.32**

(c) Include the 29 points with signal > 0.35:
Tot. Sig. = 1.0 + 4(0.890) + 4(0.792) + 4(0.628) + 8(0.559) + 4(0.394) + 4(0.351)
Tot. Sig. = 17.69
Tot. Noise = $29^{0.5}$
S/N improvement over central point = **3.29**

(d) Include the 25 points with signal > 0.39:
Tot. Sig. = 1.0 + 4(0.890) + 4(0.792) + 4(0.628) + 8(0.559) + 4(0.394)
Tot. Sig. = 16.29
Tot. Noise = $25^{0.5}$
S/N improvement over central point = **3.26**

The best case (b) gives an improvement in S/N over the central position of **3.32**.

0.5Fλ Case:

Grid step = 0.25λ/D; signal levels derived by integrating the Airy diffraction pattern over the appropriate square areas

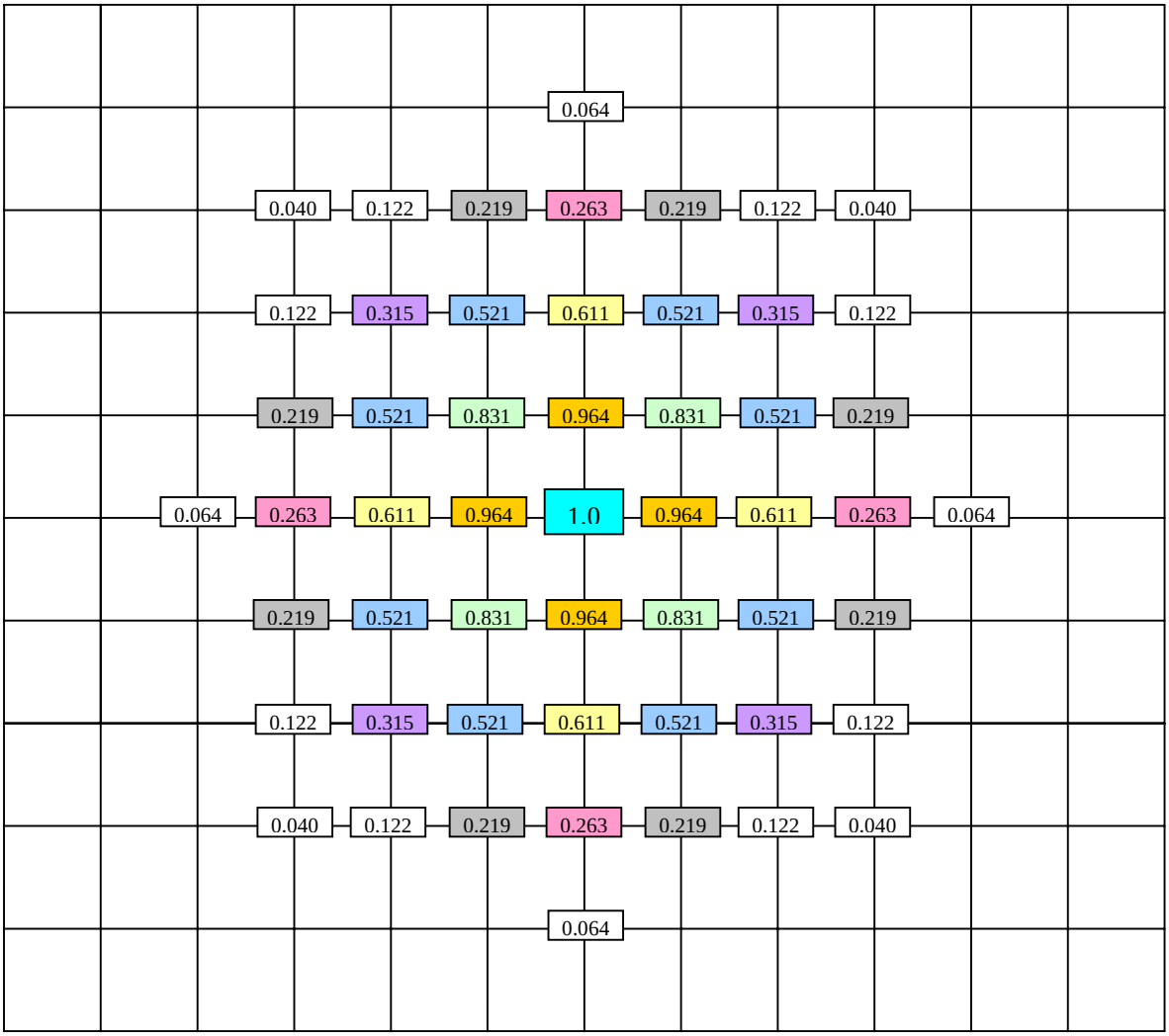

Fig. 4: Normalised signal vs. offset position for regular grid map with 0.5Fλ square detectors, assuming that the signal is proportional to the volume under the Airy function intercepted by the pixel.

(a) Include the 29 points with signal > 0.25:
Tot. Sig. = 1.0 + 4(0.964) + 4(0.831) + 4(0.611) + 8(0.521) + 4(0.315) + 4(0.263)
Tot. Sig. = 17.10
Tot. Noise = $29^{0.5}$
S/N improvement over central point = **3.18**

(b) Include the 25 points with signal > 0.3:
Tot. Sig. = 1.0 + 4(0.964) + 4(0.831) + 4(0.611) + 8(0.521) + 4(0.315)
Tot. Sig. = 16.05
Tot. Noise = $25^{0.5}$
S/N improvement over central point = **3.21**

(c) Include the 21 points with signal > 0.5:
Tot. Sig. = 1.0 + 4(0.964) + 4(0.831) + 4(0.611) + 8(0.521)
Tot. Sig. = 14.71
Tot. Noise = $21^{0.5}$
S/N improvement over central point = **3.21**

The best cases (b or c) give an improvement in S/N over the central position of **3.21**.

So on co-adding the optimum sets of pixels in each case, the ratio of the S/N values becomes

$$\frac{\sigma_F}{\sigma_H} = \left[\frac{3.21}{3.32}\right]\left[\frac{\eta_{pix\_F}}{\eta_{pix\_H}}\right]\left[\frac{A\Omega_H}{A\Omega_F}\frac{(1+\gamma_H{}^2)}{(1+\gamma_F{}^2)}\right]^{0.5}\beta^{0.5}, \qquad (25)$$

and the mapping speed advantage for the filled array case is therefore

$$\frac{\text{Speed}_F}{\text{Speed}_H} = (0.94)\beta\left[\frac{\eta_{pix\_F}}{\eta_{pix\_H}}\right]^2\left[\frac{A\Omega_H}{A\Omega_F}\frac{(1+\gamma_H{}^2)}{(1+\gamma_F{}^2)}\right]. \qquad (26)$$

6. Results of detailed calculations

Appendix A is a MathCad worksheet which calculates the S/N and mapping speed ratios for any combination of the various parameters defining the arrays. The worksheet has been run for various cases and some results are summarised below. This model is consistent with the updated sensitivity model for the SPIRE photometer (also attached as Appendix B).

6.1 Case 1: Ideal situation

- Zero gap between filled array pixels
- Completely background limited (NEP_{det} negligible)

The speed ratios (filled:feedhorn) for 250, 350 and 500 μm are:

λ	Mapping speed ratio for surface brightness	Point source observing speed ratio (on-axis)	Point source observing speed ratio (7-point with feedhorn)	Mapping speed ratio for point source extraction
λ_i	$B\_Speed\_Ratio_i$	$S\_Speed\_Ratio\_On\_Axis_i$	$S7\_Speed\_Ratio_i$	$Speed\_Ratio\_Map\_Point_i$
250	3.29	0.66	1.10	3.50
350	3.11	0.66	0.86	3.31
500	2.79	0.66	0.75	2.98

Comments:

(i) For point source observations, the feedhorn option is comparable or faster, even if a 7-point observation has to be carried out.

(ii) For surface brightness measurements or point source extraction from maps, the filled array is faster by a factor of 2.8 – 3.5.

6.2 Case 2: SPIRE, with the same NEP_{det} for both options

- 70 μm gap between filled array pixels
- $NEP_{det} = 3 \times 10^{-17}$ W $Hz^{-1/2}$ for both options

Speed ratios for 250, 350 and 500 μm:

λ	Mapping speed ratio for surface brightness	Point source observing speed ratio (on-axis)	Point source observing speed ratio (7-point with feedhorn)	Mapping speed ratio for point source extraction
λ_i	$B\_Speed\_Ratio_i$	$S\_Speed\_Ratio\_On\_Axis_i$	$S7\_Speed\_Ratio_i$	$Speed\_Ratio\_Map\_Point_i$
250	1.84	0.38	0.64	2.05
350	1.65	0.36	0.47	1.81
500	1.30	0.31	0.35	1.41

Comments:

(iii) For point source observations, the feedhorn option is significantly faster, even if a seven-point is needed.

(iv) The theoretical mapping speed advantage of the filled array option is significantly less than in the ideal background limited case. This is because the background-limited NEP per detector

for the filled array option is a factor of two lower than for the feedhorn case, and so the observations are more strongly affected by detector noise for a given NEP_{det}.

6.3 Sensitivity of the results to the assumed parameters

6.3.1 Detector NEP

The mapping speed advantage of the filled array is sensitive to the achieved detector optical NEP. If this is too high for any reason, (excess noise, stray light, etc.) then the speed advantage is reduced.

- 70 μm gap between filled array pixels
- $NEP_{det} = (3 \times 10^{-17}) * 2^{0.5}$ W $Hz^{-1/2}$ for the filled array detectors; 3×10^{-17} W $Hz^{-1/2}$ for the feedhorn array detectors

λ	Mapping speed ratio for surface brightness	Point source observing speed ratio (on-axis)	Point source observing speed ratio (7-point with feedhorn)	Mapping speed ratio for point source extraction
λ_i	B_Speed_Ratio $_i$	S_Speed_Ratio_On_Axis $_i$	S7_Speed_Ratio $_i$	Speed_Ratio_Map_Point $_i$
250	1.36	0.28	0.47	1.51
350	1.12	0.24	0.32	1.23
500	0.80	0.19	0.22	0.88

Comments:

(i) For point source observations, the feedhorn option is now considerably faster even with a seven-point (by a factor of nearly five at 500 μm).

(ii) The filled array now has a mapping speed disadvantage at 500 μm, and the advantage at the other wavelengths is reduced.

The point source and mapping speed ratios have been calculated as a function of NEP_{det} for the filled array, keeping NEP_{det} fixed at 3×10^{-17} W $Hz^{-1/2}$ for the feedhorn case. The results are plotted in Fig. 5 below.

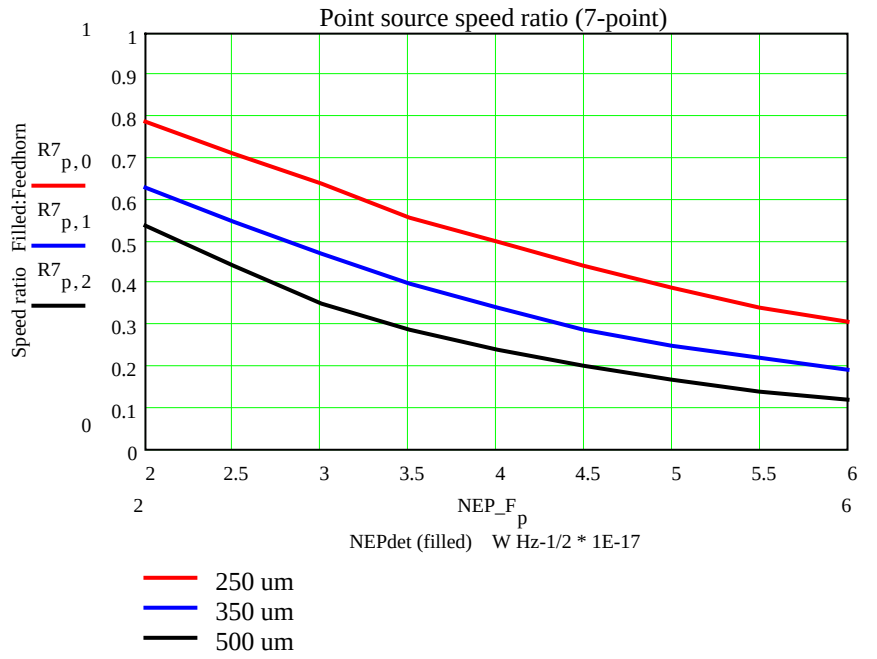

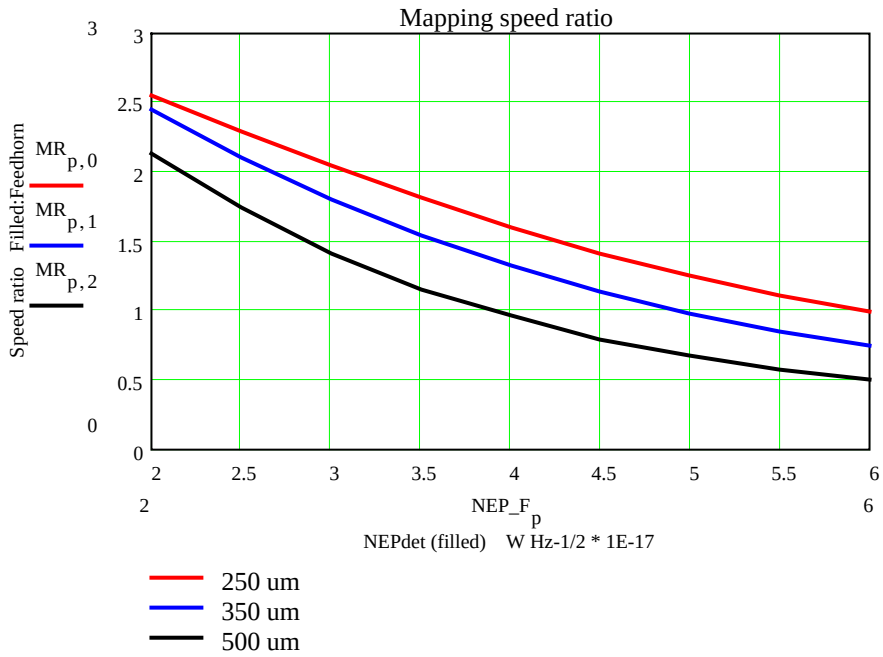

Fig. 5: Point source observing speed (7-point case) and mapping speed ratios vs. NEP_{det_F} for a fixed $NEP_{det\ H} = 3 \times 10^{-17}$ W $Hz^{-1/2}$. All other parameters are at their nominal values.

6.3.2 Telescope emissivity

We have always assumed a value of 0.04 for the FIRST telescope emissivity. This is (hopefully) slightly pessimistic. It is probably wise to design for this value, but it is possible that the emissivity could turn out to be lower or higher. (In the case of the TES option, the possibility of catastrophic loss of the detectors in the event of excess background must be avoided by design.) Figure 6 shows the speed ratios for the case of NEPdet = 3 x 10^{-17} W $Hz^{-1/2}$ for both cases.

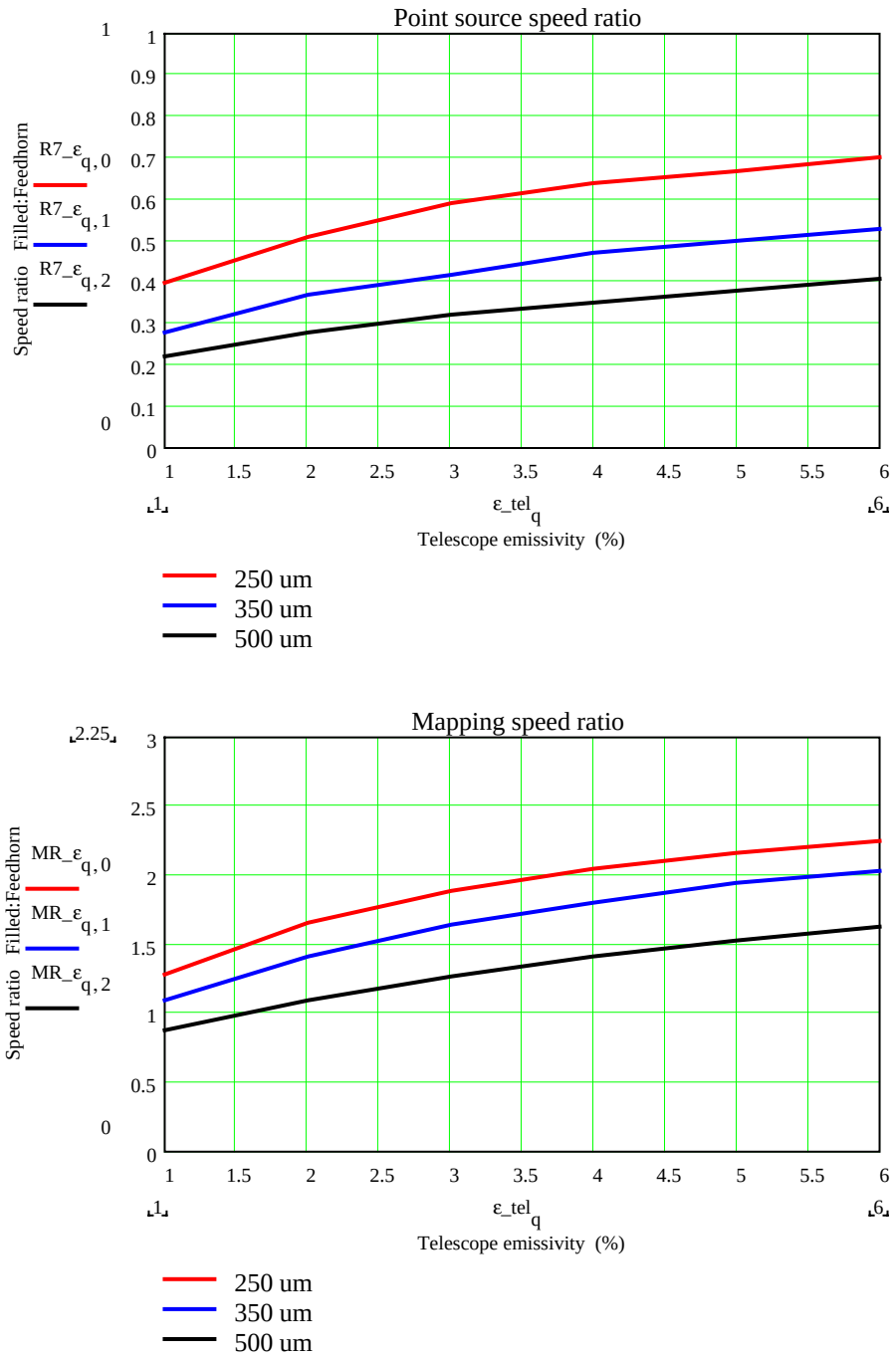

Fig. 6: Point source observing speed (7-point case) and mapping speed ratios vs. telescope emissivity for a fixed NEP_{det_H} = 3 x 10^{-17} W $Hz^{-1/2}$. All other parameters are at their nominal values.

6.3.3 Feedhorn point source coupling efficiency

The nominal value of η_{pix_H} is 0.7. The effect of adopting higher or lower values is shown in Fig. 7 (where the detector NEP has been fixed at $NEP_{det} = 3 \times 10^{-17}$ W $Hz^{-1/2}$ for all detectors). The ideal calculated value for SPIRE is 0.74. (The theoretical optimum, for perfect coupling to the aperture, is in excess of 0.8.)

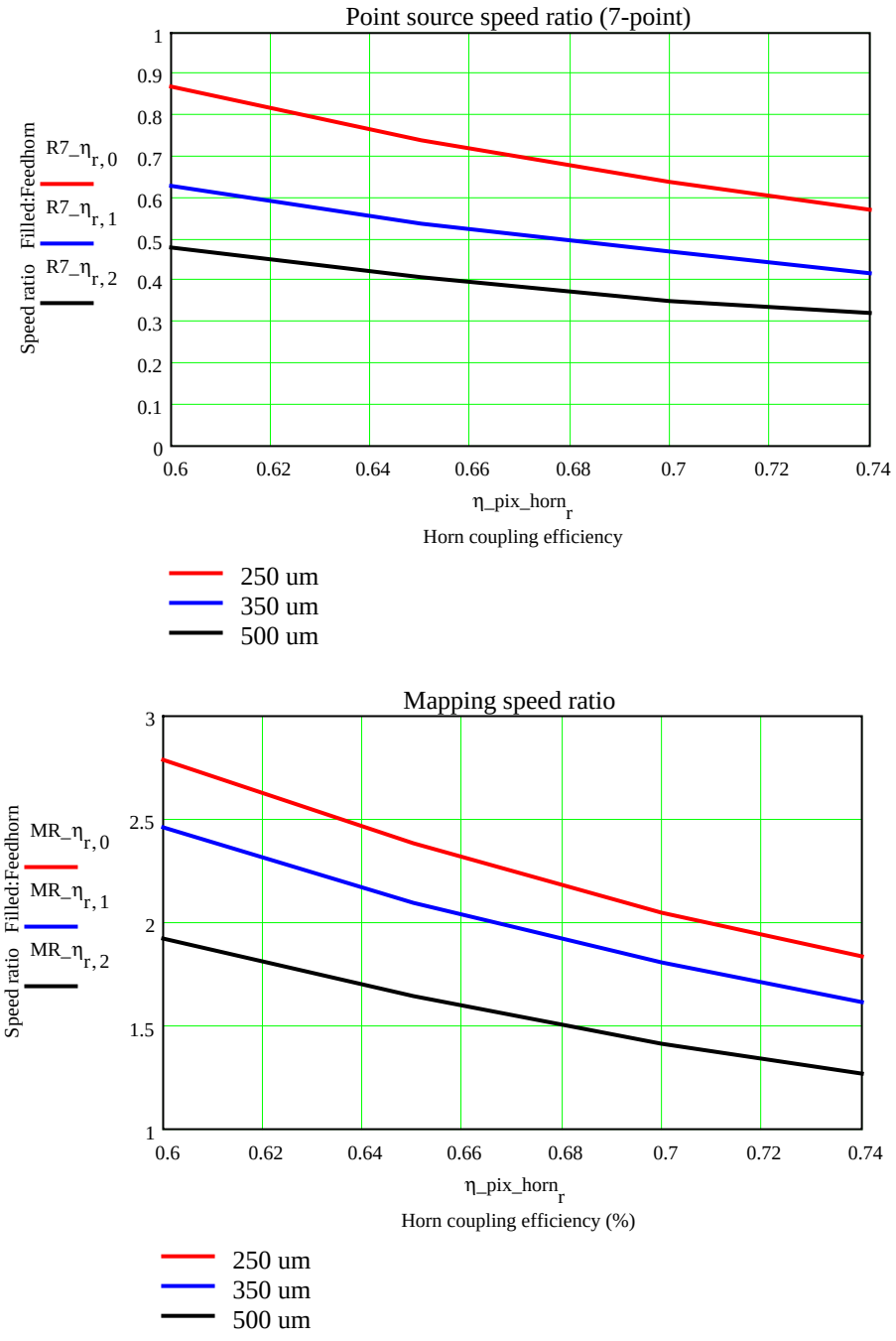

Fig. 7: Point source observing speed (7-point case) and mapping speed ratios vs. feedhorn point source coupling efficiency for a fixed $NEP_{det} = 3 \times 10^{-17}$ W $Hz^{-1/2}$. All other parameters are at their nominal values.

6.3.4 Feedhorn effective throughput

The nominal value of the feedhorn effective throughput is $0.8\lambda^2$. The effect of adopting different values is shown in Fig. 8 for the nominal case. Increasing α improves the relative performance of the filled array as the feedhorn picks up more background without picking up any more source signal. In practice, an increase in α would probably be accompanied by an increase in η_{pix_H} which would offset this effect.

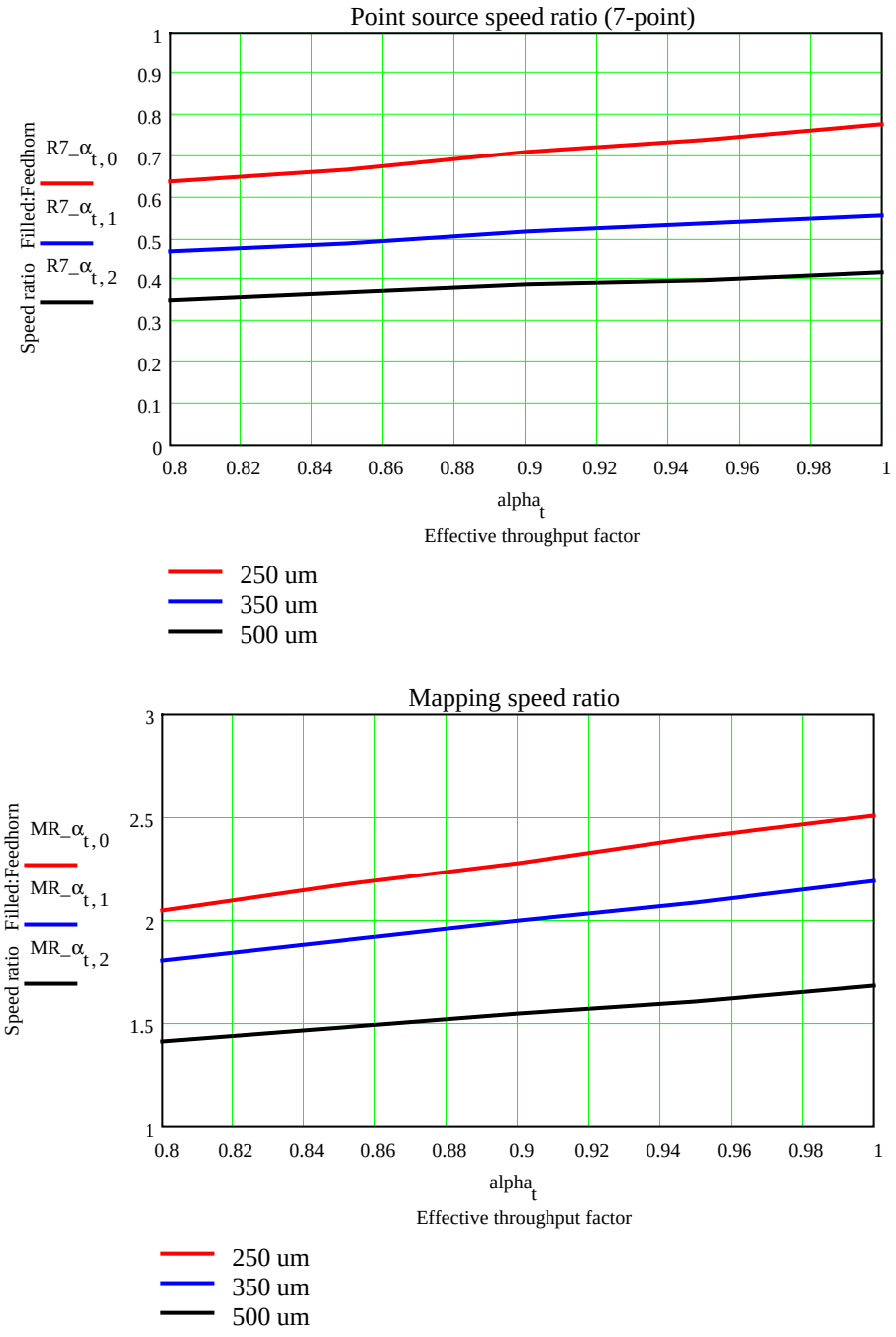

Fig. 8: Point source observing speed (7-point case) and mapping speed ratios vs. feedhorn effective throughput factor, α, for a fixed $NEP_{det} = 3 \times 10^{-17}$ W $Hz^{-1/2}$. All other parameters are at their nominal values.

6.3.5 Filled array inter-pixel gap

The nominal value of the gap between pixels has been taken to be 70 μm (appropriate for the CEA arrays). The effect of adopting higher or lower values is shown in Fig. 8 (NEPdet = 3 x 10^{-17} W $Hz^{-1/2}$ for all detectors).

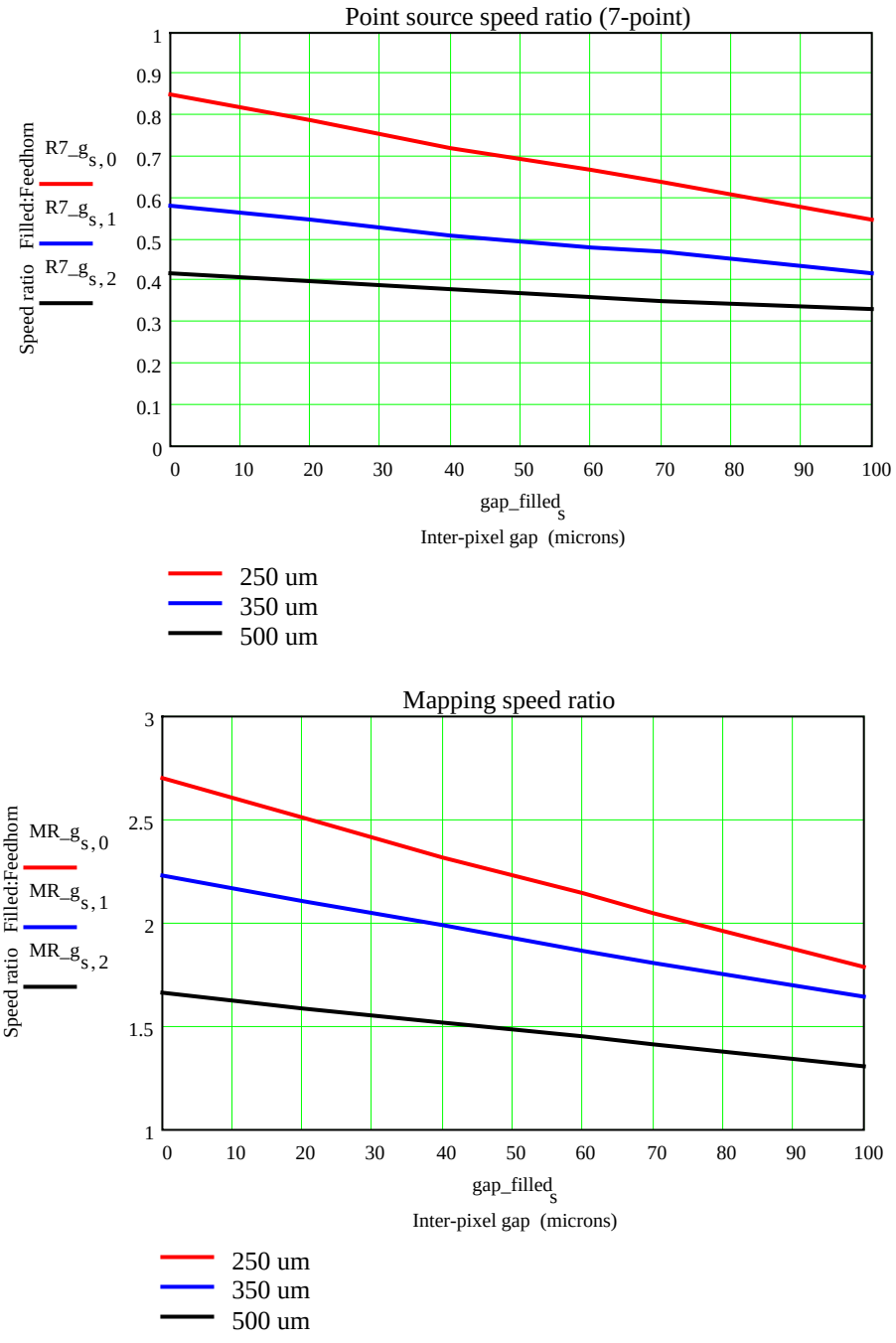

Fig. 9: Point source observing speed (7-point case) and mapping speed ratios vs. filled array inter-pixel gap for a fixed NEP_{det} = 3 x 10^{-17} W $Hz^{-1/2}$. All other parameters are at their nominal values.

7. SPIRE constraints and their implications

7.1 Scanning mode observations for deep surveys

For scanning mode observations, the telescope is scanned continuously at a rate such that:

- the maximum value of 60" per second is not exceeded;
- the signal information is encoded at frequencies high enough to be unaffected by any 1/f noise;
- the effects of finite detector speed of response are negligible.

If 1/f noise is a problem, then signal modulation by chopping or "dithering" must also be performed by the Beam Steering Mirror. (As noted above, this increases the confusion noise for deep survey observations unless the individual samples are transmitted to the ground.) To illustrate the need for signal modulation in the presence of 1/f noise, Appendix C presents an example of the results of a simplified simulation of scanning mode observations *without* such modulation. In this simulation:

- One 250-μm detector is scanned in a straight line.
- The scan rate is assumed to be the maximum of 60"/second to minimise the influence of 1/f noise. The detector speed of response is assumed to be sufficiently fast that this results in no distortion of the sky signal timeline.
- The detector trajectory includes a point source of specified strength which is manifested as a Gaussian signal timeline when convolved with an assumed 18" Gaussian beam profile on the sky. Other than this one source, the sky signal is assumed to be zero.
- Noise with a specified 1/f knee frequency is added to the signal timeline.
- The resultant noisy timeline is sampled at 7 Hz (appropriate for the filled array case)
- The signal is extracted by fitting a Gaussian plus linear baseline to a portion of the timeline around the source position (nominally one second of data on each side). This is done for various 1/f knee frequencies.
- The S/N ratios are estimated by running the simulation a number of times with different random noise timelines and calculating the rms fluctuation in the fitted amplitude.
- The S/N and corresponding mapping speed are then plotted as a function of the 1/f knee frequency to estimate the degradation in performance resulting from 1/f noise.

Fig. 10 shows the mapping speed degradation at 250 and 500 μm as a function of the 1/f knee frequency for a sampling frequency of 7 Hz. Choosing a higher value for the sampling rate made no significant difference. Mapping speed loss is worse at 500 μm because the larger beam width leads to a longer beam crossing time - the signal frequencies are lower and so more susceptible to 1/f noise.

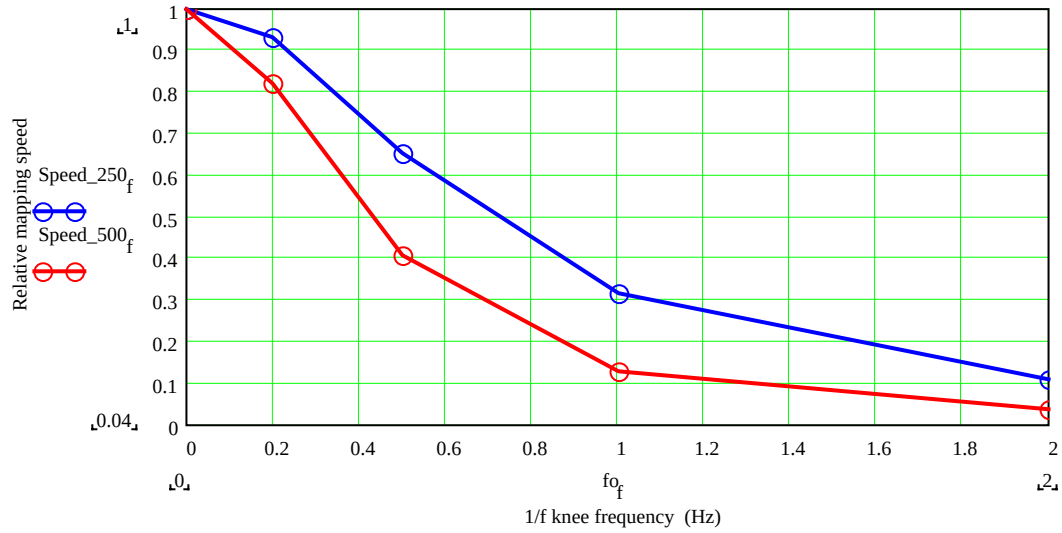

Fig. 10: Normalised mapping speed vs. 1/f knee frequency for scan mapping at 250 μm (blue) and 500 μm (red), based on simulations detailed in Appendix C.

Note: these results are independent of the array type - they give the relative loss of mapping speed per detector for a given 1/f noise knee compared to whatever is achieved by that detector in the case of a purely flat noise spectrum.

These simulations show that simple scanning mode observations are highly vulnerable to 1/f noise. Unless the 1/f knee frequency can be kept well below 1 Hz (likely to be possible only with NTD Ge detectors), this mode will not be usable without severe degradation of mapping speed. The only way to overcome this problem is to chop or "dither" while scanning. With a maximum available dithering frequency of 5 Hz, the scan rate must be less than 20 arcsec./sec, as shown in Appendix D. Note that once dithering or chopping is being implemented, it is not a fundamental requirement that the telescope also be scanned. It may be stepped (raster map mode) so that data are not taken while it is in transition between positions. In that case there will be an additional overhead associated with the telescope settling time at each new pointing. The best approach may be to scan very slowly (say, 0.1 arcseconds/second) to void telescope re-pointing overheads.

In any event, the chopping/dithering must be done at a frequency high enough to keep the signal frequency well above the 1/f regime. Currently the expected 1/f knee frequencies for the three options are:

Feedhorns with NTD Ge bolometers:	< 100 mHz
Filled array with TES bolometers:	~ 1 Hz
Filled array with CEA detectors:	Uncertain but expected to be > 1 Hz

Two consequences of this are:

(i) For the filled array, dithering/chopping must be carried out when doing deep surveys. (This may even be advisable for the feedhorn option to avoid some loss of mapping speed at 500 μm.)

(ii) For the feedhorn option, failure of the BSM would not seriously degrade the performance of the photometer for mapping, because it is not necessary to use it for signal modulation when scanning. For the filled array options, however, it would have a serious impact on performance (unless the 1/f noise for the filled array detectors can be made comparable to that for NTD Ge). This is because it would not be possible to scan the telescope fast enough to avoid the 1/f noise of the detectors.

Additional notes: It has been pointed out by Harvey Moseley and Kent Irwin that the effect of 1/f noise can be less than modelled here if an optimal filter (determined by the Gaussian point source signal template and the 1/f noise spectrum) is applied to the data. Time does not permit this to be studied in detail, but here are two comments on this for discussion:

(i) I guess that the basic conclusion is still valid that simple unmodulated scanning in the presence of 1/f will result in a severe loss of sensitivity, and that some modulation scheme must therefore be implemented to overcome any significant 1/f noise.

(ii) Although application of an optimal filter should result in better extraction of the point source signal, to what extent does this rely on good sampling of the timeline? With the filled array detectors, the sampling will actually be quite sparse (~ 7 Hz), so I'm not sure it this would be practicable. In the analogous case of infinitely small pixels, there is a lot to be gained in principle from applying an optimal filter in gaining S/N on a point source, but it turns out to be very little when one is only just critically sampled (see Section 5.2).

7.2 1/f noise and BSM spatial modulation frequency

Spatial modulation must be carried out by the BSM to generate signal frequencies high enough to be largely unaffected by 1/f noise. Assume that

(i) the noise is made up of two uncorrelated components, white noise plus pure1/f noise with a knee frequency f_{knee};
(ii) the detector frequency response is characterised by a 3-dB frequency f_{3dB}.

The S/N, normalised to the zero-frequency value for no 1/f noise, is then

$$\sigma(f) = \left[\left[1+\left[\frac{f}{f_{3dB}}\right]^2\right]\left[1+\left[\frac{f_{knee}}{f}\right]^2\right]\right]^{-1/2} , \qquad (27)$$

where f is the chopping frequency. The corresponding relative mapping speed is the square of this:

$$\text{Speed}(f) = \left[\left[1+\left[\frac{f}{f_{3dB}}\right]^2\right]\left[1+\left[\frac{f_{knee}}{f}\right]^2\right]\right]^{-1} . \qquad (28)$$

This is plotted in Fig. 11 for knee frequencies in the range 0.1 - 5 Hz for the cases of a detector with a 3-dB frequency of 20 Hz and 100 Hz.

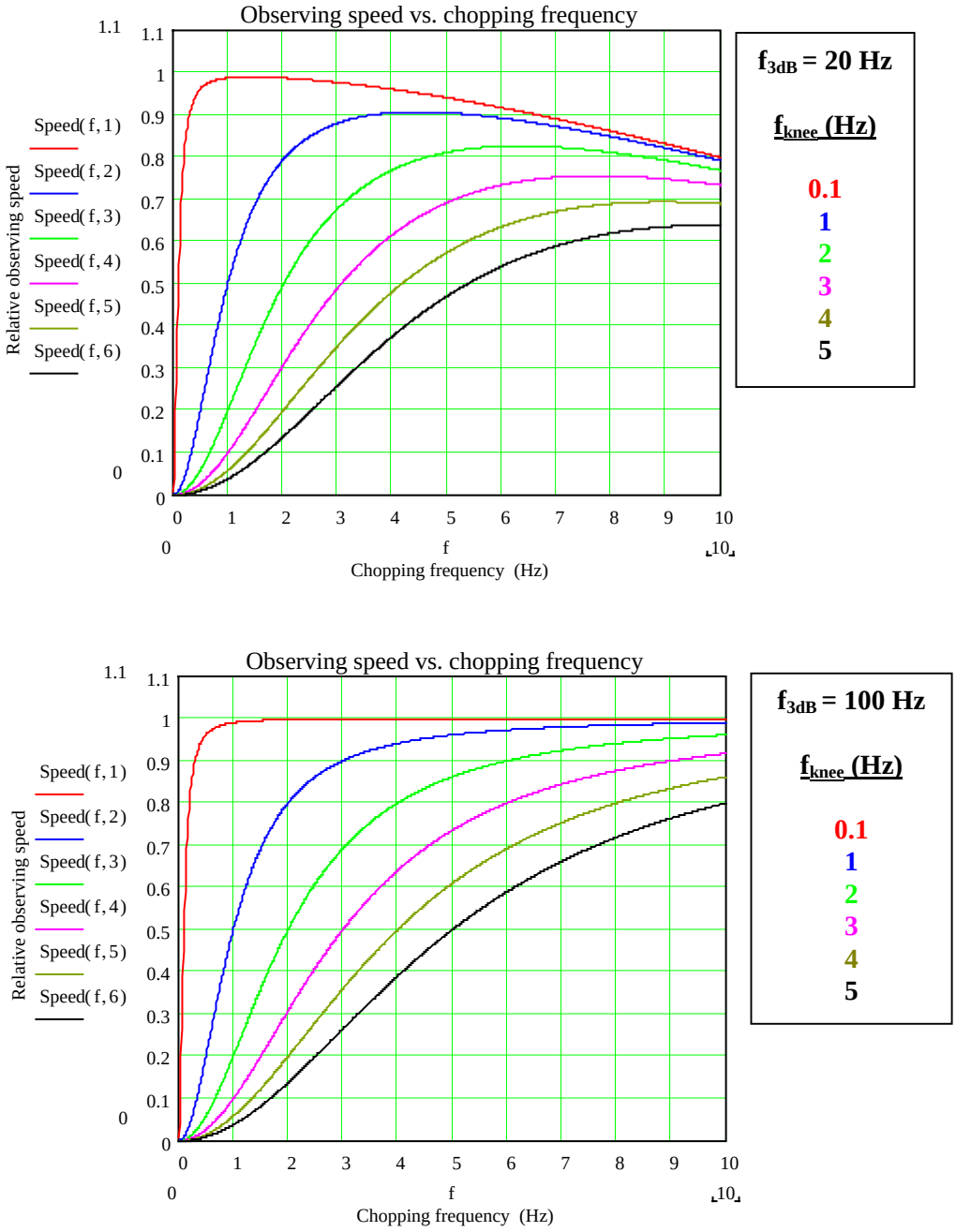

Fig. 11: Normalised observing speed vs. chopping frequency for various values of 1/f knee frequency. The responsivity is assumed to roll off with a 3-dB frequency of 20 Hz (upper plot) and 100 Hz (lower plot).

For a 20-Hz detector (SPIRE specification), assuming the maximum chopping frequency (5 Hz) and no dead time due to the chopping process, there is a 10% loss of observing speed for f_{knee} = 1 Hz and ~ 20% for f_{knee} = 2 Hz. If the 1/f knee is as high as 5 Hz, then the loss in speed is about a factor of two.

7.3 Point source extraction and confusion noise

The following section is rather inconclusive at present. It is based partly on discussions I have had with various people. I would like all of the array groups to consider the issues raised here and, hopefully, to help establish clearly what is and is not possible when it comes to point source extraction:

- avoiding additional confusion noise due to sky signal differencing, either on board or on the ground
- eliminating 1/f noise
- observing modes and constraints

The fundamental questions (I think) are:

1. Does eliminating extra confusion noise require us to produce a total power map of the sky?

2. If so, is it possible to do this

(a) with filled array detectors for which chopping/dithering is needed;
(b) with feedhorn detectors for which chopping/dithering is probably not needed?

7.3.1 Filled arrays

For chopping/dithering with a filled array, the chop throw/dither steps must be kept small to avoid losing too much of the 4 x 8 arcminute field area. The undifferenced frames contain 1/f noise, so differencing is unavoidable to get rid of it. Differencing between sky observations worsens confusion noise. A possible way of getting around this would be to adopt the proposal that Harvey Moseley has made, to surround the field by a "calibration strip" designed to replicate the dilute 80-K telescope spectrum, as shown in Fig. 12. Pixels near the perimeter can be manoeuvred onto the surround by the BSM. The surround mimics the telescope background and is assumed to be uniform and stable in temperature and emissivity. The corresponding signals from the peripheral pixels that see it *contain no confusion noise component*. So maybe they could be used as reference levels and propagated across the array by some algorithm. But can this be done practically? There will only be a few measurements of the reference source around the edge of the field, and propagating these faithfully all the way to the centre would require great accuracy in the knowledge the response of all the array pixels. Is there a <u>proven</u> observing mode and algorithm that will do this while at the same time eliminating any loss of sensitivity due to 1/f noise? Can we build such a calibrator with the required temperature stability? What loss of field area would we need to suffer to make it feasible?

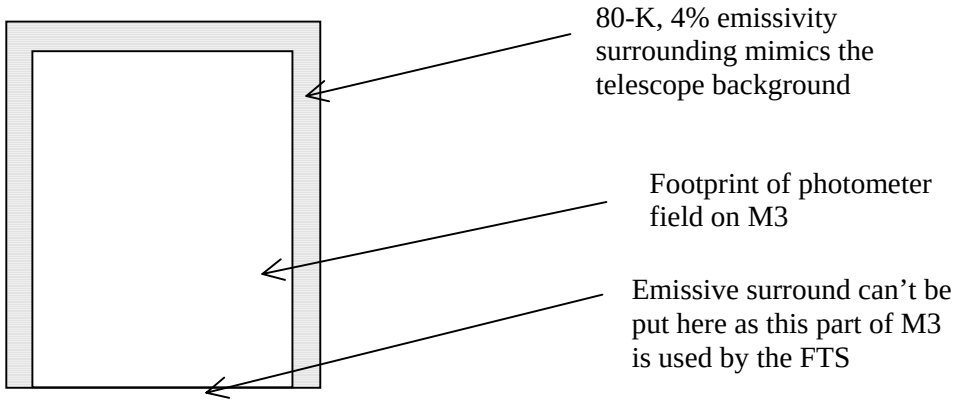

Fig. 12: Surrounding M3 by a "calibration strip" to mimic the telescope background and provide an unconfused reference level.

7.3.2 Feedhorn arrays

In my simple scheme, one extracts point sources by comparing the signals with those from patches of sky that are observed close in time, to avoid 1/f coming in. So differencing is still being done. One would like to establish a baseline by using the mean level of a *long* strip scan with the detector - the longer the better as this averages out the confusion noise. But the longer one makes it the more susceptible one is to 1/f noise even at very low frequencies.

When scanning in total power mode, one can remove an offset and slope, effectively filtering out information on the largest angular scales. The "difference" beam is averaged over the strip, and so should introduce negligible confusion noise as long as the strip is long enough - so that that the "off" beam is averaged over a large number of sky positions. More generally, one can high-pass filter the time stream data rather than taking out slope and offset, without losing much sensitivity to point sources.

The baseline level for mapping of very extended regions can also be established by this technique provided one can get some “blank” sky on either side of the source emission.

To estimate the possibility of establishing the baseline level using a long strip, the performance for point source extraction has been computed as a function of the baseline interval, using the method described in Section 7.1 above. This has been done for three cases: 1/f knee frequency = 50 m Hz, 100 mHz, and 1 Hz. The results (based on the statistics of 300 or more trials in each case) are summarised in Fig. 13 a-c. The plots are all normalised to the values for a baseline interval of 1.5 seconds (i.e., 0.75 seconds on each side of the peak).

For the case of f_{knee} = 50 mHz, baselines of 60 sec or more are feasible. For f_{knee} = 100 mHz, the baseline can be up to 25-30 seconds without any compromise to the sensitivity.

The best sensitivity is obtained for a baseline interval that represents a compromise between the detector 1/f noise and the averaging out of the noise in estimating the baseline. Generally, the longer the interval, the more accurately the baseline can be defined; but if the interval is to long, then the detector 1/f noise begins to have an effect.

Although this simulation is very simplistic in that no confusion noise is incorporated, it is indicative of the limitations on baseline interval imposed by the detector system itself. An interval of 20 seconds corresponds to 1200 arcseconds, the equivalent of around 60 beams at 250 μm, so the confusion noise could be averaged down over that sort of scale in the case of the feedhorn option Ideally, we would return to the same piece of sky in a drift scan, as will be done by Planck every one minute (with NTD Ge detectors) in order to remove the slope and offset from the bolometer signals - this would not filter the data at all. It could be implemented for SPIRE in principle, but would require coping with the 10-20 second overhead associated with telescope repointing when raster or line scanning. The 1/f stability would need to be at the 50 mHz level or less to make this feasible.

This analysis also shows again why straightforward scanning is not an option if the1/f noise knee frequency is too high. For f_{knee} = 1 Hz, any increase in the interval beyond 1 second results in severe degradation in performance due to the 1/f noise corrupting the baseline estimation. In fact, 1/f noise is already having a serious effect on the sensitivity, even for the shortest feasible baseline intervals.

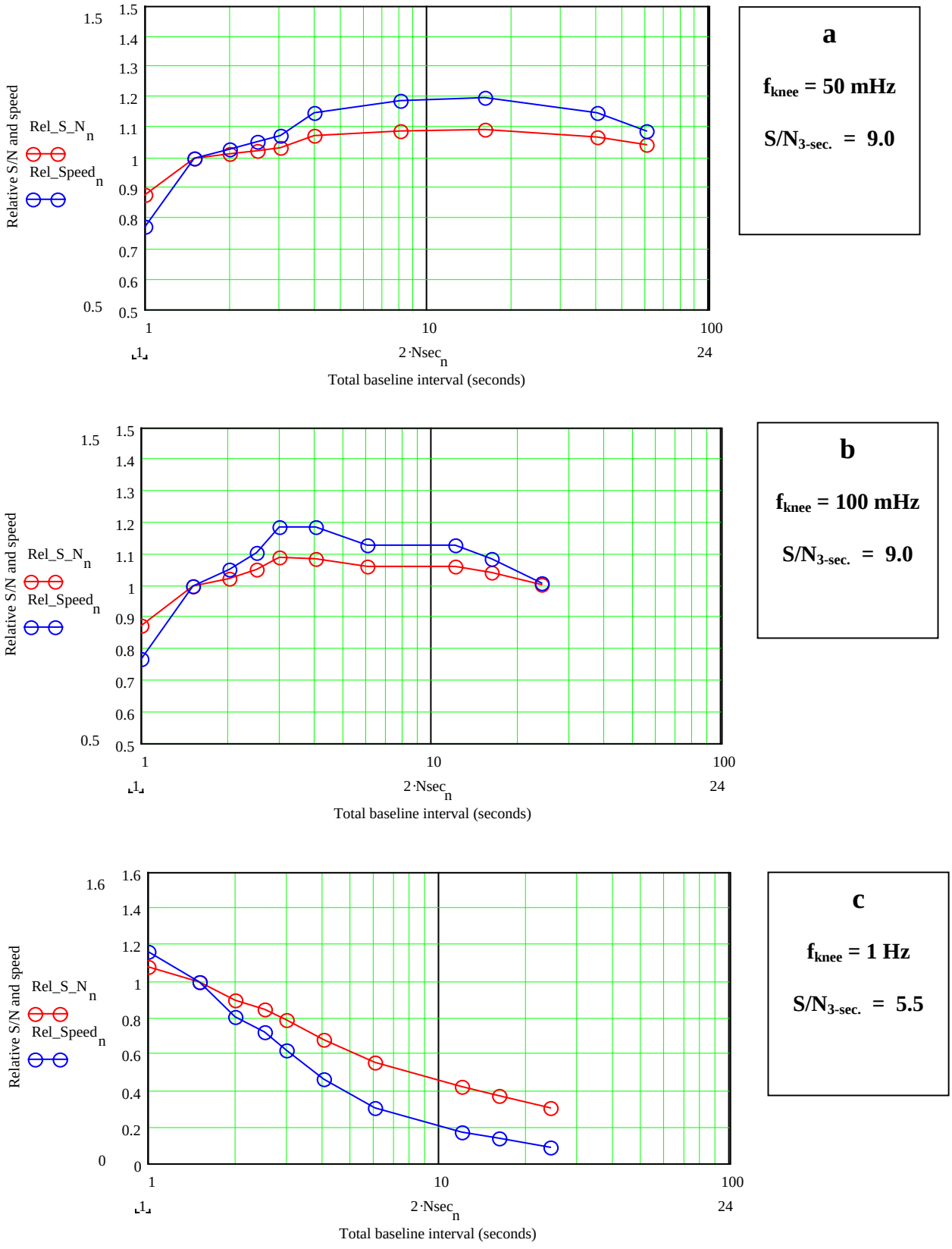

Fig. 13: Relative S/N and speed as a function of the time interval used to determine the baseline for 1/f knee frequencies of 50 mHz, 100 mHz, and 1Hz.

7.4 Data rate

Data will be transmitted by the FIRST spacecraft to the ground station during a nominal 2-hr period every 24 hrs, with the FIRST antenna pointed towards the Earth. Observations may be feasible during the telemetry dumping period, but only over a very limited part of the sky. We assume here that the instruments can effectively observe for 22 hrs out of every 24.

The available telemetry rate for SPIRE and the other instruments is 100 kbs averaged over a 24 hour period. A higher instantaneous data transfer rate from the instrument to the on-board mass memory can be used provided the total capacity is not exceeded. The data rate needs of the various SPIRE observing modes are described in *SPIRE Detector Sampling Scheme and Data Rate* (which is an appendix of the *Operating Modes of the SPIRE Instrument - OMD*). An updated version of the data rate note is appended below as Appendix D. It now includes an assessment of the data rate needs for scanning mode, which requires telemetering of undifferenced samples to avoid increasing confusion noise. **It is clear that, for the filled array options, there are problems in working within the available data rate - these should be addressed by the filled array groups for the array selection.**

A discussion at QMW on Jan. 6 (Present: Matt Griffin, Raul Hermoso, Louis Rodriguez, Rick Shafer, Bruce Swinyard) resulted in the following conclusions/questions (as noted by MJG - others please correct any misconceptions):

1. The "dithering" technique proposed by GSFC is expected to be more effective (by ~ 30-40%) than simple chopping in recovering the sky signal. It involves motions on a variety of spatial scales (not just a constant chop amplitude). It is designed to break the degeneracy between spatial variations (the sky) and temporal variations of the whole system, especially its 1/f noise. This is a generic technique (applicable also to the feedhorn array if desired, although the high 1/f stability of the NTD detectors means that it will not be essential).

2. The BSM is not so fast in moving in the "jiggle" axis as the moment of inertia is much higher than for the "chopping" axis. GSFC regard this as non-ideal, but not a major problem.

3. Section 7.2 above implies that the dithering frequency should be around 3 times the 1/f knee frequency of the system 1/f noise. Even this involves a 10% loss in mapping speed even for 100-Hz detectors. If we reduce it to only twice the 1/f knee, the mapping speed loss is 20% for a fast detector and more for a slower (20 Hz) detector.

4. A question concerning dithering or chopping to remove 1/f noise: is there any fundamental difference between the two cases below.

Let the 1/f noise knee frequency, f_{knee}, be about the same for all detectors, **but**:

(i) assume we have 1/f noise which is present in the detector timelines but **not** correlated across the array;

(ii) assume we1/f noise which **is** correlated across the array.

The question is the same for both situations: at what minimum frequency must we chop or dither to take out all the 1/f noise?

Is the answer $>3f_{knee}$ in both cases or is it less than $3f_{knee}$ for case (ii)?

5. The data rate problem (need for over 400 kbs to transmit uncompressed photometer data to the ground at 7 Hz sampling rate per detector) is essentially the same for both of the filled array options. The method of compression proposed by GSFC is as follows:

- Store on board a sequence of N images, $Image_j$, (image = one computed sample per detector) generated at $2F_{dither}$ Hz (e.g., 10 Hz for a 5-Hz dither or chop).

- Compute on board the mean of the sequence, M, and transmit this to the ground.

- Transmit also the differences ($Image_j$ - M). **As long as the images are not very different from each other**, then a much smaller number of bits should be adequate. On the ground, the N original images can be reconstructed with no loss of data.

If this method is capable of achieving a lossless compression factor of close to 4, then the filled array options will be essentially compatible with the available data rate. It is proposed that it be studied and presented at the selection meeting by someone from GSFC as a proposed solution agreed for either of the filled array options, if selected.

Appendix E is a note by Bruce Swinyard analysing the degree of compression that might be available using this technique.

An alternative approach will be described by Harvey Moseley at the selection meeting.

6. GSFC are strongly in favour of the "calibration strip" idea, regardless of the chosen detector option.

7.5 Susceptibility to microphonics

For simple scanning observations without dithering (feedhorn option), there is signal information across a broad band of frequencies, and the noise spectrum must be free of any excess noise features (due, for instance, to microphonics). No SPIRE mechanisms would be in operation, and the only source of vibration should be the spacecraft reaction wheels. The same applies to observations made by dithering without chopping (as in the SCUBA "DREAM" mode), in which the BSM is moved in a certain pattern which does not involve systematic chopping of the beam between two positions. In this case, the SPIRE BSM will be operational and will represent a possible source of microphonics.

7.6 Susceptibility to stray radiation

The field of view of a filled array pixel is much broader than for the feedhorn-coupled detector, which makes it more vulnerable to stray radiation. The relative susceptibilities of the two detector types to in-band stray light can be estimated as follows. Assume that the susceptibility is proportional to the throughput, $A\Omega$. For the feedhorn-coupled detector, $A\Omega_H = \lambda^2$. Assuming a field of view of π Sr. for the filled array pixel, its throughput is $A\Omega_F = (0.5F\lambda)^2(\pi)$. The filled array pixel is therefore $\pi F^2/4$ times more vulnerable to in-band stray light. For SPIRE, F = 5, so this is a factor of 20. Stray radiation must therefore be suppressed much more effectively for the filled array option than for the feedhorn option. Suppression of stray radiation in submillimetre instruments is often problematical, so this is a challenge for the opto-mechanical design.

For out-of band stray radiation at short wavelengths, the field of view of the feedhorn is rather broader, so its advantage over the filled array pixel in this respect is reduced. Stray light at low frequencies will be rejected by the waveguide section between the feedhorn and the detector. The response of the filled array pixel will also be reduced as the grid/reflector structure becomes de-tuned.

8. Filled arrays with larger pixels

It is possible with a filled array to use a pixel size larger than $0.5F\lambda$ could be used. There could be a number of reasons for doing this:

(i) The 250 and 350 μm arrays could be implemented with the same pixel size designed to be $0.5F\lambda$ at 300 μm. If this compromise makes little difference to the scientific performance, it might be justified on the grounds of simplicity and cost reduction.

(ii) The pixel size could be increased in order to reduce the total number of detectors. This would reduce power dissipation at 0.3 K, complexity and cost of the warm electronics, and data rate.

The viability of such options depends on whether or not they result in any unacceptable change in angular resolution, mapping speed or operating modes.

In this section, we analyse two cases: the 300 μm compromise as above, and the case where 1Fλ pixels are used.

8.1 Single array design for 250 and 350 μm

Assume that the filled array detector size is 0.5Fλ at 300 μm. Its sizes for the 250 and 350 μm bands are then 0.58Fλ and 0.42Fλ, respectively. The array sizes are changed from 32 x 64 and 24 x 48 to a common format of 28x56. The total number of detectors for the photometer is 3648 instead of 3712.

8.1.1 Effect on the beam size

A full calculation of the SPIRE beam profiles for this option has not been done. However, a reasonable assessment can be made by simply convolving the square pixel with the Airy disk and comparing the 0.5Fλ case with the slightly smaller or larger pixel case. This has been done, and the results (see Appendix F) show that there is a only very slight (< 2 %) broadening of the beam.

8.1.2 Effect on observing speed

The observing speeds have been calculated in the same way as before, and the results are summarised below for the case of a detector NEP of 3 x 10^{-17} W $Hz^{-1/2}$ for both options.

λ (μm)	Mapping speed ratio for surface brightness	Point source observing speed ratio (on-axis)	Point source observing speed ratio (7-point with feedhorn)	Mapping speed ratio for point source extraction
λ_i	$B\_Speed\_Ratio_i$	$S\_Speed\_Ratio\_On\_Axis_i$	$S7\_Speed\_Ratio_i$	$Speed\_Ratio\_Map\_Point_i$
250	2.41	0.43	0.73	2.47
350	1.34	0.29	0.38	1.55
500	1.30	0.31	0.35	1.41

These results should be compared with the equivalents for the 0.5Fλ option in Section 6.2. It can be seen that this option produces slightly better filled array performance at 250 μm, where the pixels are oversized, and slightly worse at 350 μm, where they are undersized. For the case where the filled array NEP is NEP_{det} = (3 x 10^{-17})*$2^{0.5}$ W $Hz^{-1/2}$, and 3 x 10^{-17} W $Hz^{-1/2}$ for the feedhorn array detectors, we get:

λ (μm)	Mapping speed ratio for surface brightness	Point source observing speed ratio (on-axis)	Point source observing speed ratio (7-point with feedhorn)	Mapping speed ratio for point source extraction
λ_i	$B\_Speed\_Ratio_i$	$S\_Speed\_Ratio\_On\_Axis_i$	$S7\_Speed\_Ratio_i$	$Speed\_Ratio\_Map\_Point_i$
250	1.89	0.34	0.57	1.95
350	0.86	0.19	0.25	1.00
500	0.80	0.19	0.22	0.88

So in this case there is no theoretical mapping speed advantage except at 250 μm.

8.1.3 Other considerations

Data rate: the impact is negligible since the total number of detectors is nearly the same.

Stray light susceptibility: this scales with pixel area, so the 250 μm arrays will be relatively *more* susceptible by a factor of $(250/300)^2$ = 0.7 and the 350 250 μm arrays will be relatively *less* susceptible by a factor of $(350/300)^2$ = 1.4.

Observing modes: For the 250 μm array, the instantaneous image will not be quite fully sampled, and there will be a corresponding oversampling at 350 μm. This would need to be accommodated in the scanning/dithering strategy. There is probably some advantage to be gained from having the 250 and 350 μm arrays exactly overlaid on the sky.

8.1.4 Conclusions

Overall, the results for this option are not hugely different to those for the nominal case.

8.2 Filled array with 1.0Fλ pixels

Assume that the filled array detector size is 1.0Fλ at all wavelengths. The array sizes are changed from 32 x 64, 24 x 48, and 16 by 32 to a common format of 16 x 32, 12 x 24 and 8x16. The total number of detectors for the photometer is 928 instead of 3712, a factor of 4 reduction.

8.2.1 Effect on the beam size

A full calculation of the SPIRE beam profiles for 1.0Fλ pixels has not been done. However, as before, we can reasonable assessment can be made by convolving the square pixel with the Airy disk and comparing the 0.5Fλ and Fλ. This has been done, and the results (see Annex D) show that the beam is broadened by about 14% compared to the 0.5Fλ value. This would result in FWHM values as follows:

λ (μm)	FWHM (arcseconds)		
	0.5Fλ filled pixel	**2.0Fλ feedhorn**	**1.0Fλ filled pixel**
250	16.5	17.1	18.8
350	23.1	24.4	26.3
500	32.8	34.6	37.4

8.2.2 Effect on observing speed

The observing speeds have been calculated in the same way as before, and the results are summarised below for the case of a detector NEP of 3 x 10^{-17} W $Hz^{-1/2}$ for both options.

λ (μm)	Mapping speed ratio for surface brightness	Point source observing speed ratio (on-axis)	Point source observing speed ratio (7-point with feedhorn)	Mapping speed ratio for point source extraction
λ_i	$B\_Speed\_Ratio_i$	$S\_Speed\_Ratio\_On\_Axis_i$	$S7\_Speed\_Ratio_i$	$Speed\_Ratio\_Map\_Point_i$
250	2.89	0.59	0.99	1.86
350	2.82	0.60	0.78	1.77
500	2.59	0.60	0.69	1.60

These results can also be compared to those for the 0.5Fλ case given in Section 6.2. For surface brightness mapping and known point source detection,1.0Fλ is better than 0.5Fλ by a factor of between 1.6 and 2 depending on the wavelength. For extraction of point sources from maps, the changes are small compared to the 0.5Fλ case - a bit worse at 250 μm, about the same at 350 μm and a bit better at 250 μm.

Comment: one reason why the relative sensitivity doesn't degrade so much with the bigger pixels is that the photon noise limit is now a lot higher due to the extra background on the larger pixel. This means that the detectors (with an NEP of 3×10^{-17} W $Hz^{-1/2}$ are now closer to being photon noise limited).

If the filled array detectors do not achieve an NEP as low as 3×10^{-17} W $Hz^{-1/2}$, then, as before, the relative speed is slower. The results for NEP $(3 \times 10^{-17}) * 2^{0.5}$ W $Hz^{-1/2}$ are summarised below.

λ (μm)	Mapping speed ratio for surface brightness	Point source observing speed ratio (on-axis)	Point source observing speed ratio (7-point with feedhorn)	Mapping speed ratio for point source extraction
λ_i	$B\_Speed\_Ratio_i$	$S\_Speed\_Ratio\_On\_Axis_i$	$S7\_Speed\_Ratio_i$	$Speed\_Ratio\_Map\_Point_i$
250	2.60	0.53	0.89	1.67
350	2.41	0.51	0.67	1.51
500	2.03	0.47	0.54	1.26

8.2.3 Other considerations

Data rate: the photometer data rate is a factor of four lower, and is basically compatible with the available telemetry budget.

Stray light susceptibility: the pixel area is four times larger, so the stray light susceptibility is greater. Adopting the same method as in Section 7.6, we find that the filled array pixels are approximately 80 times more vulnerable to in-band stray light than the feedhorn-coupled detectors. This make the optical design and filtering correspondingly more challenging.

Observing modes: The filled arrays no longer fully sample the image. As for the feedhorn array, a fully-sampled image must be created by scanning or jiggling.

8.2.4 Conclusions

The major advantage of this option is the lower number of detectors. Disadvantages are the higher vulnerability to stray light and some loss of angular resolution.

Appendices:

A Observing speed computation for filled and feedhorn options
B Simulations of scanning observations (without dithering)
C Revised data rate note
D Beam profile broadening for filled array pixels bigger than $0.5F\lambda$
E Updated SPIRE photometer sensitivity model
F Note by Bruce Swinyard on frame compression for the filled array option

Appendix A

Observing speed computation for filled and feedhorn options

Observing_Speed_Jan24.mcd

Matt Griffin 24 Jan 2000

origin := 1

This worksheet estimates the observing speed for the filled array and feedhorn options for SPIRE, based on the analysis given in *Observing speed for SPIRE filled array and feedhorn options* by Matt Griffin

Filter bandwidths have been updated to agree with BOLPH_8
Tabulation of sensitivity of the results to various assumed parameters has been added

All quantities in SI units unless otherwise specified

Fundamental constants

$h := 6.626 \cdot 10^{-34}$ $c := 3 \cdot 10^{8}$ $kb := 1.3806 \cdot 10^{-23}$

Planck function

$$B(nu,T) := \frac{2 \cdot h \cdot (nu)^3}{c^2 \cdot \left[e^{\left(\frac{h \cdot nu}{kb \cdot T} \right)} - 1 \right]}$$

Telescope and instrument properties

Telescope temperature and emissivity

$T \equiv 80$ $\varepsilon tel \equiv 0.04$

Telescope area

$Atel \equiv \frac{\pi \cdot 3.28^2}{4}$ $Atel = 8.45$

Transmission to detector

$\eta opt \equiv 0.3$

λ/Δλ of filters

$R := 3$

Final optics focal ratio

$F := 5$

Band number, central wavelengths and frequencies

$i := 1, 2 .. 3$

i = 1 : 250
i = 2 : 350
i = 3 : 500

$\lambda_i :=$

250
350
500

$\nu_i := \frac{c}{10^{-6} \cdot \lambda_i}$

λ_i	ν_i
250	$1.20 \cdot 10^{12}$
350	$8.57 \cdot 10^{11}$
500	$6.00 \cdot 10^{11}$

Filter passbands: lower and upper frequencies and passband widths

$\nu_i := \frac{c}{\lambda_i \cdot 10^{-6}}$ $\lambda L_i := \lambda_i - \frac{\lambda_i}{2 \cdot R}$ $\lambda U_i := \lambda_i + \frac{\lambda_i}{2 \cdot R}$ $\Delta\lambda_i := \frac{\lambda_i}{R}$ $\Delta\nu_i := \frac{\nu_i}{R}$

$\nu min_i := \frac{c}{\lambda U_i \cdot 10^{-6}}$ $\nu max_i := \frac{c}{\lambda L_i \cdot 10^{-6}}$

i	λ_i	λL_i	λU_i	$\Delta\lambda_i$	$\nu_i \cdot 10^{-9}$	$\nu min_i \cdot 10^{-9}$	$\nu max_i \cdot 10^{-9}$	$\Delta\nu_i \cdot 10^{-9}$
1	250	208	292	83	1200	1029	1440	400
2	350	292	408	117	857	735	1029	286
3	500	417	583	167	600	514	720	200

Detector properties

Filled array detector centre-centre spacing

$pix\_spacing_i := 0.5 \cdot F \cdot \lambda_i$

Horn array centre-centre spacing

$horn\_spacing_i := 2.0 \cdot F \cdot \lambda_i$

Inactive gap between pixels for filled array

$gap := 70$ μm

Gap in units of Fλ

$$ngap_i := \frac{gap}{\left(F \cdot \lambda_i \right)}$$

Active pixel size for filled array (in terms of Fλ)

$Active\_size_i := 0.5 - ngap_i$

Horn wall thickness (μm)

$wall := 100$ μm

Wall thickness in units of Fλ

$$nwall_i := \frac{wall}{(F \cdot \lambda_i)}$$

Horn clear aperture size in units of Fl

$$Active\_dia_i := 2.0 - nwall_i$$

Summary

$j := 1..2$

j = 1: 0.5Fl square
j = 2: 2.0Fl horns

0.5Fλ square

λ_i	$pix\_spacing_i$	$Active\_size_i$
250	625	0.444
350	875	0.460
500	1250	0.472
	μm	*** Fλ**

2.0Fλ horn diameter

λ_i	$horn\_spacing_i$	$Active\_dia_i$
250	2500	1.92
350	3500	1.94
500	5000	1.96
	μm	*** Fλ**

Detector NEP referred to the absorbed power

Filled $NEPdet_1 \equiv 3 \cdot 2^{0.5} \cdot 10^{-17}$ **Feedhorn** $NEPdet_2 \equiv 3 \cdot 10^{-17}$

Detector absorption efficiency (nominal assumption: 0.8 in every case)

Filled $\eta d_{i,1} :=$

0.8
0.8
0.8

Feedhorn $\eta d_{i,2} :=$

0.8
0.8
0.8

Detector numbers (β = N_filled/N_feedhorn)

$Ndets_{i,1} :=$

32·64
24·48
16·32

$Ndets_{i,2} :=$

9·17
7·13
5·9

$$\beta_i := \frac{Ndets_{i,1}}{Ndets_{i,2}}$$

β_i
13.4
12.7
11.4

Coupling efficiency to a point source (ηpix) for the a filled array detector

Define Airy function normalised for unit total energy

$$Airy(\theta) := \left(\frac{2 \cdot J1(\theta)}{\theta}\right)^2 \cdot \frac{1}{12.564}$$

Check total energy in the diffraction pattern (integral split in two to accommodate MathCad's limitations)

$limit := 1000$ $\quad Utot := \int_0^{limit} Airy(x) \cdot 2 \cdot \pi \cdot x \, dx + \int_{limit}^{50000} Airy(x) \cdot 2 \cdot \pi \cdot x \, dx$

$Utot = 1.000$

Define diffraction-limited PSF for angular position x,y in the focal plane

$$PSF(x,y) := Airy\left[\left(x^2 + y^2\right)^{0.5}\right]$$

Calculate η_pix = fraction of total energy contained within central square area of side sFλ

$$Fraction(s) := \int_{-\pi \cdot \frac{s}{2}}^{\pi \cdot \frac{s}{2}} \int_{-\pi \cdot \frac{s}{2}}^{\pi \cdot \frac{s}{2}} PSF(x,y) \, dx \, dy$$

ηpix for the filled array pixels (and the ideal value for a 0.5Fλpixel)

$$\eta pix_{i,1} := \text{Fraction}\left(\text{Active\_size}_i\right)$$

$\eta pix_{i,1}$

0.143
0.152
0.160

$$\eta pix\_ideal := \text{Fraction}(0.5)$$

$$\eta pix\_ideal = 0.177$$

Plot ηpix vs active pixel area for a square pixel

$$k := 0, 1 .. 20 \quad size_k := \frac{k}{10}$$

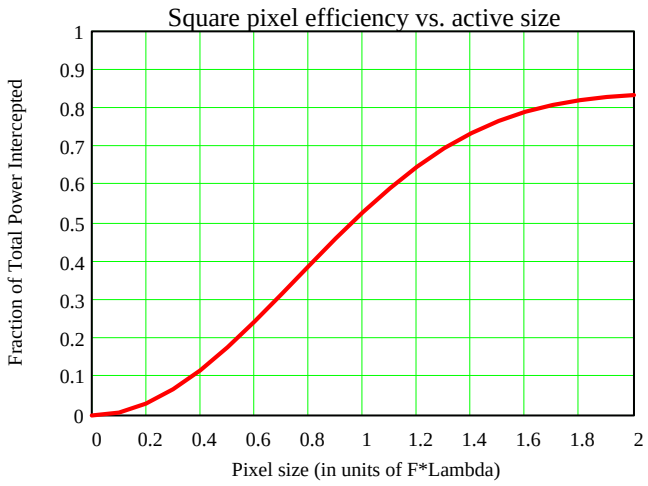

Coupling efficiency to a point source (ηpix) for a feedhorn-fed detector

Feedhorn coupling efficiency for a point source

$\eta pix_{i,2} :=$

0.7
0.7
0.7

Throughput and background power levels

Effective throughput for feedhorn in terms of λ^2

$$\alpha := 0.8$$

Throughput per detector (feedhorn array)

$$A\Omega_{i,2} := \alpha \cdot \left(\lambda_i \cdot 10^{-6}\right)^2$$

Throughput per detector (filled array)

$$A\Omega_{i,1} := \left(\text{Active\_size}_i \cdot F \cdot \lambda_i \cdot 10^{-6}\right)^2 \cdot \frac{\pi}{4 \cdot F^2}$$

Telescope power absorbed by detector

$$Pb_{i,j} := A\Omega_{i,j} \cdot \left[\int_{\nu min_i}^{\nu max_i} B(nu, T)\, d\,nu\right] \cdot \epsilon tel \cdot \eta opt \cdot \eta d_{i,j}$$

Photon noise limited NEPs

Photon noise limited NEP (full expression)

$$NEPph_{i,j} := \left[\frac{4 \cdot A\Omega_{i,j} \cdot h^2}{c^2} \cdot \left[\int_{\nu min_i}^{\nu max_i} \frac{\varepsilon tel \cdot \eta opt \cdot \eta d_{i,j} \cdot nu^4}{e^{\left(\frac{h \cdot nu}{kb \cdot T}\right)} - 1} \cdot \left[1 + \frac{\varepsilon tel \cdot \eta opt \cdot \eta d_{i,j}}{e^{\left(\frac{h \cdot nu}{kb \cdot T}\right)} - 1} \right] d nu \right] \right]^{0.5}$$

Total NEP

$$NEPtot_{i,j} := \left[\left(NEPph_{i,j}\right)^2 + \left(NEPdet_j\right)^2 \right]^{0.5}$$

γ = ratio of detector NEP to photon noise NEP

$$\gamma_{i,j} := \frac{NEPdet_j}{NEPph_{i,j}}$$

λ_i	Filled $\gamma_{i,1}$	Feedhorn $\gamma_{i,2}$
250	1.05	0.33
350	1.34	0.43
500	1.78	0.59

Summary of power levels and NEPs

Background powers (pW) and photon noise limited NEPs (W Hz-1/2 * 1E-17) for the three bands and two pixel options

λ_i	0.5Fλ square $Pb_{i,1} \cdot 10^{12}$	2.0Fλ horn $Pb_{i,2} \cdot 10^{12}$	Ratios $\frac{Pb_{i,2}}{Pb_{i,1}}$
250	0.97	5.00	5.17
350	0.83	4.02	4.81
500	0.67	3.07	4.57

λ_i	$NEPph_{i,1} \cdot 10^{17}$	$NEPph_{i,2} \cdot 10^{17}$	$\frac{NEPph_{i,2}}{NEPph_{i,1}}$
250	4.02	9.14	2.27
350	3.17	6.95	2.19
500	2.39	5.10	2.14

λ_i	$NEPtot_{i,1} \cdot 10^{17}$	$NEPtot_{i,2} \cdot 10^{17}$	$\frac{NEPtot_{i,2}}{NEPtot_{i,1}}$
250	5.85	9.62	1.65
350	5.30	7.57	1.43
500	4.87	5.92	1.22

Approximation to Pb and NEPph assuming shot noise only and neglecting to integrate B(ν,T) across the filter band

$$Pb\_approx_{i,j} := A\Omega_{i,j} \cdot B\left(\nu_i, T\right) \cdot \Delta\nu_i \cdot \varepsilon tel \cdot \eta opt \cdot \eta d_{i,j}$$

$$NEPph\_approx_{i,j} := \left(2 \cdot Pb\_approx_{i,j} \cdot h \cdot \nu_i\right)^{0.5}$$

Accuracies of the approximate formulas for Pb and NEPph

(all accurate to within a couple of percent).

λ_i	$\frac{Pb\_approx_{i,1}}{Pb_{i,1}}$	$\frac{Pb\_approx_{i,2}}{Pb_{i,2}}$	$\frac{NEPph\_approx_{i,1}}{NEPph_{i,1}}$	$\frac{NEPph\_approx_{i,2}}{NEPph_{i,2}}$
250	0.928	0.928	0.939	0.939
350	0.922	0.922	0.933	0.933
500	0.919	0.919	0.928	0.928

Measurement of sky brightness

1-σ sky brightness [B(ν,Tsky)] limit for one detector for a 1-second and 15-minute integrations

Factor of 2^0.5 included to represent the need to subtract off the baseline

$$\Delta B\_1\_sec_{i,j} := 2^{0.5} \cdot \frac{NEPtot_{i,j} \cdot 10^{26} \cdot 10^{-6}}{2^{0.5} \cdot \eta opt \cdot A\Omega_{i,j} \cdot \Delta\nu_i}$$ **MJy Sr-1**

$$\Delta B\_15\_min_{i,j} := \frac{\Delta B\_1\_sec_{i,j}}{(15 \cdot 60)^{0.5}}$$ **MJy Sr-1**

S/N ratio (Filled:Horn) for sky brightness measurement with a given integration time

$$\Delta B\_Ratio_i := \frac{\Delta B\_1\_sec_{i,2}}{\Delta B\_1\_sec_{i,1}}$$

Mapping speed ratio (Filled:Horn) for a given integration time

$$B\_Speed\_Ratio_i := \beta_i \cdot \left(\Delta B\_Ratio_i\right)^2$$

0.5Fλ square	2.0Fλ horn	0.5Fλ square	2.0Fλ horn	S/N ratio per detector	Mapping speed ratio
$\Delta B\_1\_sec_{i,1}$	$\Delta B\_1\_sec_{i,2}$	$\Delta B\_15\_min_{i,1}$	$\Delta B\_15\_min_{i,2}$	ΔB_Ratio_i	$B\_Speed\_Ratio_i$
5.0	1.6	0.17	0.05	0.32	1.36
3.0	0.9	0.10	0.03	0.30	1.12
1.9	0.5	0.06	0.02	0.27	0.80

Measurement of a point source on-axis

1–σ flux density limit for the on-axis detector for 1-second or 15-minute integrations

$$\Delta S\_On\_Axis\_1\_sec_{i,j} := 2^{0.5} \cdot \frac{NEPtot_{i,j} \cdot 10^{26} \cdot 1000}{2^{0.5} \cdot Atel \cdot \eta opt \cdot \eta d_{i,j} \cdot \eta pix_{i,j} \cdot \Delta\nu_i}$$ **mJy**

$$\Delta S\_15\_min_{i,j} := \frac{\Delta S\_On\_Axis\_1\_sec_{i,j}}{(15 \cdot 60)^{0.5}}$$ **mJy**

Calculation of S/N enhancement for filled array through co-addition of nine pixels

$a_i := Active\_size_i$

Signal in central pixel

$$Centre_i := \int_{-\pi \cdot \frac{a_i}{2}}^{\pi \cdot \frac{a_i}{2}} \int_{-\pi \cdot \frac{a_i}{2}}^{\pi \cdot \frac{a_i}{2}} PSF(x,y)\,dx\,dy$$

$Centre_i$
0.143
0.152
0.160

Signal in each of four side pixels

$$Side_i := \int_{\pi\cdot\left(\frac{a_i}{2}+ngap_i\right)}^{\pi\cdot\left(\frac{3\cdot a_i}{2}+ngap_i\right)} \int_{-\pi\cdot\frac{a_i}{2}}^{\pi\cdot\frac{a_i}{2}} PSF(x,y)\,dx\,dy$$

$Side_i$

0.078
0.083
0.087

Signal in each of four corner pixels

$$Corner_i := \int_{\pi\cdot\left(\frac{a_i}{2}+ngap_i\right)}^{\pi\cdot\left(\frac{3\cdot a_i}{2}+ngap_i\right)} \int_{\pi\cdot\left(\frac{a_i}{2}+ngap_i\right)}^{\pi\cdot\left(\frac{3\cdot a_i}{2}+ngap_i\right)} PSF(x,y)\,dx\,dy$$

$Corner_i$

0.039
0.042
0.045

Improvement in S/N through simple co-addition of the pixels:

Total signal when the 9 pixels are co-added

$$Total_i := Centre_i + 4\cdot\left(Side_i + Corner_i\right)$$

$\frac{Total_i}{Centre_i}$

4.27
4.29
4.30

Increase in S/N when the 9 pixels are coadded

$$SN\_factor_i := \frac{1}{9^{0.5}}\cdot\frac{Total_i}{Centre_i}$$

SN_factor_i

1.42
1.43
1.43

A better way to combine the signals is to give appropriate weighting to the different pixels.

We have nine estimates of the signal level in the centre pixel, which is directly proportional to the source strength:

One measurement of the centre pixel itself, with S/N = σo - let this be normalised to 1

$$\sigma o := 1$$

Four measurements from the side pixels, each with S/N = σs = σ(o)*(Ratio of signals, Side/Centre)

$$\sigma s_i := \frac{Side_i}{Centre_i}$$

σs_i

0.543
0.544
0.545

Four measurements from the corner pixels, each with S/N = σc = σ(o)*(Ratio of signals, Corner/Centre)

$$\sigma c_i := \frac{Corner_i}{Centre_i}$$

σc_i

0.275
0.277
0.279

Factor by which the final S/N is improved on combining all the nine pixels is then

$$SN\_factor_i := \left[1 + 4\cdot\left(\sigma s_i\right)^2 + 4\cdot\left(\sigma c_i\right)^2\right]^{0.5}$$

This gives a slightly better value for the improvement in S/N than the simple coaddition above

SN_factor_i

1.57
1.58
1.58

S/N ratio (Filled:Horn) for point source measurement with a given integration time

$$SN\_Ratio\_On\_Axis_i := \frac{\Delta S\_On\_Axis\_1\_sec_{i,2} \cdot SN\_factor_i}{\Delta S\_On\_Axis\_1\_sec_{i,1}}$$

Corresponding speed ratio

$$S\_Speed\_Ratio\_On\_Axis_i := \left(SN\_Ratio\_On\_Axis_i\right)^2$$

Summary for measurement of a point source on-axis

0.5Fλ square	2.0Fλ horn	0.5Fλ square	2.0Fλ horn
$\Delta S\_On\_Axis\_1\_sec_{i,1}$	$\Delta S\_On\_Axis\_1\_sec_{i,2}$	$\Delta S\_15\_min_{i,1}$	$\Delta S\_15\_min_{i,2}$
50.4	16.9	1.68	0.56
59.9	18.7	2.00	0.62
75.1	20.9	2.50	0.70
mJy	mJy	mJy	mJy

S/N ratio	Observing speed ratio
$SN\_Ratio\_On\_Axis_i$	$S\_Speed\_Ratio\_On\_Axis_i$
0.53	0.28
0.49	0.24
0.44	0.19

Seven-point map of a point source with feedhorn array compared to one frame with filled array

FWHM

$FWHM_i :=$

18
25
36

arcsec

Angular offset from centre for 7-point

$\theta := 6$ arcsec

Relative signal in offset positions

$$Offset\_Sig_i := \exp\left[\left[-\left(\frac{-\theta}{0.601 \cdot FWHM_i}\right)^2\right]\right]$$

S/N loss in doing seven-point

$$Seven\_Point\_Factor_i := \frac{1}{7} \cdot \left(1 + 6 \cdot Offset\_Sig_i\right)$$

Observing speed ratio Filled:Feedhorn

$$S7\_Speed\_Ratio_i := \left(Seven\_Point\_Factor_i\right)^{-2} \cdot S\_Speed\_Ratio\_On\_Axis_i$$

$Offset\_Sig_i$	$Seven\_Point\_Factor_i$	λ_i	$S7\_Speed\_Ratio_i$
0.735	0.77	250	0.47
0.853	0.87	350	0.32
0.926	0.94	500	0.22

Extraction of a point source from a scan map

S/N ratio (Filled:Feedhorn) for point source extraction from a map

$$SN\_Ratio\_Map\_Point_i := \left(\beta_i\right)^{0.5} \cdot \frac{\Delta S\_On\_Axis\_1\_sec_{i,2}}{\Delta S\_On\_Axis\_1\_sec_{i,1}}$$

λ_i	$SN\_Ratio\_Map\_Point_i$
250	1.2
350	1.1
500	0.9

Corresponding mapping speed ratio (Filled:Feedhorn)

$$Speed\_Ratio\_Map\_Point_i := \left(SN\_Ratio\_Map\_Point_i\right)^2$$

λ_i	$Speed\_Ratio\_Map\_Point_i$
250	1.51
350	1.23
500	0.88

Summary of mapping/observing speed ratios Filled array: Feedhorn array

λ

λ_i	Mapping speed ratio for surface brightness $B\_Speed\_Ratio_i$	Point source observing speed ratio (on-axis) $S\_Speed\_Ratio\_On\_Axis_i$	Point source observing speed ratio (7-point with feedhorn) $S7\_Speed\_Ratio_i$	Mapping speed ratio for point source extraction $Speed\_Ratio\_Map\_Point_i$
250	1.36	0.28	0.47	1.51
350	1.12	0.24	0.32	1.23
500	0.80	0.19	0.22	0.88

Tabulation of speed ratios vs. NEPdet_F for NEPdet_H fixed at 3E-17

$p := 0, 1 .. 8$

Results of running the worksheet for a range of values of NEPdet for the filled arrays

$$NEP\_F_p := \begin{bmatrix} 2.0 \\ 2.5 \\ 3.0 \\ 3.5 \\ 4.0 \\ 4.5 \\ 5.0 \\ 5.5 \\ 6.0 \end{bmatrix}$$

$$R7 := \begin{bmatrix} 0.79 & 0.63 & 0.54 \\ 0.71 & 0.55 & 0.44 \\ 0.64 & 0.47 & 0.35 \\ 0.56 & 0.40 & 0.29 \\ 0.50 & 0.34 & 0.24 \\ 0.44 & 0.29 & 0.20 \\ 0.39 & 0.25 & 0.17 \\ 0.34 & 0.22 & 0.14 \\ 0.31 & 0.19 & 0.12 \end{bmatrix} \qquad MR := \begin{bmatrix} 2.56 & 2.45 & 2.14 \\ 2.30 & 2.11 & 1.74 \\ 2.05 & 1.81 & 1.41 \\ 1.82 & 1.54 & 1.16 \\ 1.60 & 1.32 & 0.96 \\ 1.42 & 1.14 & 0.80 \\ 1.25 & 0.98 & 0.68 \\ 1.11 & 0.85 & 0.58 \\ 0.99 & 0.75 & 0.50 \end{bmatrix}$$

Plot the point source (seven-point) ratio and the mapping speed ratio vs. NEPdet filled:

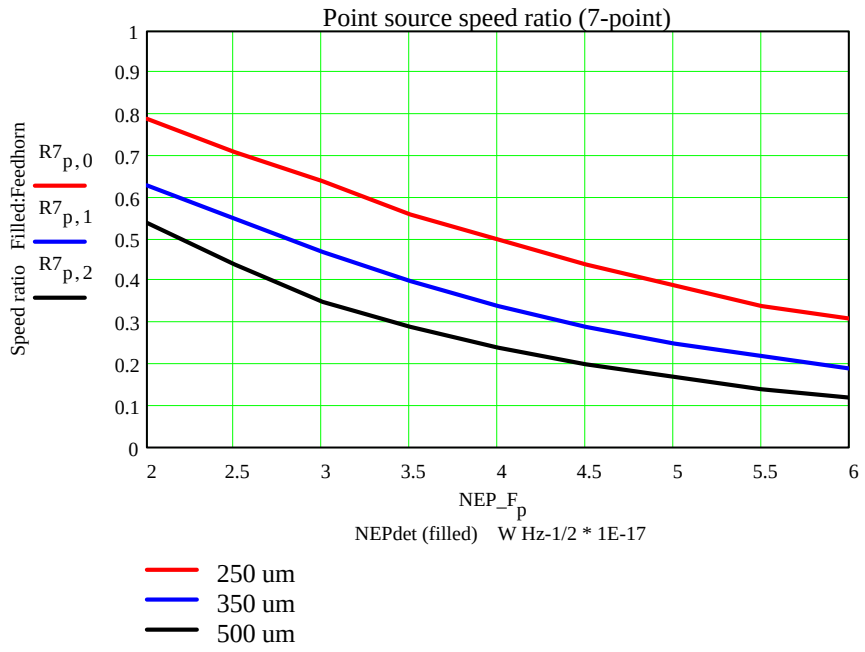

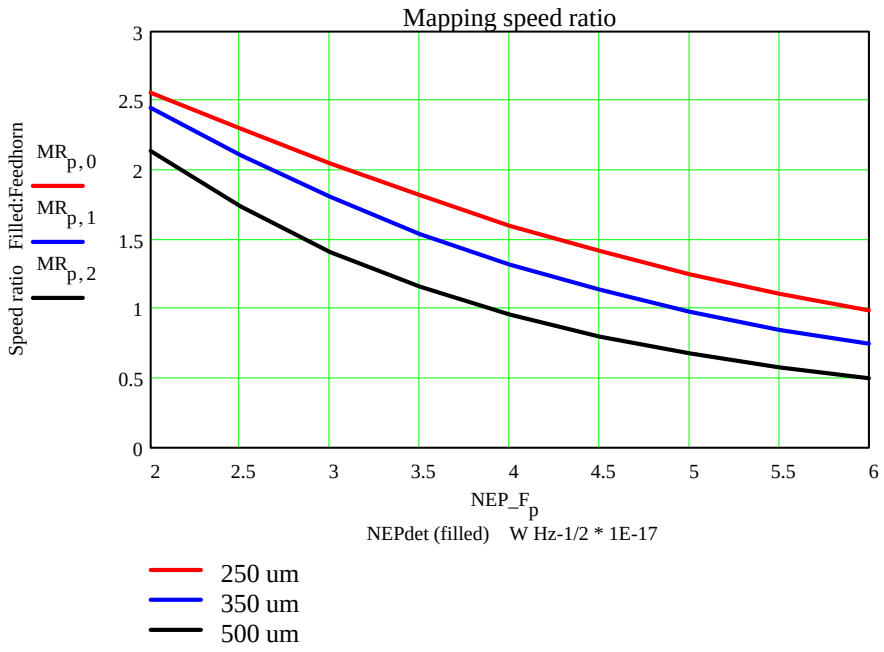

Effect of changing the telescope emissivity

$q := 0, 1 .. 5$

Fix NEPdet at 3E-17 for both options

Results of running the worksheet for a range of values of εtel for the filled arrays

$$\varepsilon\_tel_q := \begin{bmatrix} 1 \\ 2 \\ 3 \\ 4 \\ 5 \\ 6 \end{bmatrix} \quad R7\_\varepsilon := \begin{bmatrix} 0.40 & 0.28 & 0.22 \\ 0.51 & 0.37 & 0.28 \\ 0.59 & 0.42 & 0.32 \\ 0.64 & 0.47 & 0.35 \\ 0.67 & 0.50 & 0.38 \\ 0.70 & 0.53 & 0.41 \end{bmatrix} \quad MR\_\varepsilon := \begin{bmatrix} 1.28 & 1.10 & 0.88 \\ 1.66 & 1.42 & 1.10 \\ 1.89 & 1.64 & 1.27 \\ 2.05 & 1.81 & 1.41 \\ 2.17 & 1.94 & 1.53 \\ 2.25 & 2.04 & 1.63 \end{bmatrix}$$

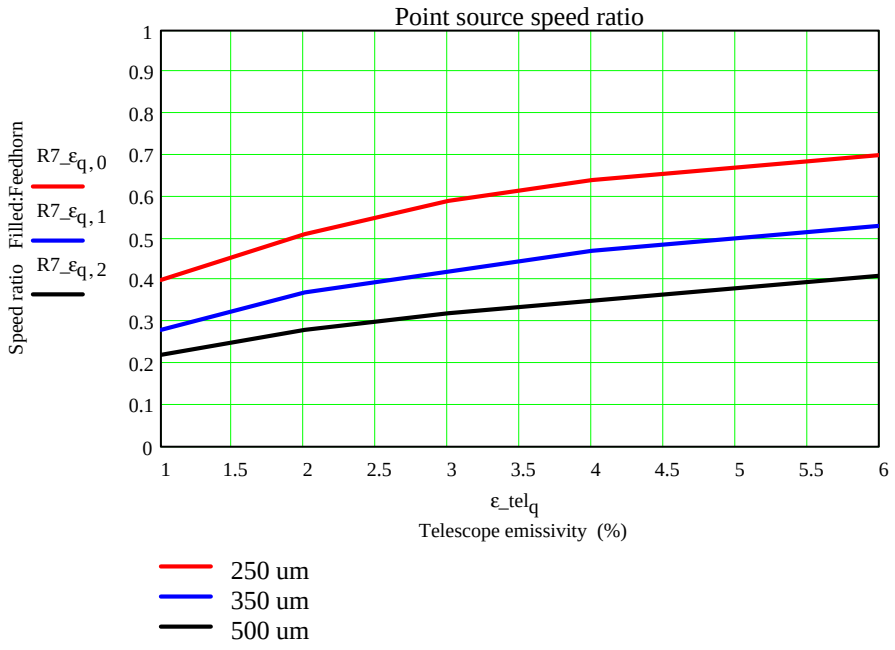

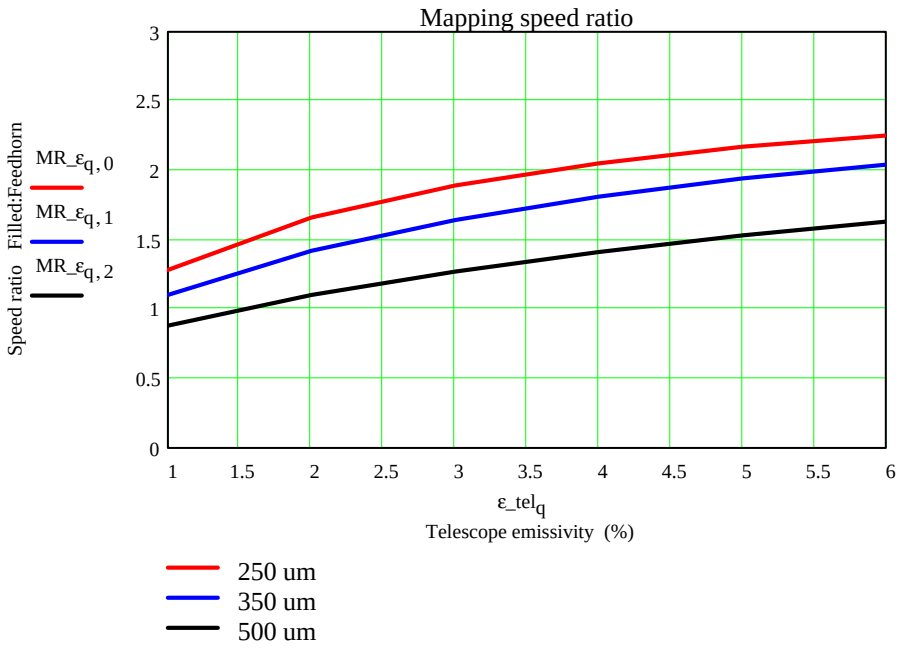

Effect of varying the point source coupling efficiency of the feedhorn:

$r := 0, 1 .. 3$

Fix NEPdet at 3E-17 for both options.

Results of running the worksheet for a range of values of ηpix for the feedhorn arrays.

0.74 is the theoretical value for SPIRE.

$\eta\_pix\_horn_r :=$

0.60
0.65
0.70
0.74

$$R7\_\eta := \begin{bmatrix} 0.87 & 0.63 & 0.48 \\ 0.74 & 0.54 & 0.41 \\ 0.64 & 0.47 & 0.35 \\ 0.57 & 0.42 & 0.32 \end{bmatrix} \qquad MR\_\eta := \begin{bmatrix} 2.79 & 2.46 & 1.92 \\ 2.38 & 2.10 & 1.64 \\ 2.05 & 1.81 & 1.41 \\ 1.84 & 1.62 & 1.27 \end{bmatrix}$$

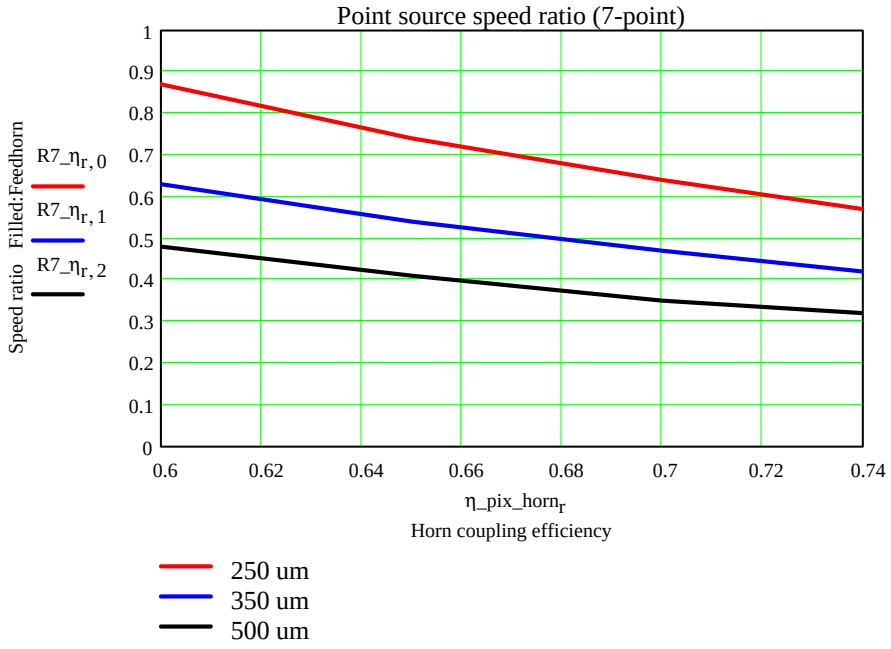

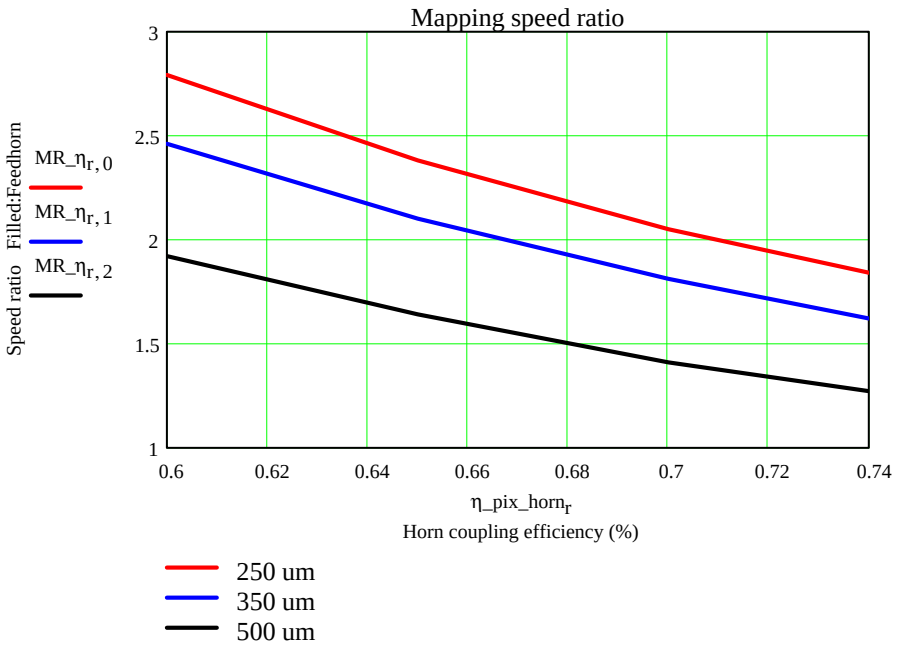

Effect of varying the inter-pixel gap for the filled array
Fix NEPdet at 3E-17 for both options.

$s := 0, 1 .. 5$

Results of running the worksheet for a range of values of gap for the feedhorn arrays.

$gap\_filled_s :=$

0
20
40
60
70
100

$$R7\_g := \begin{bmatrix} 0.85 & 0.58 & 0.42 \\ 0.79 & 0.55 & 0.40 \\ 0.72 & 0.51 & 0.38 \\ 0.67 & 0.48 & 0.36 \\ 0.64 & 0.47 & 0.35 \\ 0.55 & 0.42 & 0.33 \end{bmatrix} \qquad MR\_g := \begin{bmatrix} 2.70 & 2.23 & 1.66 \\ 2.51 & 2.11 & 1.59 \\ 2.32 & 1.99 & 1.52 \\ 2.14 & 1.87 & 1.45 \\ 2.05 & 1.81 & 1.41 \\ 1.79 & 1.64 & 1.31 \end{bmatrix}$$

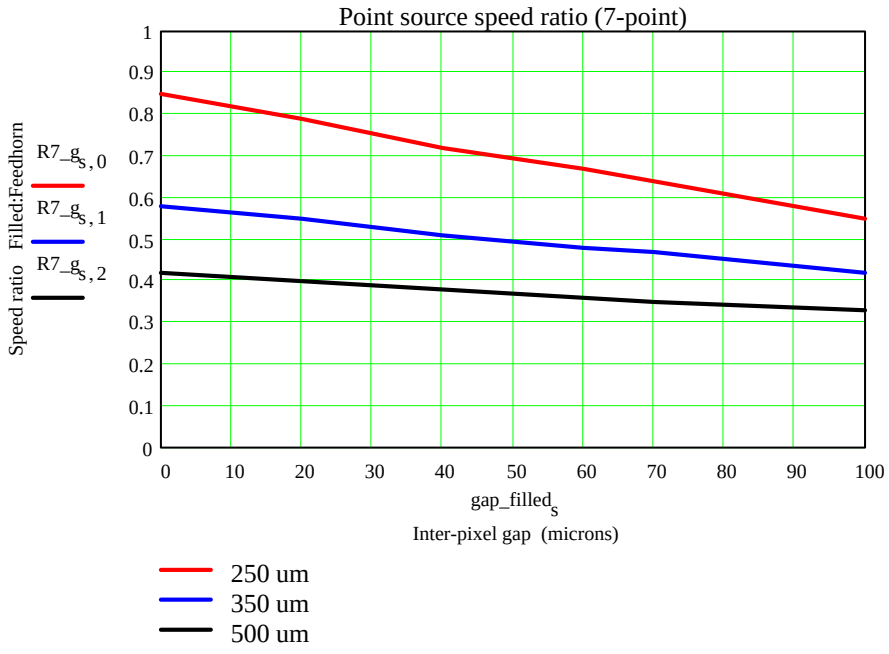

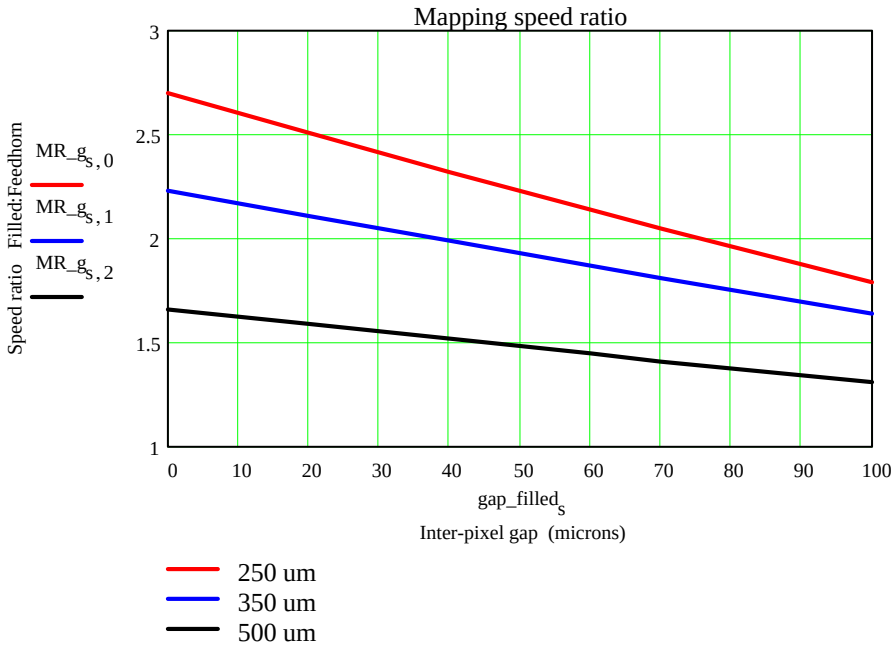

Effect of varying the feedhorn effective throughput
Fix NEPdet at 3E-17 for both options.

$t := 0, 1 .. 4$

Results of running the worksheet for a range of values of α for the feedhorn arrays.

$alpha_t :=$

0.80
0.85
0.90
0.95
1.00

$$R7\_\alpha := \begin{bmatrix} 0.64 & 0.47 & 0.35 \\ 0.67 & 0.49 & 0.37 \\ 0.71 & 0.52 & 0.39 \\ 0.74 & 0.54 & 0.40 \\ 0.78 & 0.56 & 0.42 \end{bmatrix} \qquad MR\_\alpha := \begin{bmatrix} 2.05 & 1.81 & 1.41 \\ 2.17 & 1.90 & 1.48 \\ 2.28 & 2.00 & 1.55 \\ 2.40 & 2.09 & 1.61 \\ 2.51 & 2.19 & 1.68 \end{bmatrix}$$

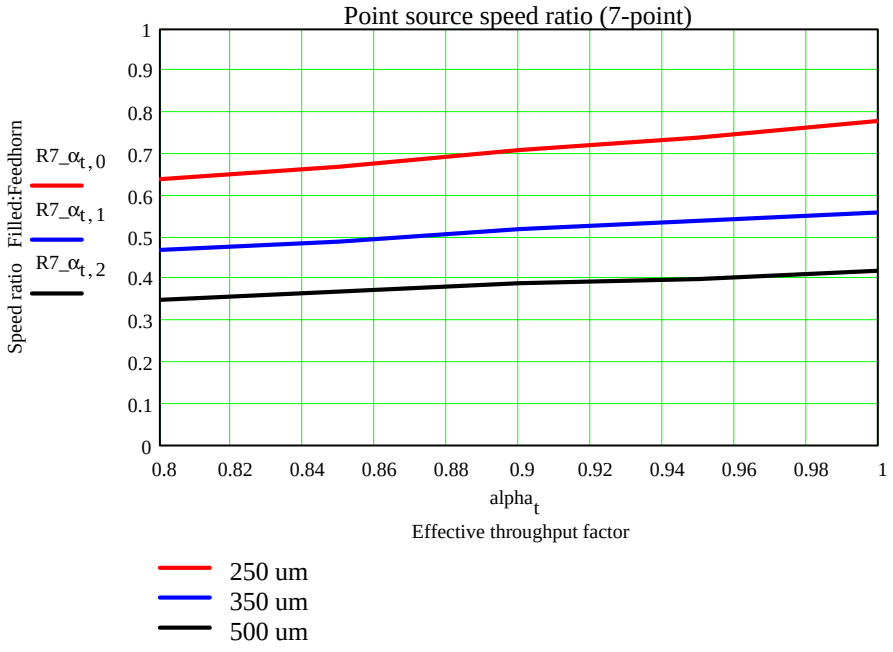

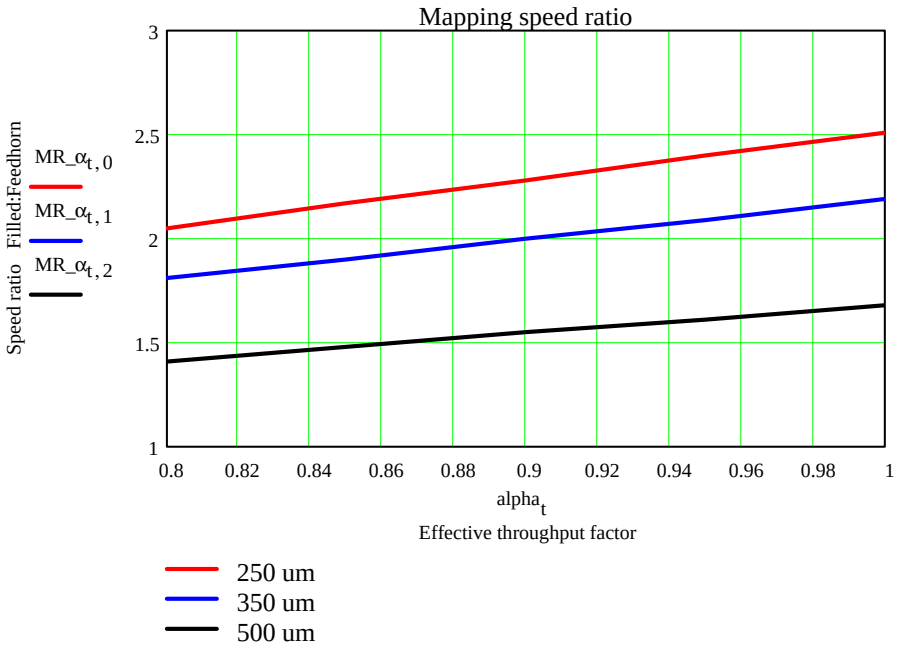

Appendix B

Simulations of the effect of 1/f noise on scanning observations (without chopping or dithering)

Scanning_250um_7Hz.mcd

Matt Griffin 13 December 1999

This worksheet simulates SPIRE scanning mode observation of an isolated point source. It models the response of a single detector scanned across a point source in the presence of 1/f noise.

Beam FWHM (arcsec.)

$FWHM := 18$

Gaussian beam profile

$$\phi o := \frac{FWHM}{2\cdot(-\ln(0.5))^{0.5}} \qquad I(\phi) := \exp\left[-\left(\frac{\phi}{\phi o}\right)^2\right] \qquad \phi o = 10.81$$

Scan rate (arcsec/sec)

$Scan\_rate := 60$ **This is the maximum possible with FIRST**

Detector sampling rate (Hz)

$Samp\_rate = 7$ **This is set globally below. Nominal values are 7 Hz for filled arrays and 28 Hz for the feedhorn array**

Define an array for computation of the timeline

$Npts \equiv 4096 \qquad i := 0, 1 .. Npts - 1$

Npts is chosen to facilitate FFT computations below

Define the position in angle and time of a point source in the scan

$Posn := 105$ **arcsec** $Time := \frac{Posn}{Scan\_rate} \qquad Time = 1.75$ **sec.**

Sky profile corresponding to scanning the detector across this source

$Amplitude := 3 \qquad Profile(x) := Amplitude\cdot I(x - Posn)$

Interval for timeline (sec.)

$$T := \frac{Npts}{28\cdot 16} \qquad T = 9.143$$

Time-steps for the timeline (sec.)

$$\Delta t := \frac{T}{Npts} \qquad \Delta t = 0.00223 \qquad t_i := i\cdot\Delta t$$

Angular positions for the timeline (arcsec.)

$\theta_i := Scan\_rate\cdot t_i$

Scan length (arcsec)

$Range := Scan\_rate\cdot T \qquad Range = 549$

Signal timeline in the absence of noise

$Signal_i := Profile(\theta_i)$

Plot signal timeline in the absence of noise

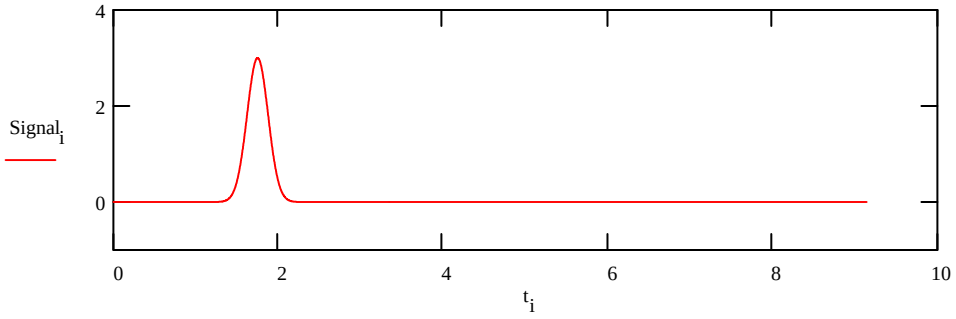

Generate a sinewave of frequency f Hz (just for diagnostic purposes)

$$fsine := 5 \qquad Sine_i := 10^{-10} \cdot \sin\left(2 \cdot \pi \cdot fsine \cdot t_i\right)$$

Generate Gaussian white noise timeline with zero mean and unit standard deviation

This is done by a setting the global variable *White* below

$$Stdev(White) = 0.99$$

White noise timeline

$$W\_Timeline_i := White_i + Sine_i$$

Sine is normally set to zero

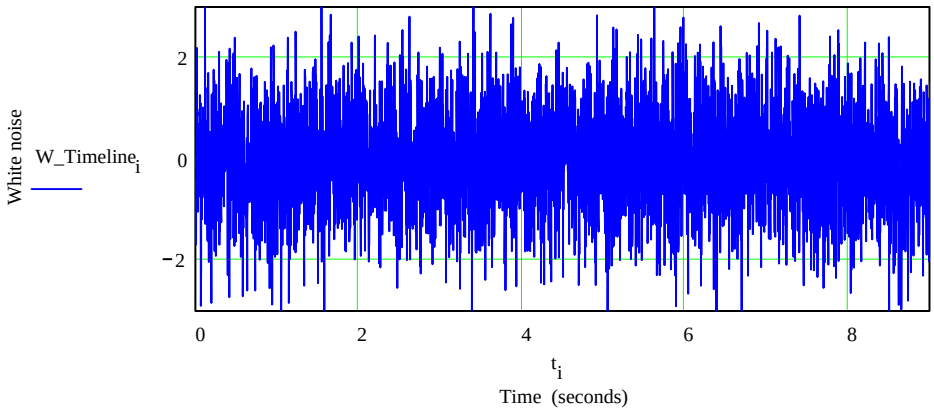

Fourier transform the white noise to derive the noise spectrum:

$$White\_spectrum := fft(W\_Timeline)$$

$$last(White\_spectrum) = 2048$$

$$j := 0, 1 .. last(White\_spectrum)$$

Define frequency scale (in Hz)

$$Freq_j := \frac{j}{T}$$

Plot the white noise spectrum

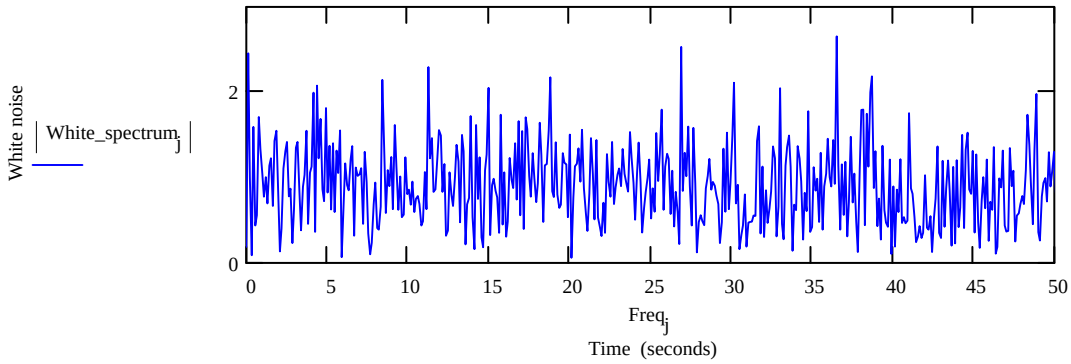

Add some 1/f noise with knee frequencies fo Hz (the set of fo values is set globally below)

fo_f
0
0.2
0.5
1
2

$k := 1, 2 .. last(White\_spectrum)$

$$Pink\_spectrum_{k,f} := White\_spectrum_k \cdot \left[1 + \left(\frac{fo_f}{Freq_k}\right)^2\right]^{0.5}$$

Plot the ratio of the (white+ 1/f) spectrum to the white noise spectrum alone (for a particular value of 1/f knee frequency as selected by global variable fknee below)

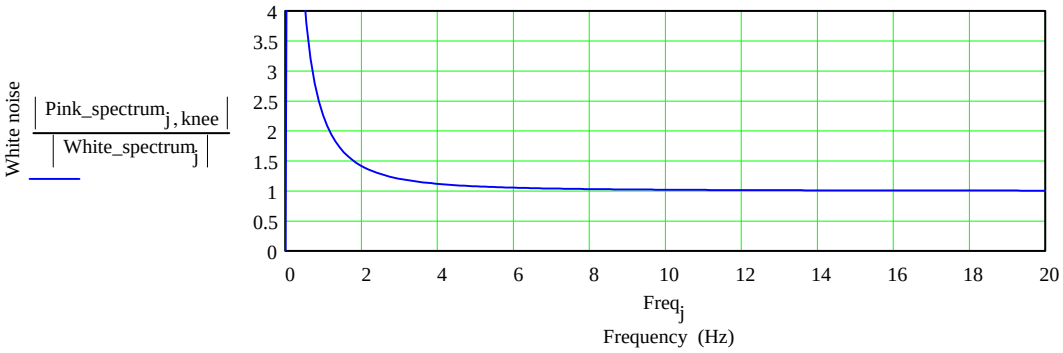

Plot the white noise and the white + 1/f noise spectra together

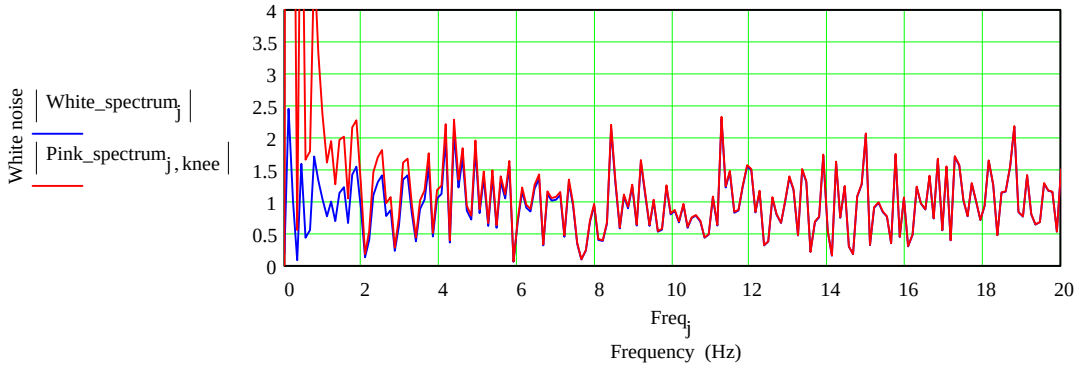

Take the inverse FFT of the (white +1/f) spectrum to get back to the time domain:

$$P\_Timeline^{<f>} := ifft\left(Pink\_spectrum^{<f>}\right)$$

Plot the white noise and (white +1/f) noise timelines for one the selected 1/f knee freq.

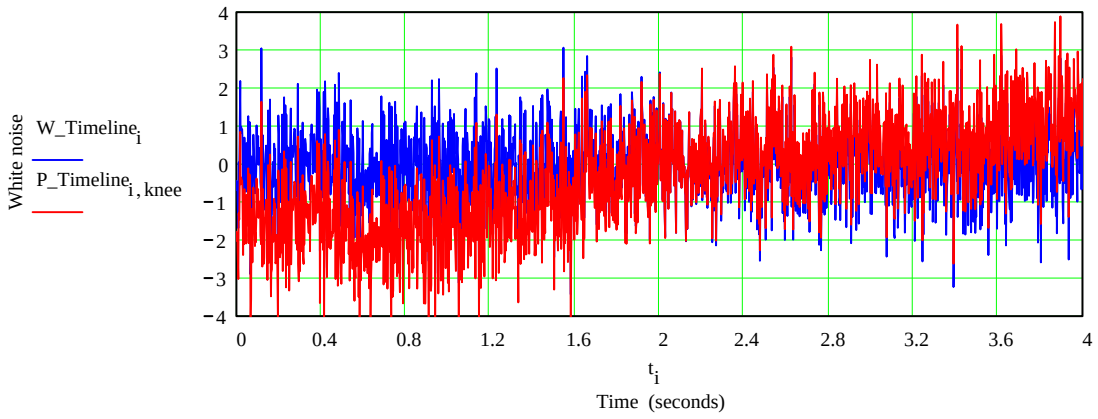

Timeline of signal + noise for one 1/f knee frequency:

$$Tot\_Timeline_{i,f} := Signal_i + P\_Timeline_{i,f}$$

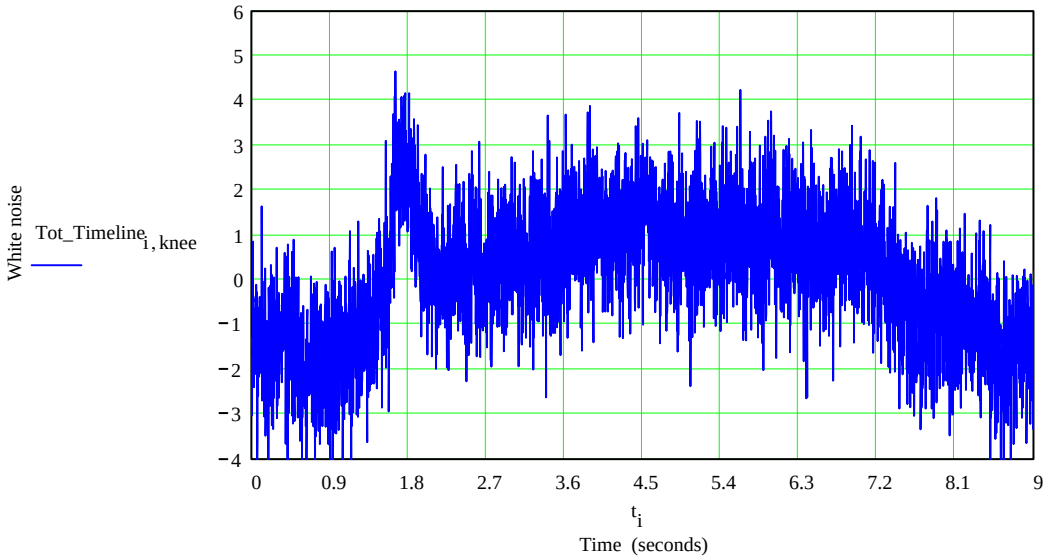

Sampling of this timeline:

Number of timeline points per sampling interval

$$Sub := \frac{28 \cdot 16}{Samp\_rate} \qquad Sub = 64$$

Index for array of sample points and corresponding sampling times

$$s := 1, 2 .. \frac{Npts - Sub}{Sub} \qquad tsamp_s := \Delta t \cdot \left(Sub \cdot s + \frac{Sub}{2} \right)$$

Sampled datapoints

$$Data_{s,f} := \frac{1}{Sub} \cdot \sum_{i = Sub \cdot s}^{Sub \cdot s + Sub - 1} Tot\_Timeline_{i,f}$$

Plot the samples

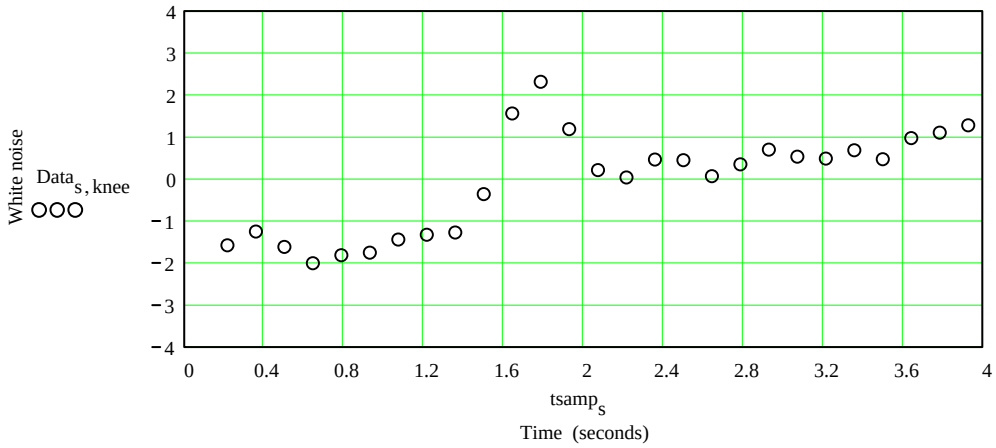

Fit a Gaussian + linear baseline to the source profile plus some data on either side

Define the interval to be used: nominally one second of data on each side of the peak

$mid := floor(Time \cdot Samp\_rate)$ $mid = 12$

$Low := mid - Samp\_rate$ $Low = 5$

$High := mid + Samp\_rate$ $High = 19$

Extract the relevant portion of the timeline

$v := 0, 1 .. High - Low$ $X_v := tsamp_{v+Low}$ $Y_{v,f} := Data_{v+Low,f}$

Width is known from scan rate and beamsize

$width := \frac{\phi o}{Scan\_rate}$ $width = 0.18$ **sec.**

Define the function and its partial derivatives with respect to the parameters

Parameters are:
ao = intercept of linear baseline
a1 = slope of baseline
a2 = amplitude of Gaussian
a3 = position (X-value) of the peak

$$F(x,a) := \begin{bmatrix} a_0 - a_1 \cdot x + a_2 \cdot \exp\left[-\left(\frac{x-a_3}{width}\right)^2\right] \\ 1 \\ -x \\ \exp\left[-\left(\frac{x-a_3}{width}\right)^2\right] \\ a_2 \cdot \exp\left[-\left(\frac{x-a_3}{width}\right)^2\right] \cdot \left[-2 \cdot \left(\frac{x-a_3}{width}\right)\right] \cdot \left(\frac{-1}{width}\right) \end{bmatrix}$$

Vector of guesses

$$guess := \begin{bmatrix} 0 \\ 0 \\ Amplitude \\ \frac{Posn}{Scan\_rate} \end{bmatrix}$$

Intercept
Slope
Amplitude
Position

Index for parameters $par := 0 .. 3$

Calculate the vectors of fitted parameters for the specified knee frequencies

$a\_fit_f := genfit(X, Y^{<f>}, guess, F)$ $a^{<f>} := a\_fit_f$

$a_{par,0}$	$a_{par,1}$	$a_{par,2}$	$a_{par,3}$	$a_{par,4}$
-0.195	-0.337	-0.705	-1.375	-2.746
-0.094	-0.155	-0.316	-0.613	-1.22
2.978	2.981	3.004	3.067	3.217
1.75	1.75	1.751	1.753	1.758

Calculate the fitted profiles and the residuals for each knee freq.

$$\text{Fitted\_profile}(x, f) := a_{0,f} - a_{1,f} \cdot x + a_{2,f} \cdot \exp\left[- \left(\frac{x - a_{3,f}}{\text{width}} \right)^2 \right]$$

$$\text{Resid}_{v,f} := Y_{v,f} - \text{Fitted\_profile}\left(X_v, f\right)$$

$$\text{Stdev}\left(\text{Resid}^{\langle 0 \rangle}\right) = 0.135$$

Crude measure of the S/N:

Use the estimated peak divided by the std. dev. of the residuals (optimisitic measure but should be OK for scaling purposes)

$$\text{S\_N\_est}_f := \frac{a_{2,0}}{\text{Stdev}\left(\text{Resid}^{\langle f \rangle}\right)}$$

Normalise this to the value for fo = 0 (white noise only)

$$\text{S\_N\_Norm}_f := \frac{\text{S\_N\_est}_f}{\text{S\_N\_est}_0}$$

S_N_est_f	S_N_Norm_f
22.0	1.00
21.8	0.99
20.6	0.93
17.8	0.81
13.1	0.59

Plot the data and fitted profile and the residuals (for the selected knee frequency)

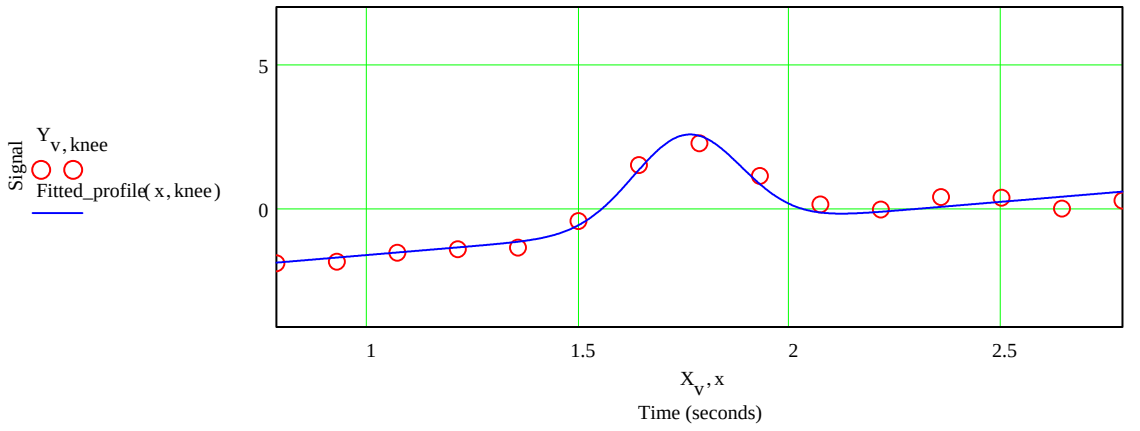

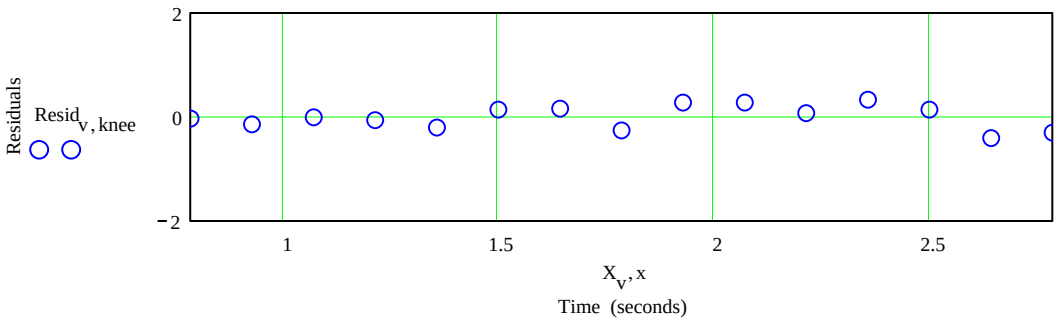

Global definitions

White noise timeline White ≡ rnorm(Npts, 0, 1)

1/f knee freqs. (Hz) f ≡ 0, 1 .. 4

Sampling rate Samp_rate ≡ 7

Knee frequency for plotting knee ≡ 4

$fo_f \equiv$

0.0
0.2
0.5
1.0
2.0

Better estimate of the S/N: Run the worksheet a number of times. Calculate the ratio of the fitted peak to the actual peak and let the S/N be estimated as the inverse of this ratio.

Measured amplitude normalised to actual value: $Nsig_f := \frac{a_{2,f}}{3}$

$Nsig_f$
0.993
0.994
1.001
1.022
1.072

Results of several runs for 250 μm; 7 Hz sampling tr := 0, 1 .. 14

7 Hz fo = 0 $N7_{tr,0} :=$

1.003
0.953
0.932
0.973
0.895
1.014
0.956
0.992
0.945
1.043
0.915
0.970
0.944
0.979
0.949

7 Hz fo = 0.2 Hz $N7_{tr,1} :=$

1.004
0.959
0.929
0.975
0.893
1.015
0.957
0.995
0.945
1.046
0.912
0.972
0.947
0.981
0.948

7 Hz fo = 0.5 Hz $N7_{tr,2} :=$

1.011
0.976
0.919
0.982
0.886
1.025
0.961
1.007
0.940
1.061
0.899
0.983
0.957
0.990
0.941

7 Hz fo = 1 Hz $N7_{tr,3} :=$

1.029
1.004
0.896
0.994
0.864
1.051
0.969
1.032
0.925
1.093
0.866
1.006
0.973
1.009
0.922

7 Hz fo = 2 Hz $N7_{tr,4} :=$

1.076
1.053
0.841
1.015
0.809
1.111
0.983
1.089
0.892
1.170
0.798
1.056
1.001
1.049
0.878

Signal-to-noise and mapping speed, normalised to values for no 1/f noise

$$Mean\_250_f := mean\left(N7^{<f>}\right)$$

$$S\_N\_250_f := \frac{1}{Stdev\left(N7^{<f>}\right)}$$

$$Speed\_250_f := \left(\frac{S\_N\_250_f}{S\_N\_250_0}\right)^2$$

fo_f	$Mean\_250_f$	$S\_N\_250_f$	$Speed\_250_f$
0	0.96	26.0	1.00
0.2	0.97	25.1	0.93
0.5	0.97	21.0	0.65
1.0	0.98	14.7	0.32
2.0	0.99	8.6	0.11

Summary of results for similar simulation for 500 μm; 7 Hz sampling

$Speed\_500_f :=$

1.00
0.82
0.41
0.13
0.04

Plot degradation in mapping speed vs 1/f knee frequency for 250 and 500μm:

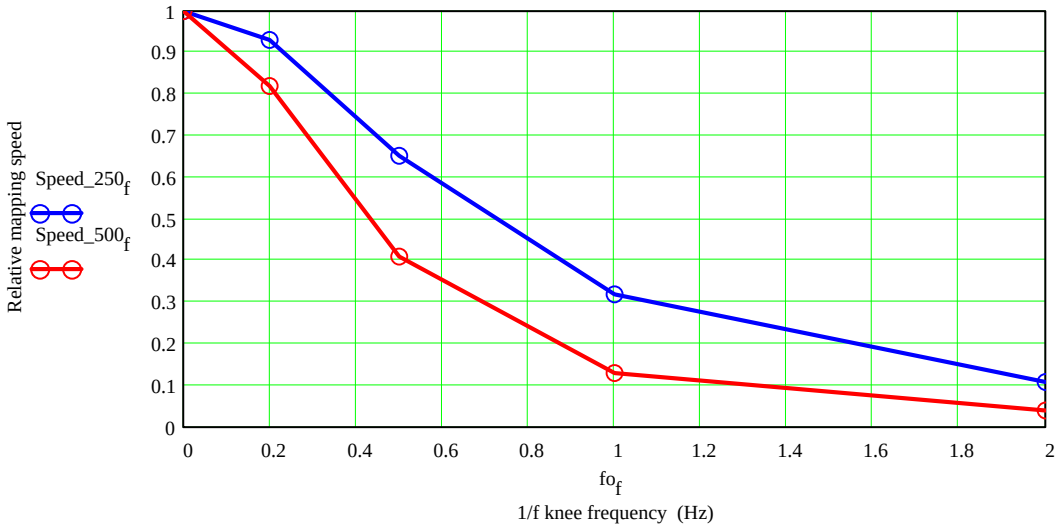

Appendix C

Revised data rate note

Revised draft of the Detector Sampling Scheme and Data Rate (which is Appendix A of the OMD)

1. INTRODUCTION

This note summarises the assumptions we currently make about data sampling and the estimated telemetry rate requirements.

The baseline data rate available to each of the FIRST instruments has been specified by ESA as 100 kbs (averaged over a 24 hr period) - see PT-06885. There may be some flexibility on this number (e.g., by increasing the downlink time over the nominal 2 hours at the expense of observing time if a larger amount of data needs to be transmitted). For the purposes of this note, we assume the following:

Available average data rate per 24-hr period	=	100 kbs
Length of observing period	=	22 hours

2. PHOTOMETER

2.1 Assumptions for photometer

- Nominal case: filled arrays with 0.5Fλ pixels (worst case for data rate).
- 4 x 8 arcminute field of view
- Filled array sizes are 32 x 64; 24 x 48 and 16 x 32 pixels at 250, 350, and 500 μm respectively
- DC coupling - so we need enough dynamic range to digitise the noise on top of the large offset from the telescope background power (which will always be greater than the power received by the detectors from even a strong source).
- No deglitching on board, but glitches may be flagged or else detected on the ground through searching for outliers, or both. It is assumed that flagging glitches does not add significantly to the data rate.
- We require 2 bits to digitise the noise.
- The effective detector sampling rate is 40 Hz. The instantaneous value may be higher, but the samples are averaged down to this level before being passed to the DRCU processing routine that deals with generating the numbers to be telemetered to the ground.

2.2 Number of bits needed for telemetry to the ground

Based on these assumptions, the required number of bits per sample *for telemetry to the ground* is 13 for filled array detectors and 14 for feedhorn detectors. Briefly this is arrived at as follows:

	Filled	**Feedhorn**
- Telescope background power on 250 μm detector (pW)	2	8
- Overall NEP for 250 μm detector (W $Hz^{-1/2}$)	$7x10^{-17}$	$14x10^{-17}$
- Signal bandwidth of detectors (Hz)	20	20
- Biggest signal we'll ever digitise and telemeter (pW)	1	4
- This is the NET signal from the strongest source we can observe (~1500 Jy at 250 μm).		
- Dynamic range required to digitise the net signal is:		

Filled: $\frac{(2)(1 \times 10^{-12})}{7 \times 10^{-17}\sqrt{20}} = 6.39 \times 10^{3} \equiv 12.6$ bits - call it 13

Feedhorn: $\frac{(2)(4 \times 10^{-12})}{14 \times 10^{-17}\sqrt{20}} = 1.28 \times 10^{4} \equiv 13.6$ bits - call it 14

2.3 Number of bits needed for detector sampling

The required number of bits per sample *for the ADC that samples the detector signals* is 15 for filled array detectors and 16 for feedhorn detectors. This is calculated arrived as follows:

When sampling the detectors, if we want to digitise the noise we actually need to digitise all the way to the GROSS signal (telescope + source). We assume, pessimistically, that we would need to do this even in the presence of the strongest source signal i.e. we sum the telescope signal and the net signal from the strongest source in the table above. So we require

Filled $\frac{(2)(3 \times 10^{-12})}{7 \times 10^{-17}\sqrt{20}} = 1.92 \times 10^{4} \equiv 14.2$ bits - call it 15

Feedhorn $\frac{(2)(12 \times 10^{-12})}{14 \times 10^{-17}\sqrt{20}} = 3.8 \times 10^{4} \equiv 15.2$ bits - call it 16

We recommend that the raw detector signals are digitised to 16 bits and only after subtraction of the chop cycles (see below) converted to 13 bits (if filled arrays) or 14 bits (if feedhorn arrays).

Note: we do not specify anything about the *instantaneous* sampling rate of the detectors or what intermediate operations need to be carried out on the raw detector data in order to get it into the form of 16-bit numbers generated at nominally 40 Hz per detector. **It is up to the array groups to specify what needs to be done here so that the DRCU processing power can be estimated. This should be included in the documentation for the Array Selectrion meeting.**

2.4 Data rates for the photometer

2.4.1 Chopping

We assume
- Chopping at f_c = 5 Hz (the maximum rate)
- Effective sampling at 40 Hz for each detector (i.e., 4 samples per chop half-cycle)
- Observing efficiency = 90%
- Averaging of each half-cycle on board to produce 10 numbers per detector per second
- Data can be
  (i) transmitted to the ground at 10 numbers per detector per second without on-board subtraction (this is essential for deep survey observations to avoid increasing the confusion noise); or
  (ii) averaged on board by computing the difference between half-cycles, with these differences transmitted to the ground at a rate of 5 numbers per detector per second (this involves loss of information, but may be acceptable for non-confusion-limited observations).

The effective data rates are then :

With on-board differencing	5 samples per detector per second x 3712 or 280 detectors (filled or feedhorn) x 13 or 14 bits per sample (filled or feedhorn) x 0.9 observing efficiency x 22/24 fraction of 24 hrs used = **199 or 16 kbs (filled or feedhorn)**
Without on-board differencing	10 samples per detector per second x 3712 or 280 detectors (filled or feedhorn) x 15 or 16 bits per sample (filled or feedhorn) x 0.9 observing efficiency x 22/24 fraction of 24 hrs used = **459 or 37 kbs (filled or feedhorn)**

Note: in the case of the feedhorns, it is possible to transmit all the undifferenced 16-bit samples at 10 Hz, with a telemetry rate of 37 kbs. This still leaves some spare telemetry capacity, so alternatives would be: (i) to dispense with averaging over the chop half-cycles and transmit all the samples at 40x280x16x0.9x22/24 = 148 kbs, assuming that some compression can be done on this to get it within the 100 kbs limit; (ii) transmit two samples per chop half cycle instead of one.

2.4.2 Scanning without dithering

This mode is likely to be applicable to the feedhorn option only as it requires very low 1/f noise (but data rates for the fileed array case are given also for completeness).

We assume that:

- The telescope is scanned continuously across the sky. The maximum scan rate is 1 arcmin/sec.(*FIRST Scientific Pointing Modes*, p8). We therefore assume a scan rate of 60 arcsec/sec.

  The FWHM beams on the sky are approximately 18, 25 and 36 arcsec. at 250, 350 and 500 μm respectively. The minimum beam crossing times are therefore 0.30, 0.42 and 0.60 sec.

- We must telemeter a minimum of two samples per FWHM, corresponding to sampling intervals of 0.15, 0.21 and 0.30 sec. or 6.7, 4.8 and 3.3 Hz.

- 1/f noise is negligible so that dithering is not necessary

It would be convenient to sample all of the arrays at the same frequency, so we assume the worst case of 7 Hz sampling for all three arrays. This can be made up of averages of four measurements with the detectors sampled at 28 Hz.

- The net telemetry rate will be		7	samples per detector per second
		3712 or 280	detectors (filled or feedhorn)
	x	15 or 16	bits per sample (filled or feedhorn)
	x	0.9	observing efficiency
	x	22/24	fraction of 24 hours used
	=	**322 or 26 kbs (filled or feedhorn)**	

In the case of the feedhorns, it would be actually be possible to transmit all the 16-bit samples taken at 28 Hz, with a telemetry rate of 28 x 280 x 16 x 0.9 x 22/24 = 103 kbs.

2.4.3 Scanning or stepping with dithering

In this case, the assumptions are as above, except that 1/f noise dictates that dithering must be carried out at some frequency f_d. The exact dithering pattern is not relevant to the data rate (although it is important for defining the movements carried out by the Beam Steering Mirror). If the telescope is scanned continuously at the same time, the scanning speed must be chosen so that the data are not smeared by significant beam motion occurring during the chop cycle. A reasonable criterion may be set by stipulating that the telescope must scan by less than one tenth of a 250-μm beam (2 arcsec.) during one half-cycle of the chop. This gives

$$\text{scan rate} < 4f_d \text{ arcsec./sec.}$$

With a maximum available dithering frequency of 5 Hz, the scan rate must be **less than 20 arcsec./sec.** The data rates in this mode are the same as for chopping with no on-board differencing, as outlined in Section 2.4.1.

2.5 Options for reducing the photometer telemetry rate for the filled array options

The uncompressed average telemetry rates for the filled arrays are greater than the 100 kbs figure that ESA have allocated. Options for reducing the telemetry rate are considered below.

2.5.1 Chopping or dithering

(i) With on-board differencing of the half-cycles:

Chop more slowly and so average on board over a longer period. Reducing the chop frequency from 5 to to 2.5 Hz while still averaging over each chop half-cyclye would reduce the uncompressed data rate to 100 kbs. As long as the 1/f noise threshold of the detectors permits this, it should not be a problem, although it is not so good for deglitching. Alternatively, we could average two frames in chopping mode before transmission to the ground.

(ii) No on-board differencing of the half-cycles:

Here we need to compress by a factor of four.

(a) Reduce the data rate by taking into account that a large part of the signal is from the telescope offset (if we are able to assume that it is constant). This could reduce the number of bits per sample to 13 instead of 15, bringing the data rate down to 398 kbs - not much of a reduction.

(b) A more drastic alternative be to subtract off a constant offset as above AND to reduce the maximum detectable signal level from around 1 pW to, say, 0.1 pW (150 Jy at 250 μm). The number of bits per sample to be telemetered is reduced to 10 and the data rate comes down to 306 kbs - still not much of a reduction.

(c) Reduce the chop frequency to around 1.25 Hz. This is feasible only if there is no 1/f noise coming in at that frequency.

The required data rate for the filled arrays is

$$(0.9)(22/24)(2f_c)(3712)N_{bits} = (6.13)f_cN_{bits} \text{ kbs,}$$

where N_{bits} is the number of bits per sample transmitted to the ground. Keeping this within 100 kbs requires $f_cN_{bits} < 16.3$. The chopping frequency must be high enough to get above any excess 1/f noise. Chopping at twice the 1/f knee frequency results in a degradation in mapping speed by a factor of 25%. Adopting this as the worst allowable case gives $N_{bits} = 8/f_{knee}$. A 1/f knee frequency well below 1 Hz is therefore essential to be able to operate within the available data rate.

2.5.2 All modes

Putting the time series signal from an individual detector or the array images through a lossless compression algorithm. Such an algorithm has been proposed by GSFC (see the Observing Speed note).

2.6 Conclusions and questions for the photometer

2.6.1 Conclusions

1. For the filleed arrays, with chopping or dithering at 5 Hz, an uncompressed telemetry rate of 460 kbs is needed to transmit all the scan mode data with no on-board differencing. This can be reduced by dithering more slowly, which can only be done if the 1/f noise performance is good enough.

2. A data rate of 100 kbs poses no significant problems for the feedhorn option.

3. For the filled arrays in chopping mode, a telemetry rate of about 200 kbs would allow us to transmit individual "photometer frames" (a frame here is defined as the result of an ON-OFF subtraction of one 0.2-second chopper cycle, for the full 4 x 8 field of view) with no deglitching and no frame averaging on board.

4. In chopping/dithering mode, slowing down the BSM by a factor of two (if 1/f noise permitting) or averaging over two half cycles, can fit the data stream into 100 kbs.

2.6.2 Questions

1. What are the filled array groups' proposals for accommodating the data rate of 100 kbs without loss of science? (Note: This is a generic issue and it would be appropriate for the two filled array groups to have a common approach.)

2. Can we design the system so that any necessary processing is done in software? That would make the system maximally flexible and enable us to adapt the compression scheme to the actual flight conditions and observing modes to achieve maximum efficiency and to prevent an inappropriate (or maybe useless) scheme being hard-wired into the system. (It is difficult to predict exactly how we may want to operate the system seven years from now!)

3. Could compression be done with a general purpose algorithm implemented in the DRCU processor, or would we need to write a special algorithm ourselves?

4. What level of processing power is likely to be needed to implement such compression on board?

3. FTS

3.1 Assumptions

- There is only one operating mode for the FTS - scanning the mirror mechanism whilst the telescope is kept at a fixed pointing.
- Baseline FTS operating parameters as in BMS note of 3 Mar 99 which updated the previous case for the selected Mach-Zehnder design - briefly the assumptions are:

  Filled arrays (worst case for data rate) - one array of 16x16 and one array of 12x12 - 400 detectors

  Detectors assumed to have 20 Hz 3-dB frequency and are sampled at 200 Hz for the 16x16 array and 133 Hz for the 12x12 array - 70 kHz total rate.

  If there is no nulling of the telescope background we will require 16-bit sampling

  If the telescope background is nulled to 5% we will require only 12 bits

  Assume 90% observing efficiency (for telescope slewing, scan dead-time, etc.).
- The instantaneous data rate - no decimation, no overhead - will be 1120 kbs for 16-bit sampling and 840 kbs for 12-bit sampling. This is what will pass from the detector read-out into whatever electronics is responsible for the interferogram processing.
- The processor will have to perform the deglitching and decimation of the interferogram back to critical sampling. After decimation and allowing for overheads, the rate for telemetry to the ground will be:

  (1120*0.9*22/24)/5 = 185 kbs for 16 bit sampling

  and (840*0.9*22/24)/5 = 139 kbs for 12 bit sampling
- For 12 bit sampling and full decimation we can almost meet the 100 kbs rate. Some compromises are possible: slow down the mirror; observe at lower data rate for fraction of the orbit; assume some lossless compression.
- For the feedhorn option we assume there will be 56 detectors. The maximum *instantaneous data rate before decimation* is therefore 130 kbs for 16 bit sampling and 97 kbs for 12 bit sampling.
- For the filled array options, a 1/5 duty cycle for SPIRE would allow us to transmit raw data as a special engineering mode.
- If desired, we could also transmit raw data from a few detectors (e.g., the central pixels)

3.2 Conclusions for the FTS

1. We are close to meeting the 100 kbs budget if we assume that we can null the telescope background to within 5%. However, for the filled arrays, this means that we will be entirely reliant on the calibration source working correctly.
2. We recommend that a 16 bit ADC is implemented and, unless the calibrator fails, only 12 bits are telemetered. This means that the instantaneous data transfer rate will be of order 1200 kbs from the detector readout to the on-board processor responsible for the decimation.
3. No averaging of interferograms should be implemented - we will cope with any restrictions on the data rate in other ways - lossless compression etc.
4. If the feedhorn option is chosen there will be no requirement for on-board processing of the interferograms.

Appendix D

Beam profile broadening for filled array pixels bigger than 0.5Fλ

Filled_array_beams.mcd

Matt Griffin **9 January 2000**

This worksheet calculates the idealised beam profiles for square filled array pixels.

Method: The square pixel is assumed to be uniformly absorbing and its geometrical area is convolved with an ideal Airy pattern

Pixel size in units of Fλ

$i := 1, 2 .. 4$ $d1 := \frac{250}{300} \cdot 0.5$ $d1 = 0.417$ $d2 := \frac{350}{300} \cdot 0.5$ $d2 = 0.583$

$Pixel_i :=$

0.5
1.0
d1
d2

i = 1: 0.5Fλ pixels
i = 2: 1.0Fλpixels
i = 3: 250 μm array with pixel design wavelength = 300 μm
i = 4: 350 μm array with pixel design wavelength = 300 μm

Pixel angular size $\theta_i := Pixel_i \cdot \pi$

Define Airy function

$$Airy(x, y) := \left[\frac{2 \cdot J1\left[\left(x^2 + y^2 \right)^{0.5} \right]}{\left(x^2 + y^2 \right)^{0.5}} \right]^2$$

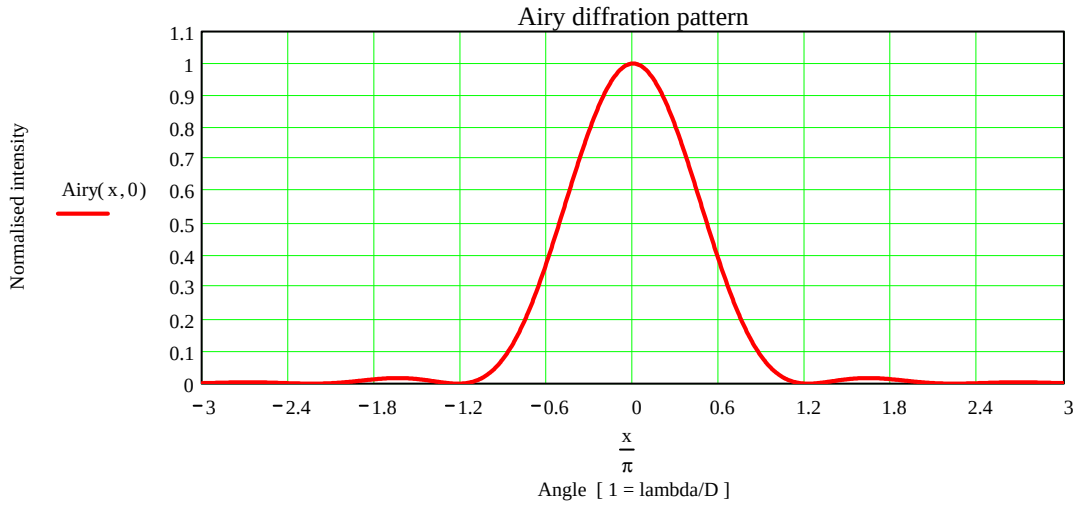

Compute the beam profile by convolving the square pixel with the Airy pattern:

$j := 0, 1 .. 60$ $z_j := \frac{j - 30}{5}$ $b_i := \frac{\theta_i}{2}$

$$Signal(z, i) := \int_{-b_i + z}^{b_i + z} \int_{-b_i}^{b_i} Airy(x, y)\, dx\, dy \qquad Response(z, i) := \frac{Signal(z, i)}{Signal(0, i)}$$

Calculate the FWHM in terms of λ/D:

$FWHM_i :=$

1.0703
1.2212
1.0573
1.0862

$Response\left(\frac{FWHM_i \cdot \pi}{2}, i \right)$

0.5000
0.5000
0.5000
0.5000

$FWHM_i$

1.0703
1.2212
1.0573
1.0862

Plot the beam profiles for 0.5Fλ and 1.0Fλ:

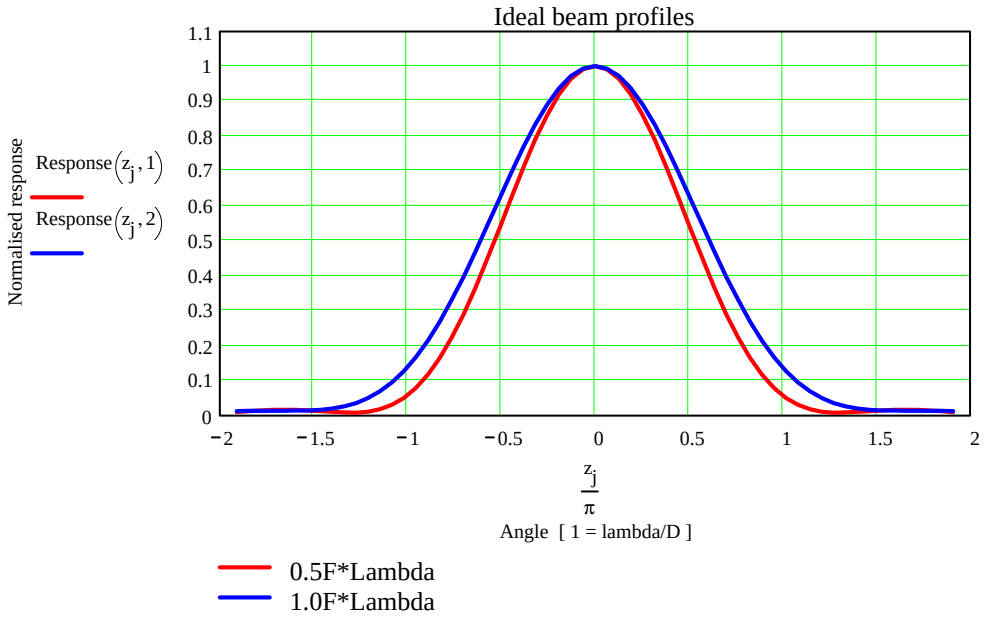

Comparison of the 0.5Fλ results with full model of SPIRE computed by Martin Caldwell:

$k := 1, 2 .. 3$ $\lambda_k :=$

250
350
500

$$Beam\_half\_F\_\lambda_k := \left(\frac{\lambda_k \cdot 10^{-6}}{3.28} \cdot \frac{360}{2 \cdot \pi} \cdot 3600 \right) \cdot FWHM_1$$

This calculation

$Beam\_half\_F\_\lambda_k$

16.8
23.6
33.7

arcseconds

MJC model

$Beam\_MJC_k :=$

16.5
23.1
32.8

arcseconds

The results are very similar

Percentage by which the beam is broader than the 0.5Fλ beam

$$Broadening_i := \frac{\left(FWHM_i - FWHM_1\right) \cdot 100}{FWHM_1}$$

0.5Fλ pixels
1.0Fλpixels
250 μm array with pixel design wavelength = 300 μm
350 μm array with pixel design wavelength = 300 μm

$Broadening_i$

0
14.1
-1.2
1.5

%

Conclusions:

1. **The beam width is not significantly affected if one array type is used for 250 and 350 μm.**
2. **The beam width for a 1.0Fλ pixel is about 14% larger than that for a 0.5Fλ pixel.**

Appendix E

Sensitivity model for the SPIRE photometer

Photometer sensitivity model for SPIRE feedhorn option — BOLPH_08.MCD — 15 Jan. 2000

BOLPH_01.MCD 18 Sept. 1997
Modified to compute mapping sensitivity correctly following discussion with WKG

BOLPH_02.MCD 11 Oct. 1997
Telescope focal ratio changed to f/9.59
Horn outside diameter changed to 2Fλ
Hours per day changed from 20 to 22

BOLPH_03.MCD 11 Nov. 1997
Telescope focal ratio changed to f/8.68
Dtel changed to 3.285 m

BOLPH_04.MCD 26 Nov. 1997
Adjusted calculation of sensitivity for frame mapping to use factors for S/N enhancement as in draft note on mapping speed by Griffin, Bock and Gear
NEPdet changed from 1E-17to 3E-1'7
Observing efficiency: 0.9 for point source ; 0.8 for field map

BOLPH_05.MCD 2 April 1999
Revised to include each optical element of photometer explicitly
15-K level makes significant additional contribution
Overall transmission still set at around 0.3

BOLPH_06.MCD 22 April 1999
Revised to incorporate 4 x 8 fov for deep surveys
Strong source power levels calculated
Internal calibrator requirements now included

BOLPH_07.MCD 16 May 1999
Detector sensitivity characterised in terms of DQE

BOLPH_07_revised.MCD 28 June 1999
New version incorporating Jamie's comments in his e-mail of June 25. Revisions are noted in purple.

BOLPH_08.MCD
Version prepared for array selection meeting
* Bands set at 250, 350, 500 μm, the nominal values used for the array selection
* Temperature table updated to reflect current optical/thermal design
* Power and NEP now referred to what is absorbed by the detector
* Only one observing efficiency factor (0.9) used for all observations
* Full NEPph calculation implemented (makes no real difference)

Constants $h \equiv 6.626 \cdot 10^{-34}$ $c \equiv 3 \cdot 10^{8}$ $kb \equiv 1.38 \cdot 10^{-23}$

$origin \equiv 1$

Planck function $B(nu, T) := \dfrac{2 \cdot h \cdot (nu)^3}{c^2 \cdot \left[e^{\left(\frac{h \cdot nu}{kb \cdot T} \right)} - 1 \right]}$

Assumptions

$i \equiv 1, 2 .. 3$

Telescope	Temp.	Emissivity	Diameter	Area	Focal ratio
	$Ttel \equiv 80$	$\varepsilon tel \equiv 0.04$	$Dtel \equiv 3.285$	$Atel \equiv 0.25 \cdot \pi \cdot Dtel^2$	$Ftel := 8.68$

Plate scale at telescope focus (arcsec/mm): $PS := \frac{1}{Dtel \cdot Ftel} \cdot \frac{360}{2 \cdot \pi} \cdot 3.6$ $PS = 7.23$

Plate scale at arrays (arcsec/mm): $PSA := PS \cdot \frac{8.68}{5}$ $PSA = 12.56$

Feedhorns	Point source coupling efficiency	Final focal ratio	No. of feedhorns
	$\eta tel \equiv 0.7$	$Ffin := 5$	$Ndets_i \equiv$

$Ndets_i \equiv$
61
37
19

Beamwidths (arcsec.): $FWHM_i := \frac{1.22 \cdot \lambda_i \cdot 10^{-6}}{Dtel} \cdot \frac{360}{2 \cdot \pi} \cdot 3600$

$FWHM_i$
19
27
38

Bolometers	NEP (*1E-17)	QE
	$NEPdet \equiv 3.0$	$\eta b \equiv 0.8$

Observing efficiencies	Chopping factor	Observing efficicency (slewing, mechanism overheads, etc.):
	$\eta ch \equiv 0.45$	$\eta obs \equiv 0.9$ **Now using just one overall efficiency factor**

Bands: defined by central wavelengths (in μm) and resolution of the filters

$\lambda_i \equiv$	$R_i :=$
250	3
350	3
500	3

$\nu_i := \frac{c}{\lambda_i \cdot 10^{-6}}$ $\lambda L_i := \lambda_i - \frac{\lambda_i}{2 \cdot R_i}$ $\lambda U_i := \lambda_i + \frac{\lambda_i}{2 \cdot R_i}$ $\Delta\lambda_i := \frac{\lambda_i}{R_i}$ $\Delta\nu_i := \frac{\nu_i}{R_i}$

$\nu L_i := \frac{c}{\lambda U_i \cdot 10^{-6}}$ $\nu U_i := \frac{c}{\lambda L_i \cdot 10^{-6}}$

Filter bands changed to 250, 350, 500

i	λ_i	λL_i	λU_i	$\Delta\lambda_i$	$\nu_i \cdot 10^{-9}$	$\nu L_i \cdot 10^{-9}$	$\nu U_i \cdot 10^{-9}$	$\Delta\nu_i \cdot 10^{-9}$
1	250	208	292	83	1200	1029	1440	400
2	350	292	408	117	857	735	1029	286
3	500	417	583	167	600	514	720	200

Transmission, emissivity and temperature of optical elements $j \equiv 0, 1 .. 11$ $k \equiv 0, 1 .. 12$

0 = Telescope
1 = 15-K filter
2 = M3
3 = M4
4 = M5
5 = 4-K filter
6 = M6
7 = 2-K filter
8 = M7
9 = Dichroic
10 = M8
11 = Bandpass filter
12 = Blocker

k	$t_k \equiv$	$\varepsilon_k \equiv$	$T_k \equiv$	td_j
0	0.960	0.04	80	0.301
1	0.900	0.100	4	0.334
2	0.995	0.005	4	0.336
3	0.995	0.005	4	0.338
4	0.995	0.005	4	0.339
5	0.900	0.100	4	0.377
6	0.995	0.005	4	0.379
7	0.900	0.100	2	0.421
8	0.995	0.005	2	0.423
9	0.900	0.100	2	0.47
10	0.995	0.005	2	0.473
11	0.525	0.300	0.3	0.9
12	0.900	0.100	0.3	

Transmission from element to detector $td_j \equiv \prod_{k=j+1}^{12} t_k$

Cold stop attenuation of telescope background: $\eta cs := 0.8$

Temperature table has been updated: all of the SPIRE optics and filters are now at 4 K or less. The contribution from the instrument iteself is now completely negligible.

Array parameters

Horn aperture outside dia. (mm)

$$Dhorn_i := \frac{2 \cdot Ffin \cdot \lambda_i}{1000}$$

Array dimension cente-centre (pixels):

$Nmax_i :=$

17 – 1
13 – 1
9 – 1

$Nmin_i :=$

9 – 1
7 – 1
5 – 1

Pixel size at telescope focus (mm):

$$Dpix_i := \left(Dhorn_i\right) \cdot \frac{Ftel}{Ffin}$$

Array dimensions at telescope focus centre-centre (mm):

$$Lmm_i := Nmax_i \cdot Dpix_i$$

$$Wmm_i := Nmin_i \cdot Dpix_i$$

Field size (arcmin):

$$Larcmin_i := \frac{Lmm_i \cdot PS}{60} \qquad Warcmin_i := \frac{Wmm_i \cdot PS}{60}$$

Lmm_i	Wmm_i	$Larcmin_i$	$Warcmin_i$	$Dhorn_i$	$Dpix_i$
69	35	8.4	4.2	2.5	4.3
73	36	8.8	4.4	3.5	6.1
69	35	8.4	4.2	5.0	8.7

Background power levels on the detectors

Throughput:

$$A\Omega_i := \eta cs \cdot \left(\lambda_i \cdot 10^{-6}\right)^2$$

Power contribution absorbed by detector from any element (pW)

$$Power_{i,j} := td_j \cdot \varepsilon_j \cdot 10^{12} \cdot \int_{\nu L_i}^{\nu U_i} B\left(\nu, T_j\right) \cdot A\Omega_i \, d\nu \cdot \eta b$$

Total power absorbed by detector (pW)

$$Pdet_i := \sum_{n=0}^{9} Power_{i,n}$$

$Power_{1,j}$	$Power_{2,j}$	$Power_{3,j}$
5.01	4.03	3.08
0.00	0.00	0.00
0.00	0.00	0.00
0.00	0.00	0.00
0.00	0.00	0.00
0.00	0.00	0.00
0.00	0.00	0.00
0.00	0.00	0.00
0.00	0.00	0.00
0.00	0.00	0.00
0.00	0.00	0.00
0	0	0

Note that this is now totally dominated by the telescope - the small contribution from 15 K is no longer present

Photon noise levels and single-detector NEFD

Photon noise limited NEP (full expression)

$$NEPph_i := \left[\frac{4 \cdot A\Omega_i \cdot h^2}{c^2} \cdot \left[\int_{\nu L_i}^{\nu U_i} \frac{\varepsilon tel \cdot td_0 \cdot \eta b \cdot nu^4}{e^{\left(\frac{h \cdot nu}{kb \cdot T_0}\right)} - 1} \cdot \left[1 + \frac{\varepsilon tel \cdot td_0 \cdot \eta b}{e^{\left(\frac{h \cdot nu}{kb \cdot T_0}\right)} 1}\right] d\,nu\right]\right]^{0.5} \cdot 10^{17}$$

Overall NEP
(W Hz$^{-1/2}$ x 10^{-17})

$$NEPtot_i := \left[(NEPdet)^2 + \left(NEPph_i\right)^2 \right]^{0.5}$$

NEFD (mJy Hz-1/2)

$$NEFD_i := \frac{NEPtot_i \cdot 10^{-17} \cdot 10^{26} \cdot 1000}{\eta ch \cdot \eta tel \cdot 2^{0.5} \cdot Atel \cdot td_0 \cdot \Delta\nu_i \cdot t_0 \cdot \eta b}$$

This assumes chopping

Summary

$Pdet_i$	$NEPph_i$	$NEPtot_i$	$NEFD_i$
5.01	9.1	9.6	28
4.03	6.9	7.6	30
3.08	5.1	5.9	34
pW	W Hz-1/2 E-17		mJy Hz-1/2

Note that Pdet and NEPph now refer to the absorbed rather than the incident power.

Values of Pdet for the filled pixels are smaller by a factor of 4.5 - 5 (see the Observing Speed note)

Point source observation

1 σ; 1 sec. sensitivity (mJy):

$$S\_1\sigma\_1s_i := \frac{NEFD_i}{2^{0.5}}$$

$S\_1\sigma\_1s_i$
19
21
24

1 σ; 1 hr limiting flux density (mJy):

$$Slim\_point\_1hr_i := \frac{NEFD_i}{2^{0.5} \cdot (3600 \cdot \eta obs)^{0.5}}$$

$Slim\_point\_1hr_i$
0.34
0.38
0.42

Deep mapping of one 4 x 4 arcmin field for 1 hour:

Loss in S/N for point source due to need to jiggle (see note on mapping speed by Griffin, Bock and Gear)

$factor_i :=$

0.45
0.43
0.41

Limiting flux density (mJy)

$$\Delta S\_field\_1hr_i := \frac{Slim\_point\_1hr_i}{factor_i}$$

These factors need to be revised based on the new Observing Speed note but these values will be basically correct

Large area deep survey:

Area of one field (sq. arcmin) $Afield := (4)\cdot(8)$ $Afield = 32$

Area to be surveyed (sq. deg.) $Asurv := 60$

Required overlap between fields: $overlap := 1.1$

Number of fields to be observed: $Nfields := \frac{Asurv \cdot 60^2}{Afield} \cdot overlap$ $Nfields = 7425$

Time for survey: $TMonths := 6$ $TDays := \frac{TMonths}{12} \cdot 365$ $THrs := TDays \cdot 22$

$TDays = 182.5$ $THrs = 4015$

Time for each field (hrs): $TField := \frac{THrs}{Nfields}$ $TField = 0.541$

Large survey 3-σ flux density limit: $\Delta S\_surv\_3\sigma_i := \Delta S\_field\_1hr_i \cdot \eta ch \cdot \left(\frac{1}{TField}\right)^{0.5} \cdot 3$

Summary of sensitivity calculations

		NEPs			Point source		Map	
λ_i	$Pdet_i$	$NEPph_i$	$NEPtot_i$	$NEFD_i$	$S\_1\sigma\_1s_i$	$Slim\_point\_1hr_i$	$\Delta S\_field\_1hr_i$	$\Delta S\_surv\_3\sigma_i$
250	5.01	9.1	9.6	28	19	0.34	0.8	1.4
350	4.03	6.9	7.6	30	21	0.38	0.9	1.6
500	3.08	5.1	5.9	34	24	0.42	1.0	1.9
mm	pW	W Hz-1/2	W Hz-1/2	mJy Hz-1/2	mJy	mJy	mJy	mJy

Large astronomical signals

$j := 1, 2 .. 11$ $S_j := 10^{j-7}$

Signal power absorbed by detector

$Psig_{i,j} := S_j \cdot 10^{-26} \cdot 10^{12} \cdot \eta tel \cdot \eta b \cdot Atel \cdot td_0 \cdot t_0 \cdot \Delta\nu_i$ pW

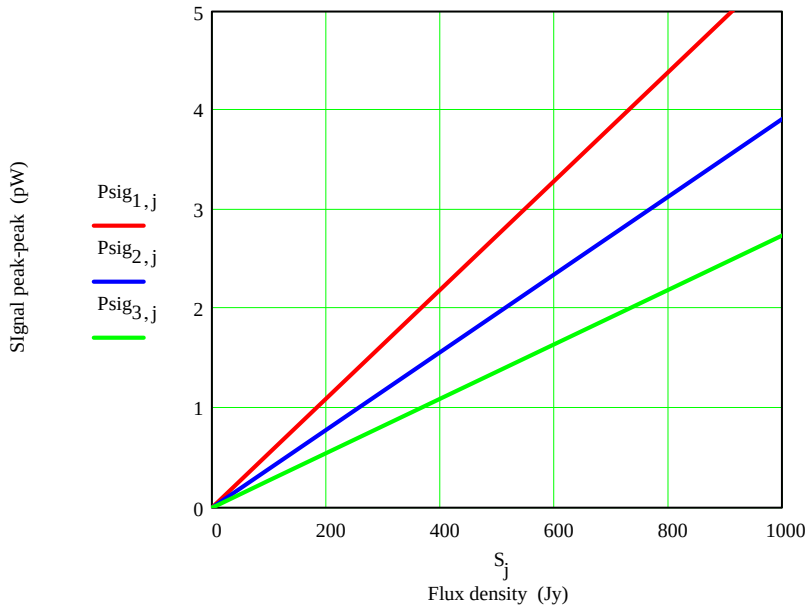

Typical 350 μm fluxes:

OMC1	1500
W3(OH)	680
K3-50	321
W75N	650
Neptune	95
Uranus	253
Saturn	7340
Jupiter	24241

Appendix F

Note by Bruce Swinyard on frame compression for the filled array option

Estimation of compression achievable by frame comparison
Bruce Swinyard (from a concept by Rick Shafer)
13 Jan 1999

Introduction

In order to comply with the restrictions on the net data rate available to the SPIRE instrument on FIRST, the filled array type detectors have to find a way of getting the raw data rate of ~460 kbits (see data rate note and observing speed note) to closer to 100 kbits. Several ways of reducing the data rate have been suggested, however those suggested so far all involve some form of integration – either directly or by slowing down the chop frequency.

Rick Shafer suggested a lossless compression method whereby several frames are averaged and then only the differences are telemetered to the ground. This note is a report on a simulation to test how much compression can be achieved by this method.

The Simulation

The simulation program is written in IDL. It takes 64 elements to simulate one row of the 64x32 array or one 16x16 array – the number and format is irrelevant. Sixty four random numbers are generated with zero mean and a sigma of 1 to simulate the noise for each frame and these are "digitised" by using FIX(N+0.5). This is equivalent to setting 3 bits for the noise – 2 bit digitisation plus 1 sign bit. To this is added a number representing the DC offset on the signal and another array representing the varying part of the signal.

The varying part of the signal is generated by having a slope of some gradient across the array plus a random distribution of signal in each pixel with the maximum signal strength being some predetermined fraction of the DC offset – or total dynamic range. Each frame then has a different random distribution of "signals" in each pixel plus some random "noise" plus the DC offset and a fixed slope. This then simulates some random distribution of sources on the sky and that each frame represents a different pointing. In fact this is a slight exaggeration of the real situation as the signal on near neighbour pixels will be more correlated than this and some portions of the array may not have the same amount of sources as another. It's not too far from the truth and serves to illustrate the possible compression factors.

Figure 1 shows the signal on the 64 elements for each of eight frames for a DC signal (dynamic range) of 10000 and a random varying component of 1% of the dynamic range. Figure 2 shows the same signal after subtraction of the average of the eight frames. Note these are integer (digitised) values. Figure 2, then, is the information that is required to be telemetered to the ground plus the averaged frame in order to reconstruct the true signal in each frame.

The program cycles through a set of fractional powers for the varying signal component and calculates the number of bits required to digitise the telemetered data by looking for the maximum signal present in all eight frames for each signal strength. One bit is added to account for the sign in each case. Note that in order to calculate the average signal 32 bits were needed to store the sum of the eight frames with no loss of fidelity. Figure 3 shows the results for a very moderate slope across the detectors (one part in sixty-four). In fact, as the slope is constant from one frame to the next, this is only relevant for the digitisation of the average signal. Figure 4 shows the same data on an expanded x-scale.

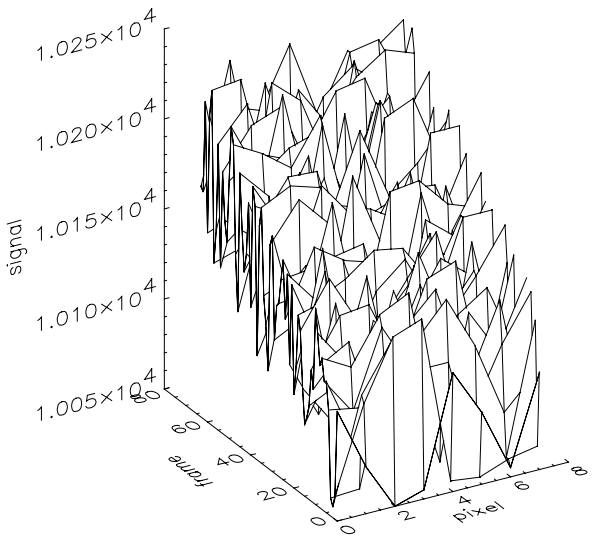

Figure 1: Input signal for 1% of dynamic range

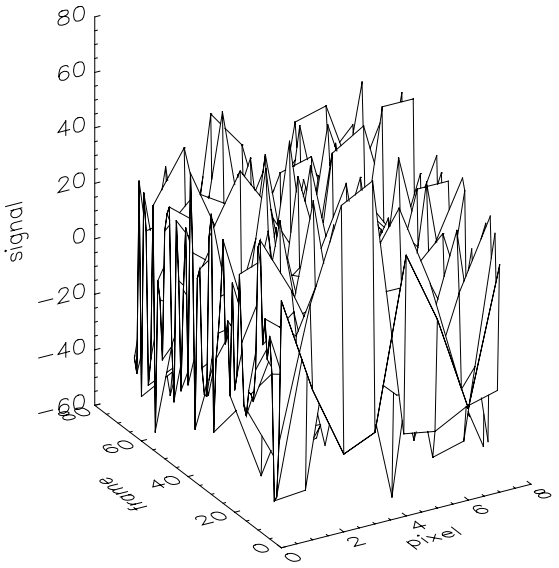

Figure 2: Difference signal for 1% of dynamic range

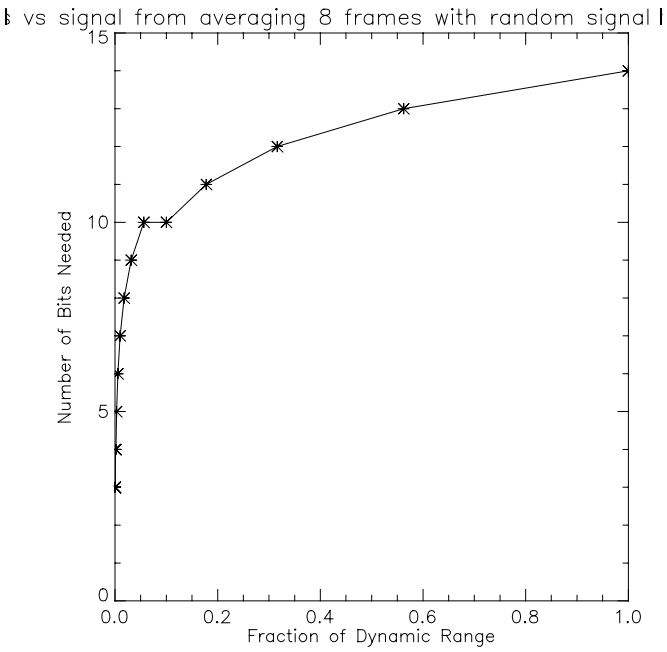

Figure 3: Number of bits required as a function of fraction of dynamic range

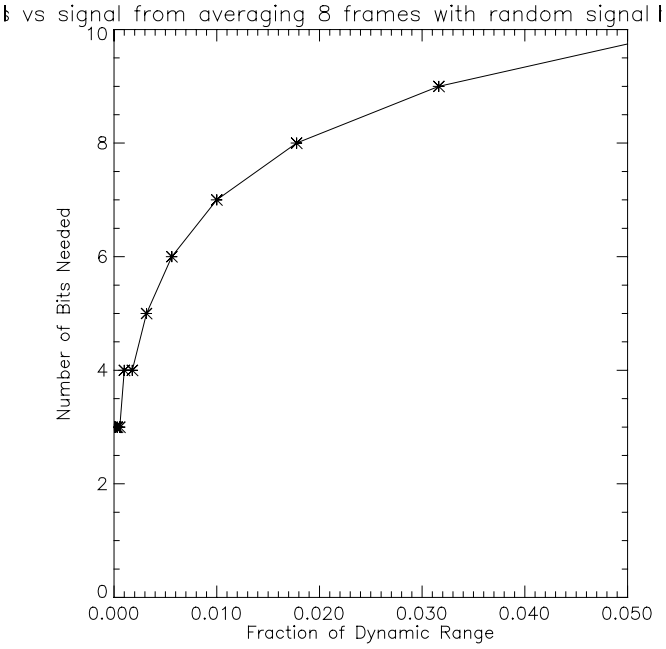

Figure 4: As figure 3 for range up to 5%

The method is feasible and appears robust. The storage requirements are modest – for 8 frames of 16 bit numbers and 3712 pixels plus one frame of 3712 32 bit numbers (the average frame), we require ~ 72 kbytes. The calculation requires only straightforward manipulations and should be well within the capabilities of the CPU.

In the absence of any fluctuation between frames, the maximum compression factor that could be achieved is 14/3 ~ 4.7. This is rapidly degraded and at 1% of the background power from the telescope (~ tens of Jy) the compression factor will be only 2.

For the deep surveys we can assume that we are only seeing noise plus a bit and we will need 4 bits – the compression factor is therefore 14/4=3.5. For almost any observations in the galaxy, and most especially for the galactic plane surveys, we will be seeing changes from pointing to pointing of 10's of Jy and the compression factor will be at best 2.

This method clearly offers some large lossless compression but there are some caveats:

i) For galactic observations the data rate will still be too high and other compression methods will be needed.

ii) To calculate the average frame with no loss of fidelity requires the calculation and storage of 32 bit numbers – is this o.k.?

iii) The sky may not be the dominating source of signal variation – for instance the background power may change from one BSM position to another. To get a compression factor of ~ 4 implies that the background power has to be stable to one part in 1000, is this realistic?